UNIVERSITÀ DEGLI STUDI DI PADOVA

Sede Amministrativa: Università degli Studi di Padova

DIPARTIMENTO DI PRINCIPI E IMPIANTI DI INGEGNERIA CHIMICA "I. Sorgato"

SCUOLA DI DOTTORATO DI RICERCA IN INGEGNERIA INDUSTRIALE

INDIRIZZO: INGEGNERIA CHIMICA

CICLO XXII

SVILUPPO E APPLICAZIONE DI METODOLOGIE PER LO SCALE-UP E L'OTTIMIZZAZIONE DI PROCESSI PER LA PRODUZIONE DI ETANOLO DA MATERIALI LIGNOCELLULOSICI

Direttore della scuola: Ch.mo Prof. Paolo Bariani

Coordinatore d'indirizzo: Ch.mo Prof. Alberto Bertucco

Supervisore: Ing. Fabrizio Bezzo

Dottoranda: Chiara Piccolo

Foreword

The realization of this work has involved the intellectual and financial support of many people and institution, to whom the author is most grateful.
Most of the research activity that led to the results summarized in this Thesis has been carried out at DIPIC, the Department of Chemical Engineering of the University of Padova, under the supervision of Dr. Fabrizio Bezzo. Part of the work has been conducted under the supervision of Prof. Gunnar Lidén, at the KEMITEKNIK- LTH - Chemical Engineering Department of Lund University (Sweden).
This study have been carried out through the financial support of Fondazione CARIPARO under the framework "Progetto Dottorati di Ricerca 2006".
The scholarship of "Fondazione Ing. Aldo Gini" (Padova, Italy) and the partial financial support from the University of Padova under Progetto di Ateneo 2007 (cod. CPDA071843) "Bioethanol from lignocellulosic biomass: process and equipment development" are also gratefully acknowledged.

All the material reported in this Thesis is original, unless explicit references to the authors are provided. In the following, a list of the publications stemmed from this project is reported.

PUBLICATIONS IN INTERNATIONAL JOURNALS

C. Piccolo, M. Wiman, F. Bezzo, G. Lidén (2010). Enzyme adsorption on SO_2 catalyzed steam-pretreated wheat and spruce material. *Enzyme and Microbial Technology*, **46**, 159-169

C. Piccolo, F. Bezzo (2009). A techno-economical comparison between two technologies for bioethanol production from lignocellulose. *Biomass and Bioenergy*, **33**, 478-491

PUBLICATION IN CONFERENCE PROCEEDINGS

C. Piccolo, G. Lidén, F. Bezzo (2009), Effect of substrate specific area on lignocellulose enzymatic hydrolysis: An experimental and modeling investigation, In: *Computer-Aided Chemical Engineering 27, 10th International Symp. on Process Systems Engineering* (R.M. Brito-Alves, C.A. Oller do Nascimento, E.C. Biscaia Jr., Eds.), Elsevier, Amsterdam, The Netherlands, 1701-1706

C. Piccolo, F. Bezzo (2008), Verso un approccio model-based per la progettazione e l´ottimizzazione dei processi di fermentazione e idrolisi per la produzione di etanolo da lignocellulosa, *Atti Convegno GRICU 2008 – 14-17 settembre 2008, Le Castella (KR), Italia*, 601-604

C. Piccolo, F. Bezzo (2007), Ethanol from lignocellulosic biomass: a comparison between conversion technologies, In: *Computer-Aided Chemical Engineering 24, 17th European Symp. on Computer Aided Process Engineering* (V. Plesu and P.S. Agachi, Eds.), Elsevier, Amsterdam, The Netherlands, 1277-1282

Padova, 28th January 2010

Abstract

The conversion of biomass into biofuels can increase fuel flexibility and reduce the related strategic vulnerability of petroleum based transportation fuel systems. Bioethanol has received considerable attention over the last years as a fuel extender or even neat liquid fuel. Lignocellulosic materials are very attractive substrates for the production of bioethanol because of their low cost and their huge potential availability. A wide variety of processes for the production of ethanol from cellulosic materials have been studied and are currently under development and complex technical problems affecting the indicators of global process have not been properly solved. Techno-financial analysis of the global processes along with the design and development of each one of the involved operations, with special care for the most critical and cost-effective steps are fundamental in order to the develop profitable processes, select the best technological options and lead the research efforts to the directions with the highest potential of costs reduction.

Process systems engineering could provide strategic tools for developing economically viable and environmentally friendly technologies for the production of fuel ethanol. The overall goal of this Thesis is to apply multi-scale modelling principles, techniques and tools to processes for the production of fuel-ethanol from lignocellulosic biomass.

First, two different conversion options, the enzymatic hydrolysis and fermentation process (EHF) and the gasification and fermentation process (GF) are considered and analysed in a macroscale approach in order to select the best alternative on the basis of their efficiency according to technical, economic, and environmental criteria. Accordingly, the EHF technology was selected as the most mature and effective process alternative in the near-term.

Afterward emphasis was placed on the single unit operations, focusing on the investigation of most critical and expensive ones. The task of enzymatic hydrolysis kinetic modelling was therefore addressed and an experimental investigation was carried out in order to characterize and better understand critical phenomena, to obtain experimental data for model validation and parameters estimation. In particular, the purpose of the study was to simultaneously assess the changes in specific surface area, surface morphology, enzyme adsorption and enzymatic hydrolysis caused by varying the pretreatment conditions in SO_2 catalyzed steam pretreatment of different lignocellulosic substrates such as wheat straw and spruce.

A simple model structure, taking into account the main phenomena occurring, and the different chemical-physical factors affecting the process, was identified and parameters estimation was performed. A preliminary sensitivity study was carried out for analysing the near-linear dependency between parameters and pointing out potential identificability issues.

Sommario

Attualmente i combustili fossili coprono il 96% del fabbisogno energetico del settore trasporti. Questa quasi totale dipendenza dai combustibili fossili determina, tuttavia, una serie di problematiche. Le riserve petrolifere sono limitate e non equamente distribuite nel mondo, con le riserve più importanti in regioni politicamente instabili. Reali o anticipate flessioni nella disponibilità del petrolio hanno condotto a rilevanti e repentini aumenti del prezzo del petrolio stesso e a incertezza economica. Negli ultimi anni anche le preoccupazioni relative all'ambiente hanno assunto particolare risonanza e le emissioni di CO_2 fossile sono indicate come uno dei fattori responsabili del riscaldamento globale.

Per tutti questi motivi una diversificazione delle fonti primarie di energia per la produzione di combustibili è necessaria, in modo particolare per quelle forme di energia che sono già disponibili o almeno più equamente distribuite del petrolio.

Il bioetanolo prodotto a partire da biomassa lignocellulosica si presenta come uno dei possibili candidati a sostituire quote di carburante fossile dal momento che la materia prima è abbondante, distribuita su tutto il territorio, e di facile approvvigionamento, e inoltre permette un'elevata riduzione delle emissioni di gas serra.

Una grande varietà di substrati può essere utilizzata per produrre etanolo: residui dell'industria agro-forestale, colture energetiche, rifiuti solidi urbani di natura organica, materiali di natura erbacea e arborea, residui dell'industria del legno e della carta. Tutti questi materiali non ricadono nella categoria di substrati, come i cereali, affetti dal problema cosiddetto "feed for fuel", ovvero l'utilizzo a fini energetici di colture destinate in precedenza ad esclusivo uso alimentare.

Nonostante tutti questi benefici, la produzione su scala commerciale di bioetanolo da lignocellulosa è tuttora impedita da una serie di barriere tecniche ed economiche: lo scale-up delle apparecchiature è complesso e affetto da problematiche di scala; l'ottimizzazione dei consumi energetici e idrici è essenziale per l'economicità del processo, così come la valorizzazione di tutte le frazioni della biomassa (organica e lignina); l'utilizzo di dati affidabili e rappresentativi per le stime di costo dell'investimento e del prodotto; la determinazione dell'impatto ambientale e socio-economico.

In generale non è ancora possibile identificare una procedura per selezionare la migliore opzione tecnologica, per ottimizzare le singole unità operative e il processo nel suo complesso, per stimare in modo inequivocabile la fattibilità tecnico-economica di un progetto.

In questa Tesi i principi della modellazione multiscala e della sintesi di processo sono stati applicati per raggiungere alcuni di questi obiettivi. Per conseguire un maggiore livello di conoscenza delle reali problematiche del processo e degli aspetti critici dell'esercizio, si è

ritenuto fondamentale affiancare all'attività di simulazione e modellazione l'attività sperimentale, condotta presso il Dipartimento di Ingegneria Chimica dell'Università di Lund, dotato di apparecchiature e strumenti analitici avanzati e con ventennale esperienza di ricerca nel campo del bioetanolo di seconda generazione. La Tesi è strutturata come segue.

Nel primo capitolo si analizza la diffusione (attuale e potenziale) nel mondo e, in particolare, in Europa del bioetanolo lignocellulosico e la distribuzione delle materie prime, si evidenziano costi e benefici derivanti dall'utilizzo di questo carburante, le iniziative governative, per promuovere l'uso dei biocarburanti. Infine, si descrivono le principali caratteristiche fisico-chimiche della biomassa che influenzano i processi di conversione e sono discusse le opzioni tecnologiche attualmente disponibili, soffermandosi sull'analisi della letteratura e sullo stato dell'arte dei diversi stadi di processo coinvolti.

La conversione dei substrati lignocellulosici in etanolo può essere ottenuta attraverso due approcci tecnologici. La via biochimica, a cui si farà riferimento con l'acronimo EHF (Enzymatic Hydrolysis and Fermentation process) prevede l'utilizzo di enzimi per convertire le frazioni cellulosica ed emicellulosica della biomassa in zuccheri semplici, successivamente fermentati da microorganismi (lieviti, batteri, funghi) in etanolo. La lignina è rimossa ed utilizzata come combustibile per la produzione di calore ed elettricità, e/o co-prodotti ad elevato valore aggiunto. Il processo è multistadio e prevede cinque step principali: pre-trattamento, idrolisi enzimatica, fermentazione, recupero del prodotto e co-generazione.

La seconda opzione tecnologica è rappresentata dal processo termochimico-biologico, nel testo menzionato con l'acronimo GF (Gasification and Fermentation process). Questo processo prevede uno stadio di pirolisi/gassificazione della biomassa al fine di produrre gas di sintesi (principalmente CO e H_2) che, dopo essere stati raffreddati e condizionati, vengono fermentati da opportuni microbi. Il gas non convertito può essere riciclato al reattore o bruciato in un sistema di combustore-turbina multistadio per produrre energia elettrica.

Nel Capitolo 2 tecniche di simulazione di processo sono utilizzate per analizzare, ottimizzare e valutare la sintesi di processo delle tecnologie EHF e GF al fine di selezionare l'opzione tecnologica più promettente, sulla base di criteri quali le rese produttive, il potenziale di ottimizzazione delle diverse apparecchiature, indici di redditività e potenziale di riduzione dei costi. I modelli hanno permesso di valutare produttività, consumi, opportunità di cogenerazione di vapore ed elettricità, possibilità di integrazioni processistiche, e sensitività ai parametri operativi. I dati raccolti sono serviti come punto di partenza per un'analisi finanziaria che ha portato alla determinazione del costo di investimento e di prodotto, e dei principali indici per la valutazione dell'investimento (NPV, IRR, ROI, EROI, ethanol pay back price). Il processo EHF è risultato essere oggi l'alternativa più matura ed efficace. Si è pertanto deciso di soffermarsi su un'analisi più dettagliata di quelli che sono emersi come gli stadi più problematici del processo EHF, al fine di supportare il lavoro di modellazione con una più profonda conoscenza dei fenomeni che sono alla base della conversione dei substrati

lignocellulosici. L'indagine sperimentale compiuta ha rivestito, in quest'ottica di acquisizione delle informazioni fondamentali sul processo, un ruolo essenziale. In particolare, molti dei meccanismi alla base degli stadi di pretrattamento e di idrolisi enzimatica della lignocellulosa non sono stati ancora pienamente compresi come pure il ruolo dei diversi parametri che caratterizzano il complesso enzima-substrato e impattano, più o meno direttamente, la cinetica e le rese finali di prodotto sono scarsamente conosciuti.

Il Capitolo 3 si apre con una panoramica dei diversi fattori che influenzano il processo di idrolisi enzimatica, distinguendo fattori legati all'enzima (composizione e attività della miscela enzimatica, inibizione da prodotto, sinergismo, adsorbimento produttivo e non produttivo al substrato) e fattori legati al substrato (cristallinità, grado di polimerizzazione, presenza e distribuzione della lignina, superficie accessibile). Sono successivamente esposte le motivazioni che hanno condotto a pianificare un'indagine sperimentale sull'effetto della superficie specifica (SSA) del substrato sottoposto a pretrattamento (*steam explosion* acido-catalizzata) sulla cinetica di idrolisi enzimatica. Un approccio a tre stadi è stato utilizzato:

- sono state determinate sperimentalmente la SSA e la distribuzione dei pori di due diversi substrati (abete e paglia di grano) sottoposti a condizioni di pretrattamento di diversa severità;
- sono stati condotti esperimenti di adsorbimento di enzima sui diversi substrati;
- si sono, infine, effettuati esperimenti di idrolisi enzimatica.

Le metodologie e gli strumenti adottati e i risultati dell'attività sono ampiamente descritti e discussi nel Capitolo.

Infine, nel Capitolo 4 si affronta nuovamente l'aspetto della descrizione quantitativa dei fenomeni. Il Capitolo presenta un'analisi critica dei principali modelli cinetici di idrolisi enzimatica, classificati in modelli empirici, deterministici, *functionally based* e *structurally based.* Una sezione a parte è dedicata ai modelli di adsorbimento, fenomeno fondamentale del processo. Un'analisi critica di questi modelli, unita alla conoscenza del processo acquisita sperimentalmente, ha portato ad individuare una struttura semplice che fosse allo stesso tempo identificabile e capace di rendere conto dei diversi fenomeni che hanno luogo nel sistema.

Partendo dalla tradizionale descrizione dell'adsorbimento attraverso l'isoterma di Langmuir, si è sviluppato un modello che incorpora la superficie del substrato accessibile all'enzima, determinata sperimentalmente, come parametro critico. Tale modello è stato inglobato nella struttura di un tradizionale modello di idrolisi a tre reazioni. I parametri del modello sono stati identificati e la sensitività delle variabili di controllo ai diversi parametri è stata valutata. La capacità del modello di predire i dati sperimentali si è rivelata soddisfacente.

Considerazioni sui possibili sviluppi e sulle opportunità di approfondimento delle tematiche di modellazione di macro e micro scala e sull'analisi tecno-economica dei processi di produzione di etanolo da lignocellulosa sono riportati nella sezione conclusiva.

La struttura della Tesi è di seguito schematizzata:

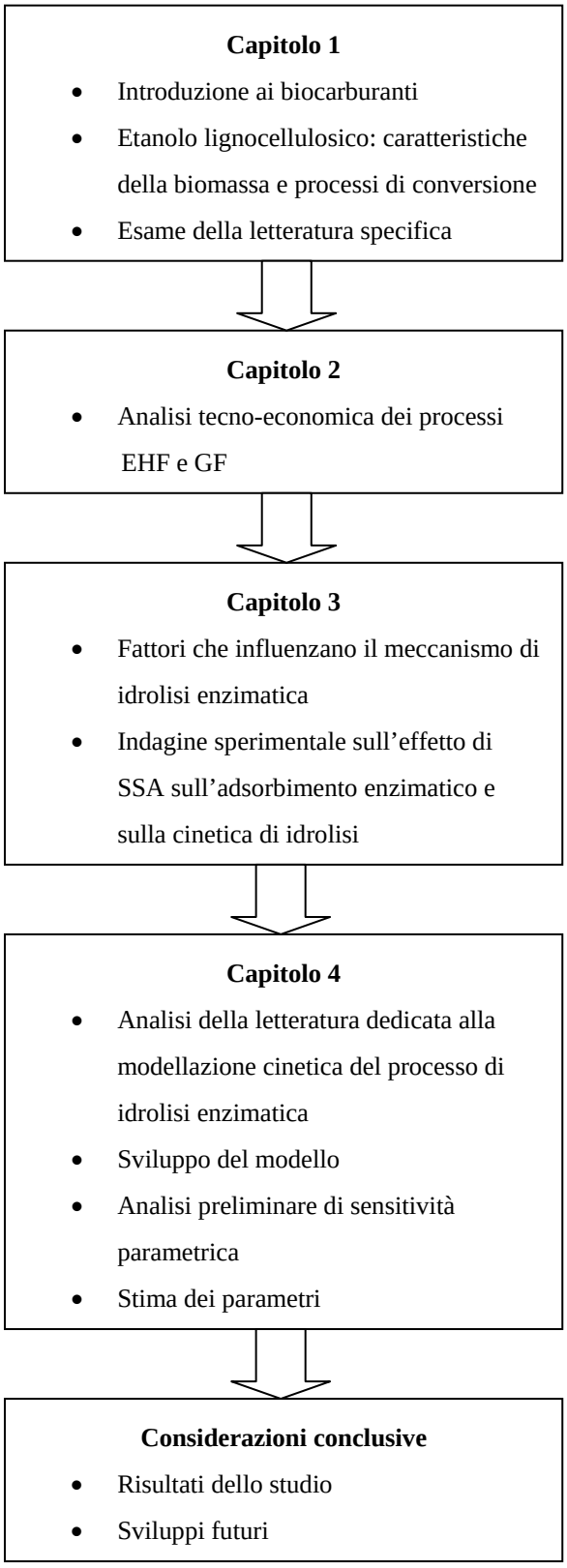

Table of contents

List of symbols

General symbols, vectors and matrices

$[CE]$ = Concentration of the enzyme-cellulose complex

A_{max} = Specific maximum cellulase adsorption

B = Generic product

C = Cellulose

c = Empirical coefficient

C_0 = Initial cellulose concentration

CrI = Cristallinity Index

E = Total enzyme concentration

e = Number of cellulose sites covered by an adsorbed enzyme molecule

E_1 = Exoglucanase enzyme concentration

E_2 = Endoglucanase enzyme concentration

E_a = Concentration of the bound enzyme

E_f = Free enzyme concentration

e_g = β-glucosidase specific activity

e_{reac} = specific acitivy of the enzyme mixture

f_C = Cellulose fraction

G = Glucose

G_2 = Cellobiose

i = fraction of total enzyme which is not inhibited by product

K_{E_2} = Endoglucanase half-saturation constant

K_{E_1} = Exoglucanase half-saturation constant

K_{eq} = Enzyme saturation constant

K_d = Equilibrium constant

k_i = Rate constant

K_{I1} = Inhibition constant

K_{I2} = Inhibition constant

K_M = Michaelis-Menten constant

k_{max} = Maximum specific reaction rate

K_P = Dissociation constant

L = Lignin

n = Empirical coefficient

N = Number of measurement

NE = Number of experiment performed

NM_{ij} = Number of measurements of the j^{th} variable in the i^{th} experiment
NV_i = Number of variables measured
P = Aggregated parameter
$Q_{a,ij}$ = Absolute sensitivity index of the j^{th} parameter
$Q_{r,ij}$ = Relative sensitivity index of the j^{th} parameter
$\mathbf{R}$ = Correlation matrix
r_i = Reaction rate
S = Substrate concentration
S_0 = Initial substrate concentration
sc_j = Scaling factor for the j^{th} parameter
SSA = Specific Surface Area
t = Time
$t_{1/2}$ = Time after which conversion reached the value ($0.5X_{max}$)
V = Hydrolysis rate
$\mathbf{V}$ = Variance matrix
V_{max} = Maximum hydrolysis rate
$V_{syn,max}$ = Maximum synergistic hydrolytic rate
W_{max} = Maximum cellulase adsorption
X = Conversion
$\mathbf{x}$ = Vector of state variables
X_{max} = Maximum conversion
$Y/[C]_0$ = Fraction of substrate hydrolyzed
y_{ijk} = k^{th} predicted value of the j^{th} variable in the i^{th} experiment
$\hat{y}_{ijk}$ = k^{th} measured value of the j^{th} variable in the i^{th} experiment
$Y_{max}/[C]_0$ = Maximum fractional conversion
ΔT_{min} = Minimum temperature difference between the hot and the cold sides in all heat exchangers

Greek symbols

α = Fraction of surface accessible to enzyme
$\boldsymbol{\gamma}$ = Heteroscedasticity parameters of variance model
$\boldsymbol{\theta}$ = Model parameters
$\boldsymbol{\Sigma}$ = Variance-covariance matrix of the measurement errors
σ_{ijk} = Variance of the k^{th} measurement of the j^{th} variable in the i^{th} experiment
φ = Lumped affinity constant
$\boldsymbol{\omega}$ = Proportionality factors of variance model
$\boldsymbol{\Phi}$ = Maximum likelihood objective function
$\eta_{isoentropic}$ = Isoentropic efficiency

Acronyms

AFEX	= Ammonia Fiber Explosion
BET	= Brunauer, Emmet, Teller method
BGL	= β-glucosidase
BIG/CC	= Biomass Integrated Gasification Combined Cycle
CBH	= Cellobiohydrolase
CBM	= Carbohydrate-Binding Modules
CI	= Confidence interval
DAE	= Differential-algebraic equations
DDGS	= Distiller Dried Grains with Solubles
DP	= Polymerisation Degree
DPV	= Viscosity Average Polymerisation Degree
DPW	= Weight Average Polymerisation Degree
EG	= Endoglucanase
EHF	= Enzymatic hydrolysis and fermentation
EROI	= Energy Return on Investment
FPA	= Filter Paper Activity
GF	= Gasification and fermentation
GHG	= Green House Gases
HEC	= Hydroxyethylcellulose
HMF	= Hydroxymethyl furfural
HPLC	= High Pressure Liquid Cromatography
HP	= High Pressure steam
LHW	= Liquid Hot Water
LP	= Low Pressure steam
NPV	= Net Present Value
NREL	= National Renewable Energy Laboratory
PB 10	= Pay back price for a 10 years pay back time
PB 5	= Pay back price for a 5 years pay back time
PTA	= Pinch Technology Analysis
ROI	= Return of Investment
S1	= Optimal pretreated spruce
S2	= Non optimal pretreated spruce
SAXS	= Small Angle X-ray Scattering
SEM	= Scanning Electron Microscopy
SHF	= Separate Hydrolysis and Fermentation
SSA	= Specific Surface Area
SSCF	= Simultaneous Saccharification and Co-Fermentation

SSF = Simultaneous Saccharification and Fermentation
TPC 10 = Total product cost for a 10 years pay back time
TPC 5 = Total product cost for a 5 years pay back time
WIS = Water Insoluble Solids
WS1 = Wheat straw treated at conditions set 1
WS2 = Wheat straw treated at conditions set 2
WS3 = Wheat straw treated at conditions set 3
WS4 = Wheat straw treated at conditions set 4
WWT = Waste Water Treatment

Chapter 1

Thesis overview and literature survey

1.1 Motivations

Growing environmental concerns over the use and depletion of non-renewable fuel sources, together with the increasing price of oil and instabilities in the oil market, have recently stimulated interest in developing processes for large-scale production of liquid transport fuels derived from renewable resources, such as bioethanol. Lignocellulosic materials offer unique and desirable features: a secure, abundant and cheap source of supply, limited conflict with land use for food and feed production, typical of first generation biofuels. Lignocellulosic ethanol used as a replacement for gasoline can reduce CO_2 emissions by 90% (Ward and Singh, 2002) and can help fulfil the commitments of the 1997 Kyoto protocol. The process alternatives for biological production of ethanol from forest and agricultural residues, or dedicated lignocellulosic crops, offers these benefits but their development is still hampered by economic and technical obstacles: process scale-up and integration to minimize energy and water demand; characterization and valuation of the lignin usage; use of representative and reliable data for cost estimation, determination of environmental and socio-economic impacts. A well-grounded methodology to select the best technological option, to address the task of single units operation and overall process optimization and to perform techno-financial assessment is still to be defined.

In this work multi-scale modelling principles, techniques and tools have been applied to fulfil these purposes. Dynamic process modelling and process synthesis methods were first integrated in a techno-economic analysis of two, regarded ad the most promising biotechnological process routes for bioethanol production, namely the enzymatic hydrolysis and fermentation process and the gasification-fermentation route. Dynamic simulation, optimization and costs assessments were performed and enabled to determine where technological and economic bottlenecks are settled and to evaluate the potential for improvements of processes' performances. As a result of this assessment the enzymatic hydrolysis and fermentation process was selected as the viable near-term option at the state of the art and the investigation of single critical unit operations within this process was addressed to tackle the obstacles that hinder process transition to commercial scale. In the past 50 years, there has been a constant influx of research publications addressing the enzymatic kinetics of cellulose degradation, which is together with pretreatment the most problematic process step. However, the kinetics of cellulose degradation is still not fully understood because of different competing effects that can hardly be distinguished from each other and that introduce large bias and

variability in the estimation of kinetic parameters. A critical analysis of models reported in literature helped in defining a suitable model structure which was at the same time capable of taking into account the main phenomena occurring in the hydrolysis step and the main factors affecting the process and which could be identified and validated through experimental data. A trade off between simplicity of the resulting model and the amount of embedded process information was thus required. The focus was put on enzymes adsorption and hydrolysis of pretreated materials and their correlation to the morphological effects caused by the pretreatment.
An experimental investigation was carried out in order to collect data needed to validate the mathematical model. All the information was than organize in an aggregated understanding, incorporating fundamentals lignocellulosic substrates morphological parameters into the traditional mathematical patterns recorded in literature.

1.2 Introduction

Worldwide energy consumption has increased 17 fold in the last century and emissions of CO2, SO2 and NOx from fossil-fuel combustion are primary causes of atmospheric pollution (Ture et al., 1997). Known oil reserves are estimated to be depleted in less than 50 years at the present rate of consumption (Sheehan et al., 1998). Energy for the transport sector represents a particularly critical area as it accounts for more than 30% of total energy demand in developed countries. Furthermore, it is 98% dependent on fossil fuel and is considered one of the main responsible for CO_2 increase in developed countries (IEA, Campbell, 2007).
Biomass has been recognized as a major world renewable energy source to supplement declining fossil fuel resources (Ozcimen and Karaosmanoglu, 2004; Jefferson, 2006). Biomass is seen as an interesting energy source for several reasons. One of the main reason is that bioenergy can contribute to sustainable development (Van den Broek, 2000; Monique et al., 2003): resources are often locally available, and conversion into secondary energy carriers is feasible without high capital investments. Moreover, biomass energy can play an important role in reducing greenhouse gas emissions; since CO_2 that arises from biomass wastes would originally have been absorbed from the air, the use of biomass for energy offsets fossil fuel greenhouse gas emissions (Lynd, 1996). Furthermore, since energy plantations may also create new employment opportunities in rural areas, it also contributes to the social aspect of sustainability. In addition, application of agro-industrial residues in bioprocesses not only provides alternative substrates but also helps solving their disposal problem. With the advent of biotechnological innovations, mainly in the area of enzyme and fermentation technology, many new avenues have opened for their utilization. Many research programs have been recently focusing on the development of concepts such as renewable resources, sustainable development, green energy, eco-friendly process, etc. in the transportation sector. In developed countries there is a growing trend towards employing modern technologies and efficient bioenergy conversion, which are becoming cost competitive with fossil fuels (Demirbas, 2000). The term biofuel is referred to liquid or gaseous fuels for the transport sector that are predominantly produced from biomass. Biofuels are generally considered as offering many

advantages over traditional oil-based fuels, including sustainability, reduction of greenhouse gas emissions, regional development, social structure and agriculture, security of supply (Reijnders, 2006).

Some governments have been announcing commitments to biofuel programs as a way to both reduce greenhouse gas emissions and dependence on oil-based fuels. The United States, Brazil, and several EU member states have the largest programs promoting bio-fuels in the world. The recent commitment by the United States government to increase the bioenergy quote threefold in ten years has added impetus to the search for viable bio-fuels (Demirbas, 2006; Demirbas et al., 2006; Chen et al., 2008). In South America, Brazil continued policies mandating at least 22% bioethanol on motor fuels and encouraged the use of vehicles that use hydrous bioethanol to replace gasoline (Stevens et al., 2004) The European Commission has indicated that biomass will play an important role in the future(Erikcsson and Nilsson, 2004).

The European Commission White Paper (White paper, 2001) calls for dependence on oil in the transport sector to be reduced by using alternative fuels such as bio-fuels. The EU bio-fuels directive (2003/30/EC) set a target of an indicative 5.75% total bio-fuel share of all consumed gasoline and diesel fuel for transport placed on the market by 2010. France established an ambitious bio-fuels plan, with goals of 7% by 2010, and 10% by 2015. Belgium set a 5.75% target for 2010. The European Commission's Green Paper on "A European Strategy for Sustainable, Competitive and Secure Energy" (March 2006) and its 2007 strategic energy review, "An Energy Policy for Europe" (January 2007) have both emphasized the need to take effective actions to address climate change (including actions to mitigate greenhouse gas emissions), promote jobs and growth and enhance security of energy supply in the internal market. On 23 January 2008, the European Commission (Proposal for a Directive, 2008) proposed a binding minimum target of 10% for the share of bio-fuels in transport in the context of the "EU directive on the promotion of the use of energy from renewable sources" that envisages a 20% share of all renewable energy sources in total energy consumption by 2020. Without the present set of subsidies, tax reductions and exemptions as well as mandatory incorporation rates, the EU production would certainly be much more limited (Jacquet et al., 2007). Fuel tax reductions are the most widely used of all the support measures for bio-fuels (Kojima et al., 2007). In 2003, the EU's framework for the taxation of energy products and electricity was amended to allow Member States to grant tax reductions and/or exemptions in favour of renewable fuels. However, to minimize the tax revenue loss for EU member states, the final tax on bio-fuels intended for transport use may not be less than 50% of the normal excise duty (Schnepf, 2006). Tax reductions for bioethanol in EU countries have been as high as US$0.84 per litre (Kojima et al., 2007).

1.3 Bioethanol as a transportation fuel

Bioethanol and bioethanol/gasoline blends have a long history as alternative transportation fuels. It has been used in Germany and France as early as 1894 by the then incipient industry of internal combustion engines (Demirbas, 2007). Brazil has utilized bioethanol as a transportation fuel since

1925. The use of bioethanol for fuel was widespread in Europe and the United States until the early 1900s. Because it became more expensive to produce than oil-based fuel, especially after World War II, bioethanol potential was largely ignored until the oil crisis of the 1970s (Balat, 2009). Since the 1980s, there has been an increased interest in the use of bioethanol as an alternative transportation fuel. Countries including Brazil and the United States have long promoted domestic bioethanol production. In addition to the energy rationale, bioethanol/gasoline blends in the United States were promoted as an environmentally driven practice, initially as an octane enhancer to replace lead. Bioethanol also has value as oxygenate in clean-burning gasoline to reduce vehicle exhaust emissions (Demirbas, 2005).

Bioethanol has a higher octane number (108), broader flammability limits, higher flame speeds and higher heats of vaporization. These properties allow for a higher compression ratio and shorter burning time, which lead to theoretical efficiency advantages over gasoline in an IC engine (Balat, 2007). Octane number is a measure of the gasoline quality for prevention of early ignition, which leads to cylinder knocking. The fuels with higher octane numbers are preferred in spark-ignition internal combustion engines. An oxygenate fuel (35% oxygen) such as bioethanol provides a reasonable antiknock value, reduces particulate and nitrogen oxides (NOx) emissions, as well as exhaust emissions normally attributed to imperfect combustion in motor vehicles, such as CO and unburned hydrocarbons (Malça and Freire, 2006).

Disadvantages of bioethanol include low energy density (bioethanol has less 66% of the energy per unit of mass than gasoline), corrosiveness, low flame luminosity, low vapour pressure (making cold starts difficult), miscibility with water, toxicity to ecosystems (MacLean and Lave, 2003), increase in exhaust emissions of acetaldehyde, and increase in steam emissions when blending with gasoline. Some properties of alcohol fuels are shown in Table 1.1.

Table 1.1 *Some properties of alcohol fuels.*

Fuel property	Isooctane	Methanol	Ethanol
Octane number	100	112	108
Auto-ignition temperature (K)	530	737	606
Latent heat of vaporization (MJ/Kg)	0.26	1.18	0.91
Lower heating value (MJ/Kg)	44.4	19.9	26.7

Bioethanol can be directly used as a transportation fuel or it can be blended with gasoline. Bioethanol is most commonly blended with gasoline in concentrations of 10% bioethanol, known as E10. In Brazil, bioethanol fuel is used pure or blended with gasoline in a mixture called gasohol (24% bioethanol and 76% gasoline) (Oliveira et al., 2005). Bioethanol can be used as a 5% blend with gasoline under the EU quality standard EN 228. This blend requires no engine modification. With engine modification, bioethanol can be used at higher levels, for example, in E85 (85% bioethanol) (Difiglio, 1997).

1.4 Bioethanol trends and projections

Global production of bioethanol has increased from 17.25 billion litres in 2000 (Balat, 2007) to over 65 billion litres in 2008 (`www.biofuels-platform.ch`), making bioethanol the most produced biofuel worldwide. This figure is mainly due to the United States (52%) and Brazil (37%) contribution. Considering all the new government programs in America, Asia, and Europe in place, total global fuel bioethanol demand could grow to exceed 125 billion litres by 2020 (Demirbas, 2007). More recently, Asia (especially China, Thailand and India) has also embarked on large scale fuel-ethanol production and that represents one of the largest production potential in the coming years. With a production of 2.82 billion litres in 2008, the EU ranks third behind the two majors productors. Figure 1.1 shows different European Countries ethanol production in 2008. The bioethanol sectors in many EU member states have been enhanced by policy initiatives and have started growing rapidly. In 2008 the production of fuel-bioethanol increased of 56% compared to 2007. The potential demand for bioethanol as a transportation fuel in the EU countries, calculated on the basis of Directive 2003/30/EC, is estimated at about 12.6 billion litres in 2010 (Zarzyycki and Polka, 2007).

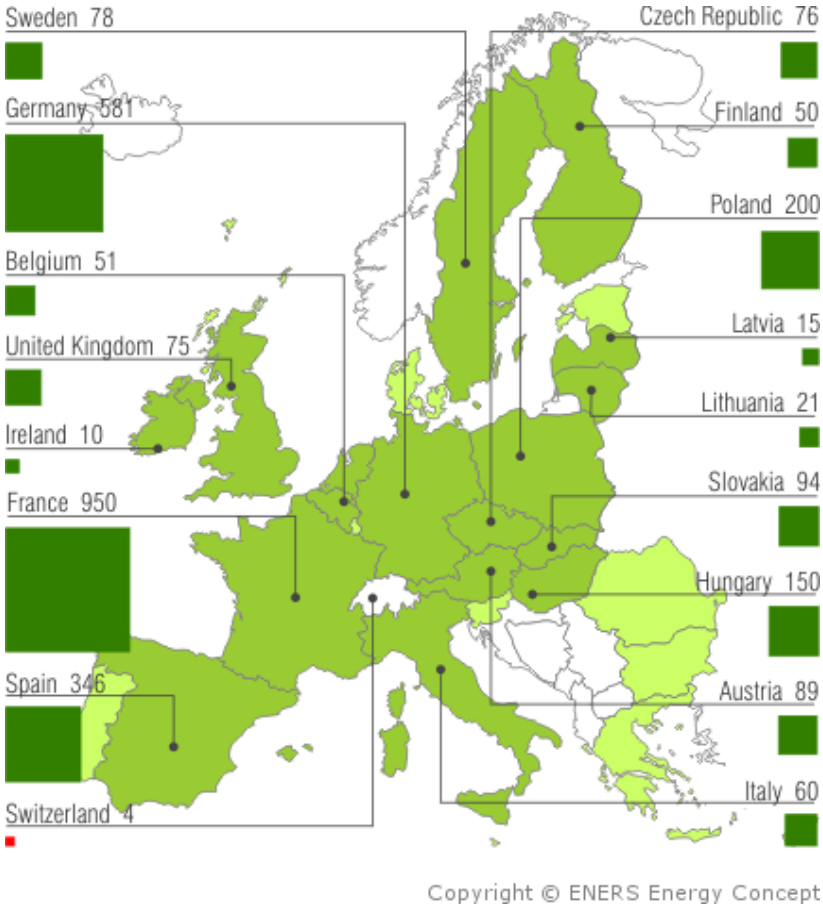

Figure 1.1 *Production of fuel-bioethanol in the EU-27 and Switzerland in 2008 (Ml).*

Table 1.2 shows the evolution of bioethanol production over the past 7 years in the 10 main producing countries in the EU.

Table 1.2 *Evolution of fuel-bioethanol production in the EU (2002-2008).*

Country		Annual production (Ml/yr)						
		2002	**2003**	**2004**	**2005**	**2006**	**2007**	**2008**
FR	France	114	103	101	144	293	539	950
DE	Germany	0	0	25	165	431	394	581
ES	Spain	222	201	254	303	402	348	346
PL	Poland	83	76	48	64	120	155	200
HU	Hungary	0	0	0	35	34	30	150
SK	Slovakia	0	0	0	0	0	30	94
AT	Austria	0	0	0	0	0	15	89
SE	Sweden	63	65	71	153	140	120	78
CZ	Czech Republic	6	0	0	0	15	33	76
UK	United Kingdom	0	0	0	0	0	20	75
-	Others	-0	0	29	49	173	119	216
EU-27	**EU 27**	**488**	**446**	**528**	**913**	**1608**	**1803**	**2855**

As already mentioned, total EU production in 2008 was an estimated 2.8 billion litres, up to 1.8 billion litres in 2007,i.e. a significant increase of 56%, i.e. an average increase of +30% per annum over the period 1992-2008, as reported in Figure 1.2.

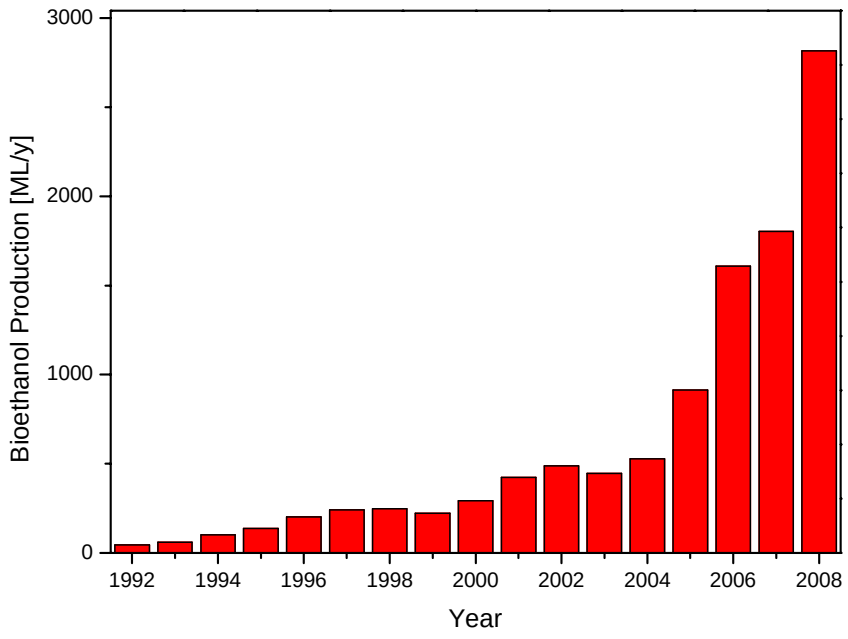

Figure 1.2 *Evolution of bioethanol production in the EU-27 (Adapted from* `www.biofuels-platform.ch`*).*

1.5 Biomass sources for bioethanol

Bioethanol feedstock can be divided into three major groups: (1) sucrose-containing feedstock (e.g. sugar cane, sugar beet, sweet sorghum and fruits), (2) starchy materials (e.g. corn, wheat, rice, potatoes, cassava, sweet potatoes and barley), and (3) lignocellulosic biomass (e.g. wood, straw, and grasses). In the short-term, the production of bioethanol is almost entirely dependent on starch and sugars from existing food crops (Smith, 2008). The drawback in producing bioethanol from sugar or starch is that the feedstock tends to be expensive and demanded by other applications as well and many concerns about major environmental problems, including food shortages and serious destruction of vital soil resources are arisen (Pimental, 2008). Lignocellulosic biomass is envisaged to provide a significant portion of the raw materials for bioethanol production in the medium and long-term due to its low cost and high availability.

The cost levels and comparison of bioethanol yield produced from different energy crops is presented in Table 1.3 (Feasibility study of the Dutch Sustainable Development Group, 2005; Wang, 2002).

Table 1.3 *Comparison of production cost and bioethanol yield from different energy crops.*

Type	Annual yield (ton/ha)	Conversion rate to sugar or starch (%)	Conversion rate to ethanol (l/ton)	Annual ethanol yield (kg/ha)	Cost (US$/m^3)
Sugar cane	70	12.5	70	4900	~160
Cassava	40	25	150	6000	700
Sweet sorghum	35	14	80	2800	200–300
Corn	5	69	410	2050	250–420
Wheat	4	66	390	1560	380–480

(Adapted from Feasibility study of the Dutch Sustainable Development Group (2005)).

About 60% of global bioethanol production comes from sugar cane and 40% from other crops (Dufey, 2006) and (Knauf et al., 2005) before 2003. Brazil utilizes sugar cane for bioethanol production while the United States and Europe mainly use starch from corn, and from wheat and barley, respectively (Linde et al., 2008). During the period 2006–2007, 6.45 million hectares of sugar cane crops were cultivated and around three million hectares were dedicated to bioethanol production, which represents more than 5% of Brazil's arable land (Trostle, 2008). In 2007, approximately 11.4 million hectares were used to provide bioethanol feedstock in the five major producing countries. This would account for about 2.2% of arable land in these countries.

In European countries, beet molasses is the most utilized sucrose-containing feedstock (Cardona and Sanchez, 2007). Sugar beet crops are grown in most of the EU-25 countries, and yield substantially more bioethanol per hectare than wheat (EUBIA, 2007). Starch is a high yield feedstock for bioethanol production (Sanchez and Cardona, 2008) and it is the most utilized

feedstock for bioethanol production in North America and Europe. Corn and wheat are mainly employed with these purposes (Cardona and Sanchez, 2007). Biomass, such as agricultural residues (corn stover and wheat straw), wood and energy crops, is attractive materials for bioethanol fuel production since it is the most abundant reproducible resources on earth. Total potential bioethanol production from crop residues and wasted crops is 491 billion litres per year, about 16 times higher than the current world bioethanol production (Kim and Dale, 2004).

1.6 First generation bioethanol

Current bioethanol, is generally derived from food crops such as sugarcane, sugar beet, maize (corn), sorghum and wheat. (van der Laaka et al., 2007). The vast majority of first-generation biofuel feedstock, especially in the case of bioethanol, constitute comestible materials, which has led to concerns about the fact that biomass previously destined for human consumption may be diverted to fuel production (van der Laaka et al., 2007), thus making food prices increase and also creating competition for water resources in some regions.

The most significant concern, however, relates to the inefficiency of first-generation biofuels. First-generation processes for bioethanol production, in the case of corn and wheat, rely on starch from the kernels of the plant or, in the case of sugar cane and sugar beet, on the sucrose produced (McCormick-Brennan et al., 2007). The remainder has no practical usage for fuel production. Thus, a large amount of energy is used for cultivating, harvesting and processing the biomass, even though only a relatively small proportion is used to derive energy (van der Laaka et al., 2007). The result is an arguably high level of inefficiency and a poor allocation of energy resources throughout. Problematic, too, is that fossil fuels are generally required in the production of biofuels (McCormick-Brennan, 2007) and only limited GHG reduction benefits are provided (with the exception of sugar cane). Biotechnology research, in the future, may alleviate the problems identified here. For example, biofuel yields from corn starch in the United States have increased almost two-fold owing to biotechnological developments and genetic manipulation (McLaren, 2005). Still, it remains to be seen whether these improvements will be more than incremental.

The two main process designs for ethanol production from starch are called wet mill and dry mill. Approximately one third of the starch-to-ethanol plants employ the wet-mill process, and the remaining the dry-mill process. The process schemes for the two configurations are presented in Figure 1.3.

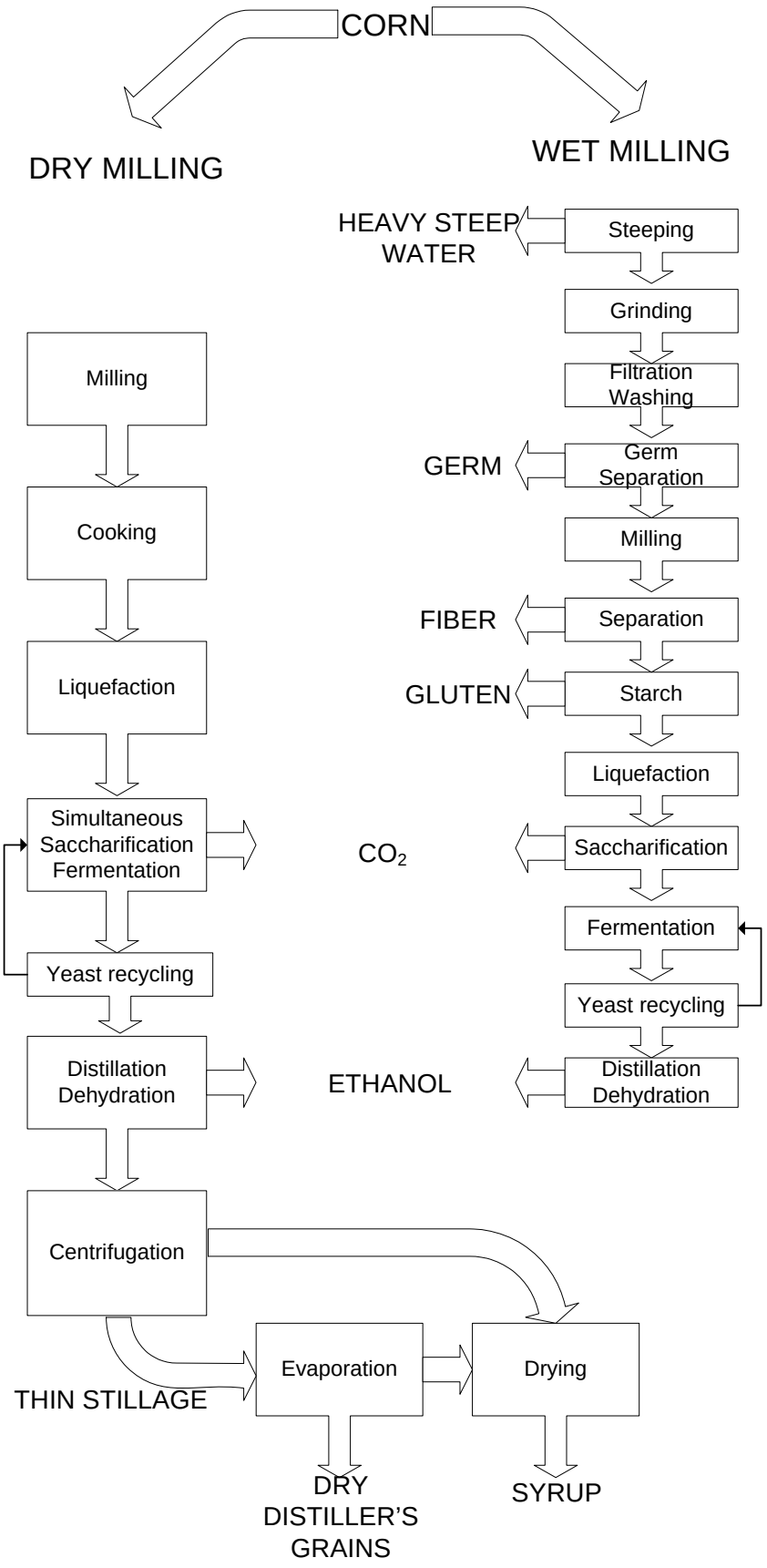

Figure 1.3 *First-generation bioethanol production process.(Adapted from USDOE, 2007).*

In the wet-mill process several products (animal feed, oil and ethanol) are obtained from grain. Separation is achieved by first steeping the corn at an elevated temperature, 49-53°C. The steeping liquor contains SO_2 and the sugars released during steeping are fermented to lactic acid. The steeping liquor softens the hulls of the grain so that the germs, fibres, gluten and starch can be separated in subsequent process steps. The germ can be further processed to give oil, and the gluten is used as animal feed. The starch, which is the main component, is used for ethanol production.
In the dry-mill process, the constituents of the grain are no separated. Instead the whole grain is milled and sieved to flour to increase the penetration depth of the water and increase the surface area accessible to the enzyme in the subsequent process step. Ethanol is the main product and the rest of the material is obtained as DDGS.
The process design for the conversion of starch to ethanol is similar for the wet-mill and the dry-mill processes. The starch or the milled grain is cooked at approximately 90-120°C and liquefied with α-amylases, which hydrolyse α-1,4 glucosidic linkages. However, α-amylases cannot hydrolyse α-1,6 glucosidic linkages, which are more abundant in amylopectin than in amylase, and a subsequent saccharification step is necessary. In the saccharification step, usually performed at 60-65°C, the glycoamylase enzymes release monomeric glucose. The monomeric sugars obtained are then fermented. The saccharification step can be performed simultaneously with fermentation, which reduces the process time, minimises the risk of infection and eliminates end-product inhibition of the enzymes (Jaques et al., 2003; Elander and Putsche, 1996).

1.7 Second generation ethanol

Second-generation biofuels are derived from feedstocks not traditionally used for human consumption. As a result, there is much less concern about the use of these fuels leading to exploitation of food resources. The benefits of using these second-generation biofuels are manifold. Aside from reducing the threat of food supplies being diverted to fuel production, second-generation biofuels be more environmentally friendly and produce less greenhouse gases (GHGs) than first-generation biofuels (Deurwaarder, 2005). Of all the attributes of cellulosic ethanol, its potential to provide very large greenhouse benefits is perhaps the least controversial. The fundamental reasons for this potential are a) the photosynthetic production of biomass removes from the atmosphere the same amount of CO_2 that is returned upon combustion of ethanol and process residues. b) the fossil fuel inputs required for production of cellulosic energy crops are modest (e.g. relative to conventional row crops). c) the energy content of lignin-rich process residues is sufficient to provide all process energy requirements, thereby obviating the need for direct fossil fuels inputs (Lynd, 1996). In addition, the choice of feedstock is wide. (Detchon, 2005). Very valuable and interesting reviews have been published on the theme of fuel ethanol production especially from lignocellulosic biomass (Chandrakant and Bisaria, 1998; Lee, 1997; Lin and Tanaka, 2006; Lynd, 1996; Wyman, 1994; Naik et al., 2009, Brown, 2007).

According to these studies the production of biofuels from lignocellulosic substrates can be achieved through different processing routes. They are:

- Biochemical route: enzymes and other microorganisms are used to convert cellulose and hemicellulose components of the feedstocks to sugar prior to their fermentation to produce ethanol. Lignin is removed and used as fuel for heat and power generation (Foyle et al., 2006; von Blottnitz and Curran, 2007). We will refer to this process as the enzymatic hydrolysis and fermentation process or EHF process.
- Hybrid thermochemical-biological process: pyrolysis/gasification technologies produce a synthesis gas ($CO+H_2$) which can be converted in bioethanol through microbial fermentation (Brown, 2007). This process will be referred to as the gasification and fermentation process or GF process

A third technological options is the indirect gasification and mixed alcohol synthesis: gasification technologies produce a synthesis gas ($CO+H_2$) from which a wide range of long carbon chain biofuels, can be reformed through a catalytic stage (Phillips et al., 2007; Badger, 2002; Naik et al., 2009).

The process steps resemble those for making FT liquids. Clean syngas is passed over a catalyst, forming a mixture of alcohol molecules. A number of different catalysts for mixed alcohol production from syngas were patented in the late 1970s and early 1980s (Nexant Inc., 2005), but most development efforts were abandoned after oil prices fell in the mid-1980s. High oil prices have reignited interest, and the United States Department of Energy recently awarded a substantial grant in support of one commercial-scale demonstration project (17). Several startup companies are developing competing technologies (Nexant Inc., 2005; Aden et al., 2005; `www.rangefuels.com, www.powerenergy.com, www.novafuels.com, www.syntecbiofuel.com`).

National Renewable Energy Laboratory in April 2007 delivered a report reporting process design and technoeconomic evaluation of the conversion of biomass to ethanol via these thermochemical pathways that are expected to be demonstrated at the pilot-unit level by 2012. Indirect steam gasification was chosen as the technology around which this process was developed based upon previous technoeconomic studies for the production of methanol and hydrogen from biomass.

This conversion route was however disregarded in this thesis since, aside from patents and patent applications, relatively little published information is available concerning these private-sector activities.

1.7.1 Lignocelluloses biomass composition

1.7.1.1 Cellulose

As it is the major component in the cell wall of living plant cells, cellulose is by far the most abundant macromolecule on earth (Brown, 2004).Cellulose is a homopolyssaccharide consisting of anhydrous glucose units connected with β-1,4 bonds. The length of the linear cellulose chain varies between 2000 and 20000 linked glucose, depending on the different sources, with the disaccharide

cellobiose as the basic repeating unit (Figure 1.4). Cellulose chain are completely linear and have a strong tendency to form intra e inter molecular hydrogen bonds. In fact cellulose chain with a degree of polymerization (DP) over 6-8 are insoluble in water. Bundles of cellulose chains are aggregated together in the form of microfibrils. It is hydrogen bonds in cellulose that make it rigid and difficult to degrade (Zhang and Lynd, 2004; Fengel and Wegener, 1989). Microfibrils have highly ordered (or crystalline) regions altered with less ordered (or amorphous) regions.

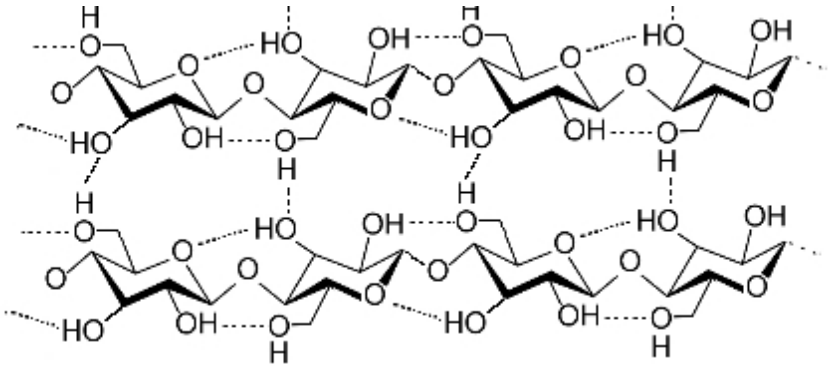

Figure 1.4 *Cellulose structure.*

1.7.1.2 Hemicellulose

The generic term *hemicellulose* comprises a group of highly branched heterogeneous polysaccharides, present in lignocellulosic materials, with degree of polymerization of 200 (Saha, 2003), i.e. much lower than cellulose (Figure 1.5). Hemicellulose is more hydrophilic and is also easier to degrade by acids into the monomeric components than cellulose. This is used in several pre-treatments methods to increase the accessible surface area of the substrate and make it available to enzymatic attack. Hemicellulose links covalently to lignin and through hydrogen bonds to cellulose. It contains a diversity of monosaccharide units, such as the hexoses glucose, galactose and mannose, and the pentoses xylose and arabinose. The composition differs depending on the origin. Especially in hardwood, the majority (60-70%) of xylose units are acetylated, i.e. some of the OH groups at C2 and C3 of the xylose units are replaced by O-acetyl groups (Shimizu, 1991; Fengel and Wegener, 1989). These are released as acetic acid when the material is hydrolysed.

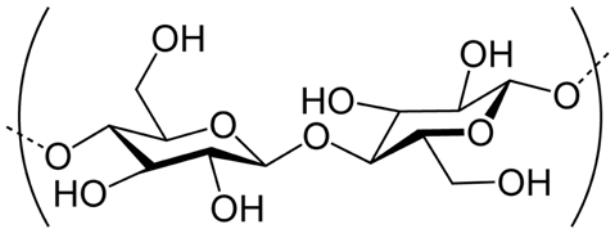

Figure 1.5 *Hemicellulose structure.*

1.7.1.3 Lignin

Lignin is a highly complex, three-dimensional polyphenolic compound, which is closely attached to cellulose and hemicellulose. Together with cellulose it gives the plants their remarkable strength. Research aimed to fully understand the structure of lignin has been under way for a long time but has proven to be difficult. The chemical structure of lignin, based on many complex carbon-carbon linkages, makes it very resistant to enzymatic or chemical degradation, and it is thought to play an important role in a plant defence against biological attack (Fan et al., 1982; Fengel and Wegener, 1989; Lee, 1997). The most common functional groups in lignin are methoxyl, aliphatic hydroxyl, phenolic hydroxyl and carbonyl groups (Figure1.6). Fraction of lignin can be extracted by both alkali (e.g. sodium hydroxide) and organic solvents (e.g. dioxane) but also partly (hardwood lignin) in acid. The solubility of lignin by solvents is also used in pretreatment methods for the EHF process. An example of this is in the ammonia fiber explosion method. Successful pretreatments often redistribute the major wood components into separate particles and by that action increase the accessible cellulose surface and decrease the surface of lignin.

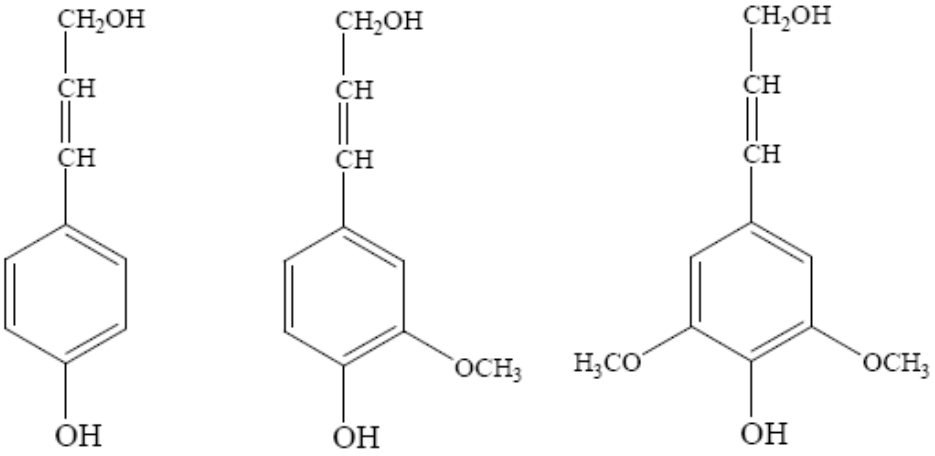

Figure 1.6 *The three precursors of lignin. From left to right: p-coumaryl alcohol, coniferyl alcohol and sinapyl alcohol.*

1.7.1.4 The composition of feedstock

Typical carbohydrate and lignin contents of some lignocellulosic materials are reported in Table 1.4. The values should be considered representative, but can differ quite significantly for each material due to environmental (region, weather, soil type) and genetic variability. The materials are categorised as softwood, hardwood or agricultural residues, not only due to their visual appearance but, more importantly, due to the general composition differences between these groups. Softwood generally has higher lignin content. The composition and the distribution of lignin within the wood cells differ compared to the other groups. So does the association of cellulose and hemicellulose to the lignin. As a consequence of these differences, softwood is more recalcitrant to degradation and more resistant to enzymatic hydrolysis (Grethlein et al., 1984 and Ramos et al., 1992). In all materials the most common carbohydrate is glucan, which makes up the cellulose and may also be present in hemicellulose. The hemicellulose in softwood is reach in mannan, whereas xylan dominates the hemicellulosic fraction of hardwood and agricultural residues.

Table 1.4 *Typical carbohydrate and lignin contents of some lignocellulosic materials.*

	Glucan	Galactan	Mannan	Xylan	Arabinan	Lignin	Ref
Softwood							
Spruce	46.5	1.7	13.5	8.3	1.2	27.9	Söderström et al, 2002
Radiata pine	42.8	2.5	11.3	5.9	1.6	27.2	Wiselogel et al., 1996
Hardwood							Wiselogel et al., 1996
Beech	42.9	n.r	0.9	20.8	1.5	26.2	Vinzant et al., 1994
Yellow poplar	49.9	1.2	4.7	17.4	1.8	18.1	Sassner, et al., 2007
Salix	43.0	2.0	3.2	14.9	1.2	26.6	
Agricultural residues							
Sugar cane bagasse	40.2	1.4	0.5	22.5	2.0	25.2	Neureiter et al., 2002
Corn stover	36.8	2.9	-	22.2	5.5	23.1	Öhgren et al., 2005
Barley straw	37.1	-	n.r.	21.4	3.1	19.5	Linde et al., 2006

1.8 Enzymatic hydrolysis and fermentation process

The first process is possibly the most mature process for the transformation of lignocellulosic materials into ethanol. It includes five main steps: biomass pretreatment, cellulose hydrolysis, fermentation of hexoses, separation and effluent treatment (Figure 1.7). Furthermore, detoxification and fermentation of pentoses released during the pretreatment step can be carried out. The key process steps will be discussed hereafter, following the here presented order. This process has been extensively described and studied (e.g., Wooley et al., 1999a and 1999b, Lynd et al., 1996, Hahn-Hägerdal et al., 2006), and pilot plants and pre-industrial facilities have recently being brought to operation. In the literature, several flowsheeting designs have been reported: for instance, Wooley

et al. (1999a and 1999b) describe the global process for ethanol production from wood chips and Cardona and Sanchez (2006) use a process simulator to assess the energy consumption for several process configurations; other works have analysed the techno-economic performance of the production process (Lynd et al., 1996; McAloon et al., 2000, Hamelinck et al., 2005).

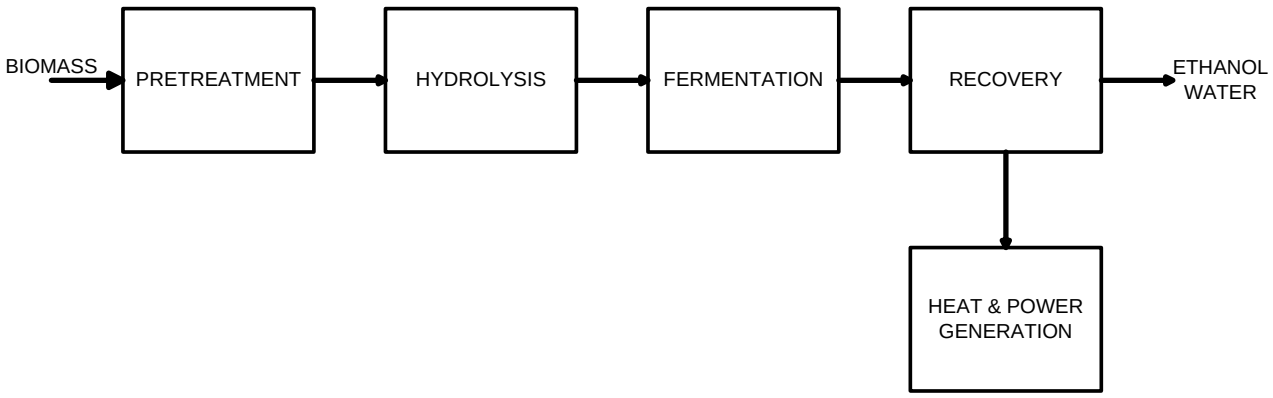

Figure 1.7 *The enzymatic hydrolysis and fermentation (EHF) process for bioethanol production.*

1.8.1 Pretreatment

Effective pretreatment should disrupt the shielding action of lignin and the hemicellulose on the cellulose to increase accessibility of the enzymes. Pretreatment should provide a high concentration and recovery of cellulose and hemicellulose sugars at low cost. The production of degradation product must be low and the pretreatment method must result in high recovery of lignin for further utilization as either chemical feedstock or solid fuel (Nguyen and Saddler, 1991).

Pretreatment can be performed in several different ways, including physical, biological, and chemical treatment or a combination of these. Over the years a number of thorough reviews of pretreatment methods have been published (Fan et al., 1982; Sun and Cheng, 2002; Duff and Murray, 1996; Mosier et al., 2005). An optional mechanical pretreatment of comminution, including dry, wet, and vibratory ball milling (Millett et al., 1979; Rivers and Emert, 1987), and compression milling (Tassinari et al., 1982) is sometimes needed to make material handling easier through subsequent processing steps. Physical pre-treatment methods use steam explosion or liquid hot water (LHW). Steam explosion is one of the most promising methods to make biomass more accessible to cellulase attack (Szengyel, 2000). The material is heated using high-pressure steam (20–50 bar, 210–290 1C) for few minutes; these reactions are then stopped by sudden decompression to atmospheric pressure.

The LHW process uses compressed, hot liquid water (at pressure above saturation point) to hydrolyse the hemicellulose. Development of the LHW process is still in laboratory stage.

Common chemical pre-treatment methods use dilute acid (Wooley et al., 1999a and 1999b, and Sun and Cheng, 2002), alkaline (US DOE. Advanced bioethanol technology), ammonia (Dale, 1986), organic solvent (Botello et al., 1999). Biological pre-treatments use fungi to solubilise the lignin (Graf and Koehler, 2000). Biological pretreatments have the advantages of low energy use and mild environmental conditions; however, the very low hydrolysis rate presently impedes the implementation (Sun and Cheng, 2002).
Several pre-treatment processes combine physical and chemical elements: acid catalyzed steam explosion (see § 1.9.1.1), ammonia fibres explosion (AFEX), CO_2 explosion (Sun and Cheng, 2002).

1.8.1.1 Steam explosion acid catalyzed

Steaming of wood and other kind of cellulose-containing materials has been thoroughly examined throughout the years. Some of the major reasons for this are its relative cheapness, its harmlessness to humans and the possibility of avoiding chemicals. The idea of using steam pretreatment prior to enzymatic hydrolysis stems from the early investigations of Mason in 1927 (Mason, 1927). He found that heating wood chips to high temperature, by means of saturated steam and sudden release of pressure in the vessel, resulted in a brownish fibre mix, which resulted very sensitive to enzymes (Jusarek ,1979; Mac Donald and Mathews, 1979). Michalowicz et al. (1991) showed that the accessibility of enzymes increased from 30% for the untreated material up to more than 70% when the material is soaked in H_2SO_4 and then steam treated. Impregnation of aspen chips with SO_2 and H_2SO_4 before steam treatment was investigated by Mackie (1985). Both acid catalysts improved the recovery of pentose sugars substantially compared with non-acid-treated substrate. They considered 210°C to be the optimal temperature, since a 90% recovery of pentosans is possible in the subsequent washing.
These conditions also solubilise some of the lignin in the feedstock and “expose” the cellulose for subsequent enzymatic hydrolysis. A small portion of the cellulose is converted to glucose. In addition, acetic acid is liberated from the hemicellulose hydrolysis. Degradation products of pentose sugars, primarily furfural, and hexose sugars, primarily hydroxymethyl furfural (HMF), are also formed.
Acid catalysed steam explosion is one of the most cost-effective processes for hardwood and agricultural residues, but it is less effective for softwoods. Limitations include destruction of a portion of the xylan fraction, incomplete disruption of the biomass structure, and generation of compounds that may inhibit microorganisms used in downstream processes. (Hamelinck et al., 2005).

1.8.2 Enzymatic hydrolysis

A large variety of microorganisms naturally produce enzymes that degrade lignocellulosic materials in order to provide substrate for their own survival. Cellulose- and hemicellulose-degrading enzymes are often grouped into cellulases and hemicellulases, respectively. The material after

pretreatment is hydrolyzed with a cocktail of enzymes to further degrade the cellulose and hemicellulose to obtain the desired monomeric glucose. The most commonly used and commercialized enzymes cocktails for lignocellulosic degradation are obtained from the fungus *Trichoderma reesei*. Cellulose is degraded by three classes of enzymes: cellobiohydrolases, endoglucanases and β-glucosidases. Figure 1.8 illustrates how enzymes hydrolyze cellulose. Endoglucanases cut the cellulose chain, preferably at the amorphous regions, while cellobiohydrolase attack the end of the cellulose chain.

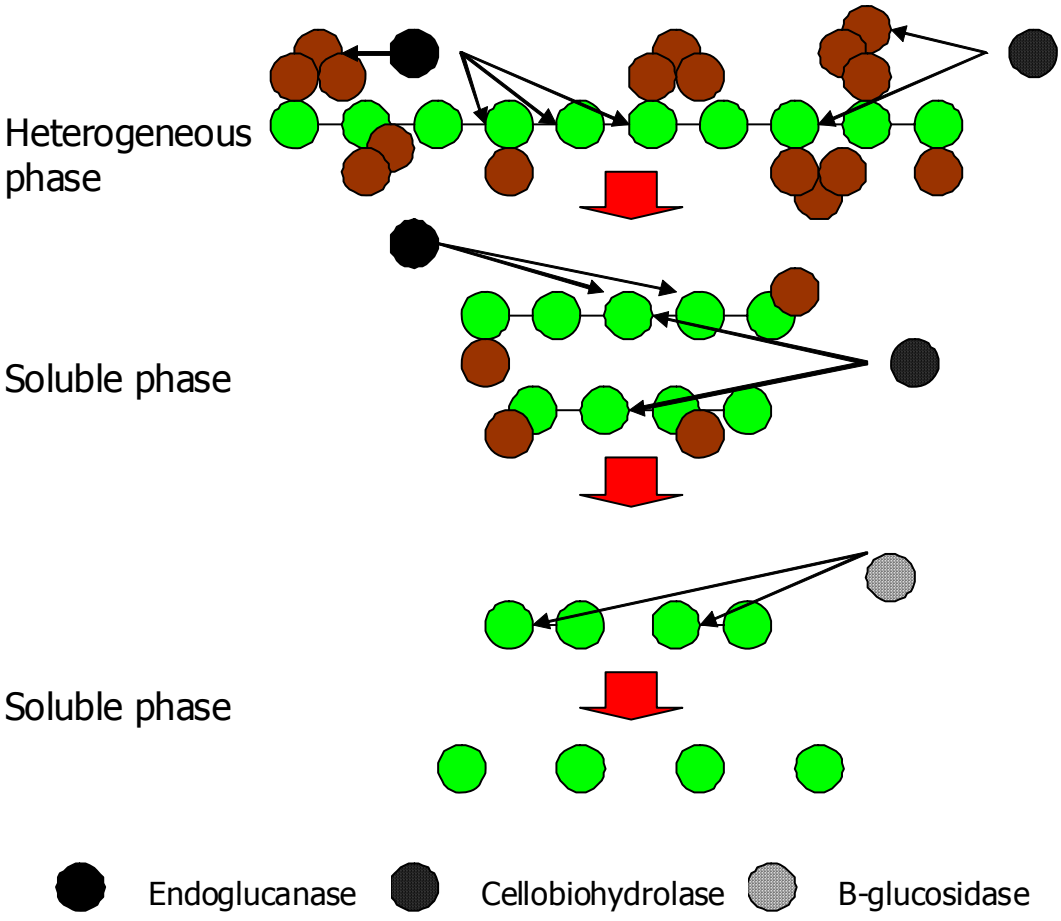

Figure 1.8 *Enzymatic hydrolysis mechanism.*

Cellobiohydrolases and endoglucanases together depolymerise cellulose to cellobiose. The cellobiose is then hydrolyzed to monomeric glucose units by β-glucosidases.

Different microorganisms secrete various ratios of specific enzymes. *Trichoderma reesei* secretes mainly endoglucanases and cellobiohydrolases but is deficient in β-glucosidase, which should be supplemented to avoid the accumulation of cellobiose, causing end-product inhibition. β-glucosidase could be produced by the microorganism *Aspergillus niger*.

The rate of hydrolysis by a specific enzyme cocktail differs depending on the substrate. In lignocellulosic materials the cellulose is highly crystalline and surrounded by hemicellulose and

lignin, thus making it recalcitrant to the enzymatic attack. One goal of the pretreatment step is to enhance the rate of hydrolysis by increasing the accessibility of the enzyme. Initially, enzymatic hydrolysis is fast, but the rate slows down as the amorphous areas of cellulose decrease and the number of free chain-ends decreases. Additionally, the rate of hydrolysis is affected by the thermal and mechanical deactivation of the enzymes (Zhang and Lynd, 2004, Gregg and Saddler, 1996).
To improve the yield and rate of the enzymatic hydrolysis, research focuses both on enhancing enzyme activity in distinctive hydrolysis and fermentation process steps (Sun and Cheng, 2002), as well as combining the different steps in fewer reactors (discussed in § 1.9.4).
Nowadays enzymes are expensive and constitute a significant contribution to the overall cost of ethanol production (Sassner et al., 2007).

1.8.3 Fermentation

A variety of microorganisms, generally either bacteria, yeast, or fungi, ferment carbohydrates to ethanol under oxygen-free conditions. According to the reactions, the theoretical maximum yield is 0.51 kg ethanol and 0.49 kg carbon dioxide per kg sugar:

$$3C_5H_{10}O_5 \rightleftarrows 5C_2H_5OH + 5CO_2 \tag{1.1}$$

$$C_6H_{12}O_6 \rightleftarrows 2C_2H_5OH + 2CO_2 \tag{1.2}$$

All microorganisms have limitations: for example they process both pentoses and hexoses, or they co-produce of cell mass at the cost of ethanol yield. Furthermore, the oxygen free condition of fermentation slowly exterminates the microorganism population (Lynd, 1996). Therefore, in the early processes, the different sugars were fermented in different sequential reactors. There is a tendency towards combining reaction steps in fewer reactors in order to avoid hydrolysis intermediate inhibitive products, to reach higher yields. Genetic engineering and new screening technologies are devoting a great effort to bring bacteria and yeast capable of fermenting both glucose and xylose (US DOE), with improved efficiency (higher fermentation rates) and resistance to high temperatures, and requiring a less intense detoxification of the hydrolysate(Wooley et al, 1999b and Graf and Koehler, 2000).

1.8.4 Integration options

Enzymatic hydrolysis performed separately from the fermentation step is known as separate hydrolysis and fermentation (SHF). Cellulose hydrolysis carried out in the presence of the fermentative microorganism is referred to as simultaneous saccharification and fermentation (SSF). The key of the SSF of biomass is its ability to rapidly convert the sugars into ethanol as soon as they are formed thus diminishing their accumulation in the medium. Bearing in mind that the sugars are much more inhibitory for the conversion process than ethanol, SSF can reach higher rates, yields and ethanol concentrations with respect to SHF (Wyman et al., 1992). SSF offers an easier

operation and a lower equipment requirement than the sequential process since no hydrolysis reactors are needed; moreover, the presence of ethanol in the broth makes that the reaction mixture less vulnerable to the action of undesired microorganisms (Wyman, 1994). Nevertheless, SSF has the inconvenient that the optimal conditions for hydrolysis and fermentation are different, which implies a difficult control and optimization of process parameters (Claassen et al., 1999); in addition, larger amounts of exogenous enzymes are required. (Cardona and Sanchez, 2007). The concept of SSF process was first described by Takagi et al. (1977). Since that time, after the technology had been patented (Gauss et al., 1976), the duration of the batch process have decreased from 14 d required for the conversion of 70% of cellulose into ethanol with final concentrations of 20 g/L, to 3–7 d needed for reaching 90–95% conversions with final ethanol concentrations of 40–50 g/L (Wyman, 1994).

Simultaneous saccharification of both cellulose (to glucose) and hemicellulose (to xylose and arabinose) and co-fermentation of both glucose and xylose (SSCF) would be carried out by genetically engineered microbes that ferment xylose and glucose in the same broth as the enzymatic hydrolysis of cellulose and hemicellulose. Actual SSCF process has been demonstrated in the case of ethanol production from yellow poplar through a benchscale integrated process that included the dilute-acid pretreatment of feedstock, conditioning of hydrolyzate for fermentation, and a batch SSCF (McMillan and Newman, 1999). In this case, the recombinant *Z. mobilis* assimilating xylose was used. SSCF is the process on which is based the technology designed as a model process by the NREL for the production of fuel ethanol from aspen wood chips (Wooley et al., 1999a). In this design, the utilization of recombinant *Z. mobilis* exhibiting a glucose conversion to ethanol of 92% and a xylose conversion to ethanol of 85% is assumed.

1.8.5 Separation and cogeneration

Ethanol is recovered from the fermentation broth by distillation combined with molecular sieve adsorption (Gulati et al., 1996; Ladisch and Dyck, 1979; Ladisch et al., 1984). The residual lignin, unreacted cellulose and hemicellulose, ash, enzyme, organisms, and other components end up in the bottom of the distillation column. Due to the relative high costs of ethanol from biomass and other feedstocks, different strategies are being developed for making the process more profitable. In the specific case of lignocellulosic biomass, the thermal conversion of non-fermentable lignin produced as a by-product can provide the energy required by the entire process remaining a surplus that can be commercialized in form of electricity. This is possible due to the high energy value of the lignin (29.54 MJ/kg) that is released during its combustion. To generate electricity and heat, at small scale (up to30MWe) a boiler with steam turbine has been proposed as a viable options (Hamelinck et al., 2005)

Reith et al. (Reith et al., 2002) point out that, at larger scale, the use of BIG/CC (Biomass Integrated Gasification Combined Cycle) technology for the thermal conversion of the non-fermentable residues can supply all the steam and electricity needed by the biomass-to-ethanol process. In

addition, the electricity surplus can be sold to the grid giving a total system efficiency of 56–68%. In this case, the cogeneration of steam and electricity is crucial for obtaining a competitive process. New trends in process engineering of bioethanol are aimed at producing co-products other than fuels that contribute to balance the economy of the global ethanol production process. In this way, many materials generated during the process and considered as wastes could become valuable and marketable co-products. Typical co-products are shown in Table 1.5 (Cardona and Sanchez, 2007).

Table 1.5 *Bioethanol production and land use by major producing countries, 2006/07.*

Co-product	Stage where co-product is formed	Application	Remarks	References
Xylitol	Xylose solutions obtained during pretreatment of lignocellulosic biomass can be converted into xylitol by chemical or biotechnological means; co-culture of *Saccharomyces cerevisiae* and *Candida tropicalis*	Anticariogenic sweetener, sugar substitute for diabetics	US$7/kg xylitol	Converti and Del Borghi (1996), Latif and Rajoka (2001), Leathers (2003), Saha (2003)
2,3-butanediol	Arabinose and xylose solutions obtained during pretreatment of lignocellulosic biomass especially corn fiber) can be converted into 2,3-butanediol by bacteria	Chemical feedstock as a precursor of synthetic polymers and resins		Saha (2003)
CMA	Xylose solutions obtained during pretreatment of lignocellulosic biomass can be converted into acetic acid by fermentation using *Clostridium thermoaceticum*	Road deicer	Stillage could be used to supply nutrients for fermentation process	Bungay and Peterson (1992), Wilkie et al. (2000)
Furfural	Xylose solutions obtained during pretreatment of lignocellulosic biomass can be converted into furfural	Valuable chemical	US$1580/ton furfural	Kaylen et al. (2000)
Single cell protein	Xylose solutions obtained during pretreatment of lignocellulosic biomass can be utilized for growing *Candida utilis*	Animal feed		Ghosh and Ghose (2003)
Unaltered lignin	Delignification of biomass by solvent pretreatment	Fuel additive	US$200/ ton	Ghosh and Ghose (2003)
Pelletized hydrolysis residue	Dilute acid pretreatment of wood	Fuel pellets for residential appliances (stoves, burners)		Öhman et al. (2006)
Lignin	Fractionation of pretreated biomass or centrifugation of stillage	Raw material for production of adsorptive materials by chemical modification		Dizhbite et al. (1999)

1.8.6 State of the art of commercial ethanol plants

While significant milestones have occurred in the laboratory, cellulosic ethanol has yet to be produced on a commercial scale.

The transition of lignocellulosic fuel ethanol production into a mature industrial technology requires further research and development efforts in these areas:

Biotechnology issues

- Improving enzymatic hydrolysis with efficient enzymes, reduce enzymes production cost and novel technology for high solids handling
- Developing robust fermenting organisms, which are more tolerant to inhibitors and ferment all sugars in the raw material in concentrated hydrolysates at high productivity and with high ethanol concentration

Engineering issues

- Design of more effective pre-treatment
- Extending process integration to reduce the number of process steps and the energy demand and to re-use process streams to eliminate the use of fresh water and to reduce the amount of waste streams
- Reducing separation costs
- Control and optimisation of process parameters
- Supply chain issues

As a result of these open issues no lignocellulosic bioethanol commercial plant is available nowadays, even if several near-term commercial facilities projects are being developed in the recent years (Table 1.6). Nevertheless, as the economic analysis (Aden et al., 2002) of the cellulosic bioethanol process shows that reliable cost estimations require laboratory results are verified in pilot and demonstration plant, where all steps are integrated into a continuous process, a number of these pre-commercial facilities have being spreading throughout the world (Table 1.7). This plant scale provides the possibility to explore the benefits of process integration to reduce the number of process steps and the energy demand, and to recirculate process streams to eliminate the use of fresh water and to reduce the amount of waste streams

Table 1.6 *Near-term cellulosic ethanol commercial plants, capacity in* $m^3\ year^{-1}$.

Company	Location	Feedstock	Capacity	Date
Bioethanol Japan Kansai	Sakai, Japan	Construction wood residues	$1.4–4.0\times10^3$	2007
Abengoa Bioenergy & SunOpta	Babilafuente, Spain	Wheat straw (co-located w/grain ethanol Wheat straw (co-located w/grain ethanol plant)	5.0×10^3	2007
Iogen	Shelley, ID	Wheat, barley and rice straw	110×10^3	2008
Xethanol & Spring Hope	Spring Hope, NC	Hardwood chips, wood residues, other	130×10^3	2007

BioFuels Xethanol & Coastal	Augusta, GA	Wood residues, other	190×10^3	2007
Maui Ethanol	Kauai, HI	Bagasse	45×10^3	2007
Dedini	Brazil	Bagasse	20×10^3	2007
Colusa Biomass Energy	Colusa, CA	Rice straw and hulls, corn stover	38×10^3	2007
Future Fuels	Toms River, NJ	Wood residues, other	200×10^3	2008
Genahol	Orrville, OH	Municipal garbage	15×10^3	2008
Pencor-Masada OxyNol	Middletown, NY	Municipal garbage	34×10^3	2008

Source: (Solomon et al., 2007)

Table 1.7 *Cellulosic ethanol pilot and demonstration plants.*

Company	Location	Feedstock	Capacity or feed rate	Start date
Pilot plants				
Iogen	Ottawa, Canada	Wood chips	9.0×10^2 kg day^{-1}	1985
Iogen	Ottawa, Canada	Wheat straw	9.0×10^2 kg day^{-1}	1993
Masada/TVA	Muscle Shoals, AL	Wood	NA	1993
SunOpta	Norval, Canada	Various (non-woody)	4.5×10^2 kg h^{-1}	1995
Arkenol	Orange, CA	Various	9.0×10^2 kg day^{-1}	1995
Bioengineering Resources	Fayetteville, AR	Softwood & bark	NA	1998
NREL/DOE	Golden, CO	Corn stover, others	9.0×10^2 kg day^{-1}	2001
Pearson Technologies	Aberdeen, MS	Wood residues, rice straw	27 Mg day^{-1}	2001
NEDO	Izumi, Japan	Wood chips	3.0×10^2 l day^{-1}	2002
Dedini	Pirassununga, Brazil	Bagasse	1600 m^3 year^{-1}	2002
Tsukishima Kikai Co.	Ichikawa, Chiba, Japan	Wood residues	9.0×10^2 kg d^{-1}	2003
Etek EtanolTeknik	Ornskoldsvik, Sweden	Spruce sawdust	5.0×10^2 l day^{-1}	2004
PureVision	Ft. Lupton, CO	Corn stover, bagasse	9.0×10 kg day^{-1}	2004
Universal Entech	Phoenix, AZ	Municipal garbage	1.0×10^2 l day^{-1}	2004
Sicco A/S	Odense, Denmark	Wheat straw	1.0×10^2 kg h^{-1}	2005
Abengoa Bioenergy	York, NE	Corn stover (co-located with grain ethanol plant)	2000 m^3 year^{-1}	2006
Iogen	Ottawa, Canada	Wheat, oat and barley straw	3000 m^3 year^{-1}	2004

ClearFuels Technology	Kauai, HI	Bagasse and wood residues	11,400 m^3 $year^{-1}$	2007
Celunol	Jennings, LA	Bagasse, rice hulls (co-located with grain ethanol plant)	5000 m^3 $year^{-1}$	2007
Etek EtanolTeknik	Sweden	Softwood residues (spruce and pine)	30,000 m^3 $year^{-1}$	2009

Source: (Solomon et al., 2007)

1.9 The gasification-fermentation process

Thermochemical processing of biomass to produce substrates suitable for fermentation is a relatively new approach to bioethanol production. A number of microorganisms are able to utilize the gaseous compounds resulted from biomass gasification as substrates for growth and production. Among the fermentation products are carboxylic acids, alcohols, esters, and hydrogen.
A block diagram for the gasification-fermentation (GF) process for bioethanol production is sketched in Figure 1.9.

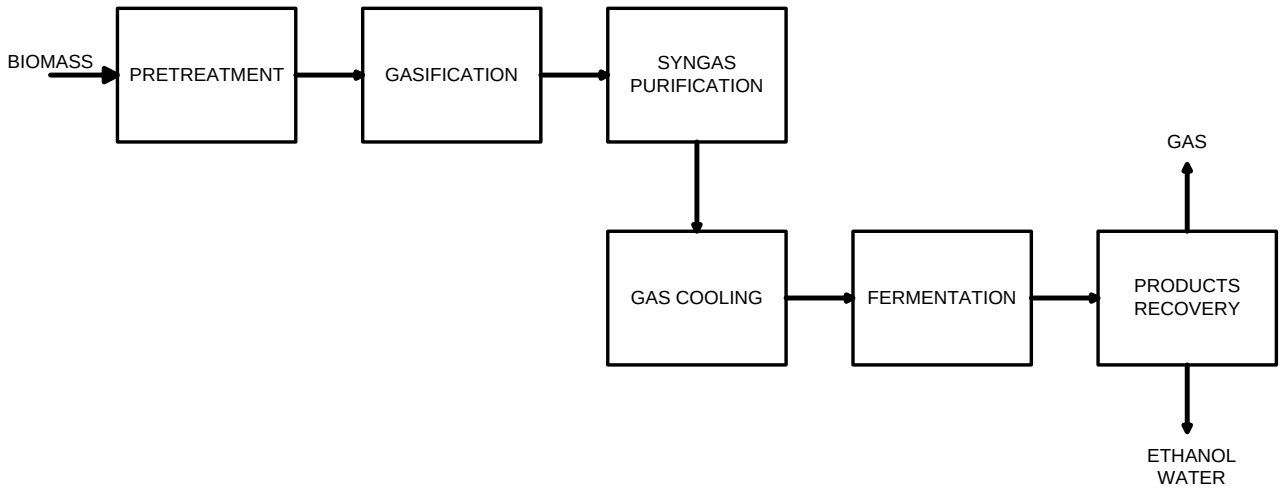

Figure 1.9 *The thermochemical/biological process for bioethanol production.*

This process has been somehow neglected in the scientific literature (at least when compared to the EHF process), notwithstanding the promising results demonstrated in the few works appeared in the literature (e.g. Datar et al., 2004; Brown, 2007). The reason for this is easy to understand: the original feedstock of the fermentation industry were naturally occurring sugars and starches that

easily hydrolyzed to sugar. The fact that both starch and cellulose are both polymers of glucose encouraged similar approaches to depolymerising these two carbohydrates. In fact, cellulose is not only more recalcitrant than starch but it is embedded in a matrix of lignin, which makes the process of releasing sugar from lignocellulose much more difficult than for starch. Considering these difficulties, hybrid thermochemical/biological approaches to bio-based products deserves increased attention. Although biomass gasification has long been studied (Bridgwater, 1995), its integration with the fermentation process has been studied only in few reports (Mississippi Ethanol LCC, 2002; BRI Energy, 2006). However, the technology potential (which is already available as a commercial process) has nonetheless been widely recognised (Ragauskas et al, 2006) and recently awarded through financing by the U.S.A Department of Energy. The syngas route, by transforming all plant constituents into CO and H_2, is attractive for its efficient use of biomass. The process has an advantage over cellulose hydrolysis since it is able to process a wider variety of substrates. In a comprehensive review on the prospects for ethanol from cellulosic biomass, Lynd (1996) noted that syngas fermentation represents and "end run" with respect to acid or enzymatic hydrolysis of biomass because it avoid the costly and complicated steps of extracting monosaccharide from lignocellulose. It also has the potential for being more energy efficient because it effectively utilizes all the constituents of the feedstock, whether cellulose, hemicellulose, lignin, starch, oil or protein.

Syngas fermentation also presents some advantages if compared with the use of inorganic catalyst in the production of synthetic fuels (Grethlein and Jain, 1993). Most catalysts used in the petrochemicals industry are readily poisoned by sulphur-bearing gases whereas gas-consuming anaerobes are sulphur tolerant. In conventional catalytic processing, the CO/H_2 ratio of the syngas is critical to commercial operations whereas biological catalyst are not sensitive to this ratio; indeed, the water-gas shift reaction is implicit in the metabolism of autotrophic and unicarbonotrophic anaerobes. Gas phase catalysts typically use temperature of several hundreds of degree Centigrade and at least 10 atm whereas syngas fermentation proceeds at near ambient conditions. Finally biological catalysts tend to be more product specific than inorganic catalysts.

Nevertheless, as described by Grethlein and Jain (1993), syngas fermentation has several barriers to overcome before it can be commercialized. For instance, the rate is low, yield is limited and there are difficulties in avoiding product inhibition by acids and alcohols, and issues at guaranteeing an acceptable mass transfer rate from the gas to the liquid phase. A study by Worden and coworkers (Worden et al., 1997) give encouragement that the use of nontoxic surfactants and novel dispersion devices can enhance mass transfer through the generation of microbubbles to carry syngas into bioreactors (see §1.10.2).

1.9.1 Gasification

Gasification is the high temperature conversion of solid, carbonaceous fuels into flammable gas mixtures, sometimes known as synthesis gas or syngas, consisting of CO, H_2, CO_2, methane, nitrogen and smaller quantities of higher hydrocarbons. Gasification is best performed with pure oxygen in order to decrease the size of the equipment via reducing the load of nitrogen. For the production of ethanol only CO, CO_2 and H_2 are interesting gases. The other hydrocarbon gases will not ferment or in the worse case will even inhibit the fermentor bacteria. This fact already limits the choice of the gasifier operating conditions because the maximum of yield of CO and H_2 can be thermodynamically achieved at high temperature, higher than 1000°C. High temperature gasifying system are therefore needed. The most important reactions that take place in the reduction zone of gasifier between different gaseous and solid reactants are given below.

$$C + CO_2 \rightleftarrows 2CO \qquad \Delta H_1 = 164.9 kJ/mol \qquad (1.3)$$

$$C + H_2O \rightleftarrows CO + H_2 \qquad \Delta H_2 = 122.6 kJ/mol \qquad (1.4)$$

$$C + 2H_2 \rightleftarrows CH_4 \qquad \Delta H_3 = -74.8 kJ/mol \qquad (1.5)$$

$$C + 3H_2 \rightleftarrows CH_4 + H_2O \qquad \Delta H_4 = -205.9 kJ/mol \qquad (1.6)$$

As reaction 1.3 and 1.4 requires heat, the gas temperature will decrease during reduction. Part of the feed can be used to heat up the gasifier through combustion.
Reaction 1.5 and 1.6 are unwanted side reactions, which produce components not useful in the rest of the process. They must be inhibited as much as possible by choosing the right process conditions.

1.9.2 Fermentation

Several acetogenic microbes are capable of metabolizing cleaned syngas into ethanol. Two of the more promising strains are described below.
Butyribacterium methylotrophicum is a gram-positive, motile, rod-shaped anaerobic bacterium, which grows on a wide variety of substrates, including glucose, formate and methanol, H_2 and CO_2, and CO. The products achieved are acetic acid, butyric acid, ethanol and butanol. Unfortunately, the yield in butanol, and especially ethanol, is usually low.
The second clan of bacteria belongs to the clostridium species which were isolated from chicken waste and demonstrated to grow well on syngas to produce acetate and ethanol. The first optimization of these species resulted in an approximate 1:1 ratio of ethanol and acetate under optimal conditions. The *Clostridium ljungdahlii* is a gram-positive, motile, rod-shaped anaerobic bacterium, which converts CO, H_2 and CO_2 into a mixture of acetate and ethanol. The ratio of these products can be adjusted by pH. When the pH is lowered to 4 the ratio ethanol:acetate becomes 3:1. Further medium adjustments has reportedly nearly insignificant acetate production and led to an ethanol concentration of 48 g/L (approximately 1mol/L) on day 25 when using an optimised medium.

Clostridium carboxidovorans is a gram-positive, motile, rod-shaped anaerobic bacterium, which converts CO, H_2 and CO_2 into a mixture of acetate, butanol and ethanol. The ratio ethanol:butanol:acetate is 6:3:1 in absence of hydrogen.
Bacterial fermentation of CO, CO_2 and H_2 using *Clostridium ljungdahlii* follows the pathway reactions:

$$6CO + 3H_2O \rightleftarrows C_2H_5OH + 4CO_2 \qquad \Delta G=-216kJ/mol \qquad (1.7)$$

$$6H_2 + 2CO_2 \rightleftarrows C_2H_5OH + 3H_2O \qquad \Delta G=-97kJ/mol \qquad (1.8)$$

1.9.2.1 Reactor design issues

Experimental studies have shown that, like aerobic fermentations, the rate-limiting step in synthesis-gas fermentations is typically the gas-to-liquid mass transfer (Bredwell et al., 1999). Mass-transfer limitations are expected to be even more severe in synthesis-gas fermentations than in aerobic fermentations. The solubilities of CO and H_2 are only 60% and 4% of that of oxygen, respectively (on a mass basis). A common approach used to enhance gas-to-liquid mass transfer in stirred tanks is to increase the agitator power-to-volume ratio. Increasing the power input increases bubble breakup, thereby increasing the interfacial area available for mass transfer. However, this approach is not economically feasible for the very large reactors being considered for commercial synthesis-gas fermentations, due to excessive power costs. Consequently, alternative bioreactor configurations that may provide more energy-efficient mass transfer, including trickle-bed reactors and airlift reactors, have been evaluated for synthesis-gas fermentations. Both suspended-cell and immobilized-cell cultures have been used in these reactors. Microbubble dispersions have been used to enhance gas mass-transfer rates in synthesis-gas fermentations (Kaster et al., 1990). Summarizing common reactor-engineering approaches used to increase the productivity of synthesis-gas fermentations are: increased pressure, higher power-to-volume ratios, different reactor and impeller configurations, and the use of microbubble sparging.

1.9.3 Recovery and cogeneration

Product is recovered through conventional distillation and optional dehydration is obtained with molecular sieves. Due to ethanol law concentrations achieved in the fermentation broth (2-3% w/w) this is the most energy intensive process operation. Multi-columns distillation schemes and direct injection of steam could be used in order to decrease the energetic cost of this step.
Exhausted gas, exiting fermentation reactors, is useful as a fuel for power and heat generation: turbogas systems or a combustor-multistage steam turbines systems could meet process energy requirements and also produce a surplus available on the grid (Magnusson, 2005).

1.9.4 Pennsylvania Cellulosic Fuel Ethanol Plant Begins Production

In November 1st 2009 Coskata Inc. has started production of fuel ethanol at its new semi-commercial plant in Madison, PA (U.S.A). This facility is designed to demonstrate the company's new flex-ethanol process—which can manufacture ethanol from virtually any cellulose-based feedstock, ranging from sustainable energy crops to construction waste, from wood biomass, to agricultural waste. The process is based on a plasma gasification technology (Westinghouse Plasma Corporation, WPC), followed by the fermentation step and product recovery stage. Process main features are briefly described.

Heat, produced by plasma technology, breaks chemical bonds in the feedstock and completely converts organic matter into synthesis gas (syngas), primarily a mixture of carbon monoxide, hydrogen, and carbon dioxide. The syngas passes through a scrubber to remove particulates, providing recoverable energy in the cooling process.

The syngas is sent to a proprietary bioreactor where patented microorganisms consume both carbon monoxide and hydrogen, simultaneously. As the syngas passes through the bioreactor, the microorganisms consume it as food and create ethanol. Ethanol and water then exit the bioreactor.

Ethanol is separated from the water using traditional distillation or membrane permeation. Water is recycled back into the bioreactor. The final product is fuel-grade ethanol.

Coskata's technology is said to reduce greenhouse gases by as much as 96% over conventional gasoline, while using less than half the water that it takes to get a gallon of gasoline. The specific biological fermentation technology used in the process is ethanol-specific and enzyme independent, contributing to high energy conversion rates and ethanol yields. Coskata says the process requires no additional chemicals or pre-treatments, which streamlines operational costs and should allow it to compete directly with conventional gasoline without long-term government subsidies.

1.10 Aims of the work

Current development of ethanol industry shows that complex technical problems affecting the indicators of global process have not been properly solved. The growing cost of energy, the design of more intensive and compact processes, and environmental concern, have forced the necessity of employing totally new approaches for the design and operation of bioethanol production processes, quite different to those utilized for the operation of the old distilleries and other commodity chemicals.

Many studies are continuously carried out aimed at reducing the ethanol production costs for a profitable industrial operation. Research tendencies are related to the different steps of processing, nature of utilized feedstocks, and tools of process engineering, mainly process synthesis, integration and optimization. Process systems engineering could provide strategic tools for developing economically viable and environmentally friendly technologies for the production of fuel ethanol.

The overall goal of this Thesis is to apply multi-scale modelling principles, techniques and tools to processes for the production of fuel-ethanol from lignocellulosic biomass.

First, a macroscale approach will be used to analyse, optimize and assess the process design of EHF and GF to select the most promising technological option on the basis of criteria such as production yields, technical facilities optimization potential, economic profitability indexes, potential of costs reduction. The methodology will allow identifying processes critical issues and potentials. Accordingly, the EHF technology us selected as the most mature and effective process alternative in the near-term.

Successively, one of the most critical EHF processing steps is chosen for a more detailed analysis aiming at deliver further insight for a more conscious modelling effort. In particular, many mechanisms underlying lignocellulose pretreatment and hydrolysis, namely the most expensive and critical process steps, are still unclear. Several phenomena not only are not properly described but not even fully understood. For instance, the impact of different parameters characterizing the substrate-enzyme complex affecting the kinetics and the final yields of these steps are barely known. Thus, a reliable dynamic modelling of pretreatment and hydrolysis would be of great practical interest and could provide valuable tools to orientate research efforts and optimize single units and eventually the overall process design and operations. Here, the focus will be on the enzymatic hydrolysis.

A critical analysis of lignocellulose hydrolysis kinetic models reported in literature was carried out in order to select a suitable model structure. On the one side the model should be capable of taking into account the main phenomena taking place. On the other side, it should be "simple" enough to allow for an experimental assessment and identification.

Among phenomena that are worth being described in detail we decided to focus on the microscale correlation between substrate morphological features after pretreatment and the extent of enzyme adsorption and its final rebound on sugars released kinetic.

An experimental investigation was considered essential in order to characterize and better understand critical phenomena, to obtain experimental data for model validation and parameters estimation. Methodology, results and motivations of the experimental work performed, in collaboration with the Chemical Engineering Department of Lund University, will be critically presented and discussed.

Starting from traditional Langmuir isotherm description of enzyme adsorption a new concept model was developed embedding specific surface area, determined through experimental measurements, as critical parameter. The following step was to include the adsorption model in an overall hydrolysis process kinetic model.

Chapter 2

Techno-economic comparison between conversion technologies

A wide variety of processes for the production of ethanol from cellulosic materials has been studied and is currently under development. In fact, the large amount of technologies and processing options advocates for a more diffuse application of process engineering modelling, design and optimisation in order to help the research effort and guide investors and policy-makers towards the most effective technologies. In this Chapter[1], two of the most promising processes will be analysed and assessed: the conversion of lignocellulosic biomass by hydrolysis and subsequent fermentation and the gasification of lignocellulose followed by syngas fermentation. The Chapter is structured as follows: first literature concerning techno-economic modelling of lignocellulose ethanol conversion processes is extensively reviewed, then the EHF process is considered in terms of modelling, process optimisation, heat and power generation and assess its performance when varying some critical parameters. The financial assessment closes this section. Secondly the GF process is then taken into account: the technical and financial performances evaluations mirror the analysis and optimisation previously carried out for the EHF process. The last section discusses and compares the main results concerning the two production processes and draws some conclusions.

[1] Portions of this Chapter have been published in Piccolo and Bezzo (2007) and Piccolo and Bezzo (2009).

2.1 Literature survey

In the early ‘90s a network for the study of biomass-to-ethanol conversion called ‘‘Biotechnology for the Conversion of Lignocellulosics’’ under the sponsorship of the International Energy Agency with the participation of research groups from USA, Canada and Sweden has been promoted (Saddler, 1992), aiming of the design of a feasible biomass-to-ethanol process. One of the strengths of this task force was the active participation of different groups with expertise in each of the multi-component steps that constitute a feasible biomass-to-ethanol process, which were meant to provide information for the development of more accurate techno-economic models. Before a techno-economic model could be developed, the key equipment and process steps were defined (Gregg and Saddler, 1995). This effort led to the first generic process from wood design (Gregg and Saddler, 1995).

Other early works dealing with process synthesis for the production of fuel ethanol from biomass were oriented to the estimation of production costs of ethanol from wood chips and to the analysis of the interdependence of process parameters. In particular, the following parameters were defined as the most significant: wood cost, enzyme costs, efficiency of the cellulose hydrolysis, ethanol yield from pentoses, efficiency of fractionation process, and the selling price of the by-product lignin (Nguyen and Saddler, 1991). These parameters were assumed as useful to benchmark a conceptual process design.

The significant variety of pretreatment methods of biomass has led to the development of many flowsheet options for ethanol production. Von Sivers and Zacchi (1995) analyzed three pretreatment process for the ethanol production from pine: concentrated acid hydrolysis, two-stage hydrolysis by steam explosion using SO_2 and dilute acid, and steam explosion using SO_2 followed by the enzymatic hydrolysis. Through sensitivity analysis, these authors showed that none of the processes could be discarded as the less rentable. Using commercial process simulators like Aspen Plus® (Aspen Technologies, Inc., USA), this group of authors have evaluated different modifications of the ethanol production process from willow wood employing separate fermentations of hexoses and pentoses.

Alternative process configurations development followed hand in hand biotechnological advancement aiming of engineering microorganisms capable of efficiently fermenting both hemicellulosic and cellulosic substrates. Lynd (1996) and Lynd et al. (1996) gave an excellent overview of 1996 state of the art technology, assessed the different processing steps and the merge of conversion steps into fewer reactors (consolidation) that may have occurred over time, and especially focused on the microorganisms development (Lynd et al. 2002). However, there is only a qualitative indication of the technological and economic impacts of future technologies without detailed systems analysis.

A pilot plant designed for the conversion of lignocellulosic biomass into ethanol was built by the US National Renewable Energy Laboratory (NREL) and operated with the aim of supporting industrial partners for the research and development of biomass ethanol

technology (Nguyen et al., 1996). In this plant, tests in continuous regime for the utilization of lignocellulosic residues of low cost and great availability like corn fiber were carried out (Schell et al., 2004). The objective of these tests consisted in the assessment of the operation of the integrated equipments and in the generation of data type of plants allowing for the acquisition of valuable experience considering the future implementation of the industrial process, as well as the feedback of the models utilized during the design step. In addition, feasibility studies carried out by NREL were supposed to help industrial partners in making decisions about the potential implementation of these technologies for fuel ethanol production (Kadam et al., 2000; Mielenz, 1997).

Along with the experience gained in the pilot plant runs, NREL has developed an exhaustive model for the design and costing of biomass- to-ethanol process (Wooley et al., 1999a and b). The motivation for such a model was the demand for greater reliability and credibility in predicting the costs of bioethanol production considering the increasing demand for cost competitiveness and guiding the process development (Wooley et al., 1999b). The model process designed by NREL comprises a hydrolysis of wood with dilute acid followed by a simultaneous saccharification and co-fermentation (SSCF, see § 1.8.4) process utilizing cellulases produced in situ by genetically engineered *Z. mobilis* with the ability of transforming both glucose and xylose into ethanol. The process is energetically integrated using the heat generated during the combustion of methane formed in the anaerobic treatment of wastewater from pretreatment and distillation steps (Wooley et al., 1999a). In addition, the burning of lignin allows for the production of energy for the process and a surplus in form of electricity. For the simulation with Aspen Plus®, a database of the physical–chemical properties of the main compounds involved during fuel ethanol production from wood chips has also been structured (Wooley and Putsche, 1996).

This model is completed with capital cost estimations obtained from vendor quotes and using the Icarus® cost estimation software (by Aspen Technologies, Inc., USA). It allowed for the definition of the most promising research directions through simulation and process analysis of the best proposals aimed at reducing ethanol production costs using lignocellulosic feedstocks (Wooley and Ibsen, 2000). The production of one litre of ethanol by this process was calculated US$0.396, whereas the ethanol production cost from corn was US$0.232 (McAloon et al., 2000).

Nagle et al. (1999) proposed an alternative configuration that involves a total hydrolysis of yellow poplar using a three-stage countercurrent dilute-acid process validated at experimental level. The obtained hydrolyzate is co-fermented by the recombinant strain of Z. mobilis. In this case, the lignin is recovered prior the fermentation.

Gong et al. (1999) report a fractionation process employing corn cob and aspen wood chips as feedstocks and utilizing alkaline pretreatment with ammonia that favours the separation of lignin and extractives. After this step, the hemicellulose is hydrolyzed with dilute acid and

releasing sugars are fermented by xylose assimilating yeast; finally the cellulose is converted into ethanol by batch SSF using a thermotolerant yeast strain.

Iogen Corporation, a major manufacturer of industrial enzymes in Canada, developed a SHF process comprising a dilute-acid-catalyzed steam explosion and the removal of the major part of the acetic acid released during the pretreatment, the use of Saccharomyces cerevisiae as a fermenting organism, distillation of broth, ethanol dehydration and disposal of stillage in landfill (Tolan, 2002).

Reith et al. (2002) have reviewed different processes for production of biomass ethanol and concluded that verge grass, willow tops and wheat milling residues could be potential feedstock for fuel ethanol production in the conditions of the Netherlands. These authors constructed a model using Excel® for the system description of generic biomass-to-ethanol process. This process involves the evaporation of the stream from saccharification step in such a way that the sugar concentration allows for a final ethanol concentration of at least 8.5 vol.% in the fermentation broth. In addition, pretreatment using $Ca(OH)_2$ was included in the analysis. The advantage of using this type of pretreatment is that inhibitors are not formed implying that a detoxification step is not necessary. The evaluation showed that currently available industrial cellulases accounts for 36–45% of ethanol production costs, and therefore, a 10-fold reduction in the cellulase costs and a 30% reduction in capital costs are required in order to reach ethanol production costs competitive with starch ethanol.

Wingren (2003) proposed a techno-economic comparison between the two dominating process configurations for softwood conversion: SHF and SSF and determined where bottlenecks in the two process lie. A sensitivity analysis was also conducted for evaluating the impact of the cost and/or the load of enzymes on the overall production cost of ethanol.

Later modifications involve the co-fermentation of both hexoses and pentoses using genetically modified strains of microorganisms like yeasts or bacteria.

Using the recombinant Z. mobilis strain patented by NREL, Lawford and Rousseau (2003) tested two configurations for ethanol production using the conceptual design based on SHF developed by Iogen. These authors demonstrated that a configuration involving the continuous pentose fermentation using the recombinant Z. mobilis strain, and the separate enzymatic hydrolysis followed by continuous glucose fermentation using a wild type strain of Z. mobilis is the most appropriate in comparison to the use of the co-fermentation process after the enzymatic hydrolysis or the use of an industrial yeast strain during the glucose fermentation.

Ghosh and Ghose (2003) report the model process for bioethanol production proposed by the Indian Institute of Technology (IIT) in Delhi (India). This process involves two pretreatment steps: steam explosion for xylose production followed by solvent pretreatment for delignification of biomass. The released pentoses are utilized for single cell protein production, whereas the cellulose undergoes simultaneous saccharification and fermentation.

The SSF reactor is coupled with vacuum cycling and has a stepwise feeding of cellulose. The process has been tested in pilot plant using rice straw as a feedstock. However, the obtained product is hydrous ethanol (95% v/v) and the production costs (US$0.544/L) are higher than those expected for the production of dehydrated ethanol through the NREL model process (US$0.39). The adoption of an adsorption separation stage (instead of distillation) increases the cost of ethanol by about 50%.

Hamelinck et al. (2005) gave new insight in the development pathway of producing ethanol from lignocellulosic, by modelling and comparing routes for the research, development and implementation of large-scale conversion processes. In this study poplar is used as the base feedstock. Improvement options for both individual process steps and the whole plant (integration, scale up) are assessed, which lead to key configurations that are claimed to come available in time, as development progresses. These configurations were analysed for their technical and economic performance. An inventory was made of the process components, their stage of development, and their applicability in different process configurations. Experts were consulted to identify the potential barriers, uncertainties, and development time. The assessment includes technologies that are not yet commercially available. Promising system configurations for present and future, were selected. These configurations were analysed using Excel® and Aspen Plus®. The results on technical modelling, process economics and the sensitivity towards several parameters were reported.

Pan et al. (2005) from the University of British Columbia and Lignol innovations (Canada) report the preliminary evaluation of the so-called Lignol process for processing softwoods into ethanol and co-products. This process makes use of the organosolv process for obtaining high quality lignin allowing the fractionation of the biomass prior to the main fermentation. For this, the process utilizes a blend of ethanol and water at about 200°C and 27.6 bar. For ethanol production, SHF or SSF has been tested. Streams containing hemicellulose sugars, acetic acid, furfural and low molecular weight lignin are also considered as a source of valuable co-products. Until now, the Lignol process has only been operated in a three-stage batch mode but simulations studies indicate an improved process economics by operating the plant in continuous mode (Arato et al., 2005).

Cardona and Sanchez (2004, 2006) simulated several technological configurations for the production of fuel ethanol from biomass considering variations in the pretreatment, cellulose hydrolysis, fermentation, separation and effluent treatment steps and taking into account the integration possibilities. The simulations were performed using mostly Aspen Plus®. Energy expenditures were utilized for the analysis and comparison of the proposed flowsheets. The obtained results showed that the most appropriate flowsheet should include a dilute-acid pretreatment, SSCF, distillation coupled with pervaporation, and evaporation and recycling of part of the wastewater to be utilized as process water.

Only few recent reports, mostly related to private-sector initiatives deal with the techno-economic evaluation of the GF process. A feasibility study, concerning the process design development and the investment and production cost assessment was performed by the Eindhoven University of Technology in connection with Ingenia Consultants & Engineers (VanKasteren, 2005). They concluded that ethanol production via gasification and fermentation is competitive with the cellulosic process in Europe, even on the relatively small scale studied (30.000 tons/year) and they calculated ethanol prices in the range of 0.60 €/L.
In the US at least two private company (BRI Energy, Inc., Mississippi Ethanol LLC) are actively seeking to commercialize technology for fermentation of syngas (Bruce, BRI Energy Inc., 2006). BRI Energy, Inc. has announced their intention to build two commercial facilities near Oak Ridge, Tennessee, United States. One facility would convert coal-derived syngas to ethanol, and the other would convert municipal solid waste via gasification to ethanol (Powelson, 2006). Nevertheless little detailed documentation is publicly available to enable an independent evaluation of BRI's technology.
A more detailed report (Mississippi, LLC, 2002) was published in 2002 by NREL and Mississippi Ethanol, LLC (ME), owner of a gasification facility, and of much of the infrastructure necessary for the entire plant. As a result of this evaluation, a fermentation process and facility has been defined that can match the pre-existing gasification process. For an input stream of 30 tons/day of dry cellulosic waste products to the gasifier, this plant is supposed to produce 4000 gallons of ethanol per day. The team estimated that a capital cost in the range of 7-10 millions of dollars. The report concluded that there is an excellent potential and that the ME process and intended facility can be used to profitably and successfully produce ethanol.

2.2 Aim of the study

The EHF process is possibly the most mature process for the transformation of lignocellulosic materials into ethanol. On the other hand, as reported in § 2.1, the GF process has been somehow neglected in the scientific literature (at least when compared to the EHF process), notwithstanding the promising results demonstrated in the few works appeared so far (e.g. Datar et al., 2004). However, the technology potential (which is already available as a commercial process) has nonetheless been widely recognised (Ragauskas et al., 2006) and recently awarded through financing by the U.S.A. Department of Energy. Therefore, here the process has been chosen and assessed as a possible alternative to EHF for the production of bioethanol. This study aims at achieving the following goals. The first one is to deliver a technical and economical comparison between two of the most important processes for the conversion of lignocellulose to bioethanol. In general, it is difficult to assess different processes when analysed by different research groups as preliminary assumptions, process

design, financial modelling and data are rather "sensitive" to specific expertise, simplifying hypotheses and data availability. Our purpose is to apply the same methodology to carry out the technical and financial analyses for both processes so that the final results are indeed comparable. Secondly, this work is willing to represent the first comprehensive analysis of the GF process (with the partial exception of Mississippi Ethanol LCC, 2002). Although the process is still in its early development (at least from what can be derived from published material) and some data definitely still exhibit a significant uncertainty, the work aims at assessing process design, potential optimisation directions and the effect of most important parameters on the overall yield and financial indexes. Finally, a step forward in the optimisation and analysis of the EHF process, is intended too. The use of pinch analysis and a new design approach aim further reduction in the utilities demand. The effect of the improved design is assessed in terms of energy efficiency, overall yield, product costs and financial profitability. A processing capacity of 700,000 t/yr of dry biomass wood is assumed.

2.3 The EHF process: modelling

The process model was implemented on the Aspen Plus® v. 13.2 process simulator, a modelling tool performing rigorous material and energy balance calculations. The accuracy of the property data bank is of paramount importance for the reliability of the simulation results. The physical property database for biomass material, specifically developed by NREL (Wooley and Putsche, 1996), is used. The system thermodynamics are described by using an NRTL model (except for the CO_2 solubility modelled in terms of Henry's law).

Several flowsheet configurations have been proposed in the recent literature from ethanol production for biomass (Cardona and Sànchez, 2006). The NREL's design for ethanol production (Wooley et al., 1999a) and (Wooley et al., 1999b) with a new concept recovery section is taken as a base case. The flowsheet is illustrated in Figure 2.1.

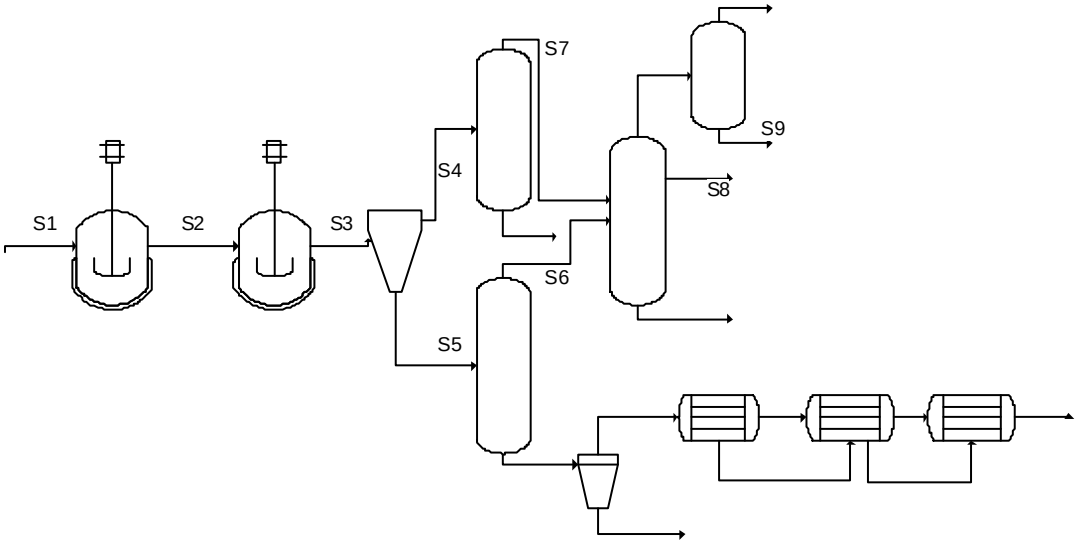

Figure 2.1 *Flowsheet for the SSCF process with a new concept recovery section.*

The process feed (160,950 kg/h) is assumed to be constituted of wet hardwood chips with the following composition (Wooley et al., 1999a and b) and (Cardona and Sànchez, 2006):

- cellulose 22.1%;
- hemicellulose 9.9%;
- lignin 20.4%;
- moisture 47.4%.

A dilute acid steam explosion is taken as the pre-treatment step. The operating conditions are defined as follows: temperature $T = 190$ °C, pressure $P = 10$ bar, residence time $\tau = 10$ min (Wyman et al., 2005). The above pre-treatment is chosen as it is one of the most extensively tested technologies; however, note that, in general, the pre-treatment process should be tailored to the specific lignocellulosic material (Galbe and Zacchi, 2007).

The conversion yield in terms of mass fraction of hemicellulose hydrolysed to hemicellulose content is 0.75.

Ethanol production takes place in the SSCF reactor. Cellulase is used as a biocatalyst for the cellulose hydrolysis and is assumed to be bought from dedicated producers. The fermenter is operated at 40 °C and atmospheric pressure. The cellulose conversion into fermentable sugar is 0.80; the actual sugar fermentation into ethanol is carried out by a recombinant *Z. mobilis* bacterium: it is assumed that 92% of hexoses (glucose and fructose) and 80% of pentoses (mainly xylose) are converted into ethanol. The outlet flow is a *beer* at 5.0% w/w ethanol. The streams compositions are given in Table 2.1.

Table 2.1 *EHF process: main streams variables (streams' numbers refer to Figure 2.1)*

Stream	S1	S2	S3	S4	S5	S6	S7	S8	S9
T [°C]	30	40	30.0	115	85.0	93.3	148.3	76.8	146.8
P[bar]	1	1	1	5	1	1	5	1	10
Mass flow [kg/h]	160950	236927	425329	114449	304813	35457	29000	22220	458
Vapor fraction	0	0	0	0	0	0	1	1	1
Mass fraction									
EtOH	-	-	0.050	0.055	0.047	0.412	0.217	0.920	0.920
CO_2	-	-	0.001	0.001	0.001	0.010	0.005	0.000	-
Water	0.474	0.636	0.835	0.931	0.800	0.573	0.775	0.072	0.059
Glucose	-	-	0.006	0.007	0.006	-	-	-	-
Xilose	-	0.059	0.005	0.006	0.005	-	-	-	-
Lights		-	0.001	0.001		0.005	0.003	0.007	0.020
Xylan	0.103	0.017	0.013	-	0.013	-	-	-	-
Cellulose	0.221	0.150	0.023	-	0.023	-	-	-	-
Lignin	0.203	0.138	0.105	-	0.105	-	-	-	-

The effect of small amounts of side-products has been considered in the simulation: this is an important (and often neglected) point as side-products (particularly, light ones) affect the final recovery configuration. Light side-products have been represented by including a small amount of acetaldehyde (after the CO_2 removal stage, the fermentation broth still contains 0.1% w/w CO_2 and 0.06% w/w acetaldehyde). As illustrated in Fig. 2.2, an integrated separation scheme is designed. The separation scheme is patterned after those used in the existing corn ethanol industry (Jacques et al., 2003) and (Franceschin et al., 2008). A multi-effect distillation scheme is adopted in order to minimize steam consumption.

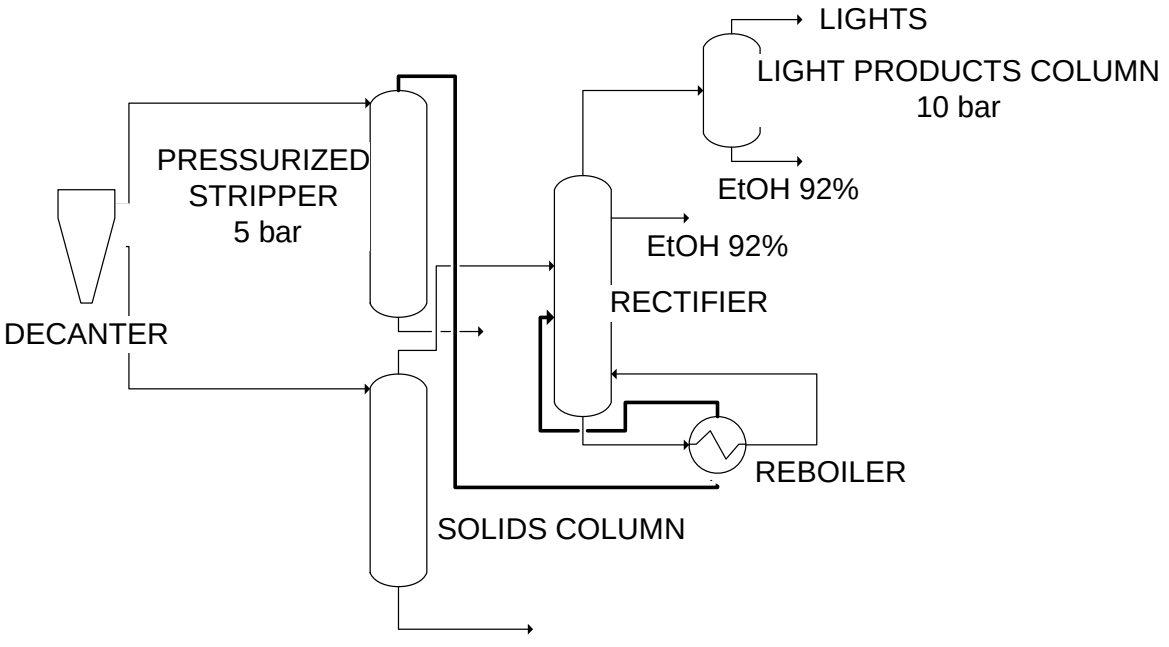

Figure 2.2 *EHF process: recovery system diagram (bold lines represent the hot streams).*

A decanter splits the input stream into two substreams: i) a fraction rich in solids, which is fed to an atmospheric column (first stripper) recovering 99% of the product in the distillate (composition: about 40% ethanol by weight); ii) a second fraction with no solids, which is sent to a pressurized column (second stripper): the distillate (20% ethanol by weight) is used to deliver some of the duty required by the reboiler in the final rectifying column. The stream compositions are reported in Table 2.2. This unit is designed to obtain at least a 92% purity in the side stream so that molecular sieves can be used to dehydrate the ethanol. A 2% of ethanol, dragged along by light products, purged from rectifier head, is recovered in a 10-tray still, operating at 10 bar.

Table 2.2 *EHF process: steam and related energy requirements for most energy intensive unit operation; HP and LP stands for High Pressure (13 bar) and Low Pressure (4 bar) steam, respectively.*

	HP [kg/L EtOH]	HP [MJ/L EtOH]	LP [kg/L EtOH]	LP [MJ/L EtOH]
Pre-treatment	1.67	3.32	0.64	1.37
Distillation	1.22	2.39		
Evaporation			2.03	4.34

The bottoms of the first stripper are fed to a centrifuge to separate the solids from the liquid solution, which is further concentrated through a triple-effect evaporator (the effects operate at 0.6 bar, 0.31 bar and 0.20 bar, respectively).
The pressurized stripper and rectifier stillage are conveyed to a water treatment section where biogas is produced through anaerobic fermentation: the methane generated in the water treatment section is obtained from literature data (Cardona and Sànchez, 2006).
The base case simulation results in an ethanol production of 312 L/ton of dry biomass (in the specific case, 20.9 t/h of ethanol are obtained, while CO_2 emissions are equal to 20 t/h).

2.4 The EHF process: energy optimisation

The flowsheet previously described can be further optimised to reduce the energy consumption. A Pinch Technology Analysis (PTA) (Linnhoff and Flower, 1978) approach has been carried out with concern to the recovery section. According to acknowledged practice, all the heat exchangers and the hot (i.e. to be cooled) and cold (i.e. to be heated) streams were identified. The ΔT_{min} representing the minimum temperature difference between the hot and the cold sides in all the process heat exchangers is set to 10 °C. The pinch point (i.e. the single temperature at which ΔT_{min} occurs) is found at 81.8 °C. Accordingly, for the hot streams the pinch temperature is 86.8 °C and for the cold streams is 76.8 °C. The construction of the composite curve allows pointing out the minimum amount of external heating and cooling for

global process (Figure 2.3). A cascade of heat exchangers is defined between hot and cold streams, in order to recover all the heat according to the composite curve construction.

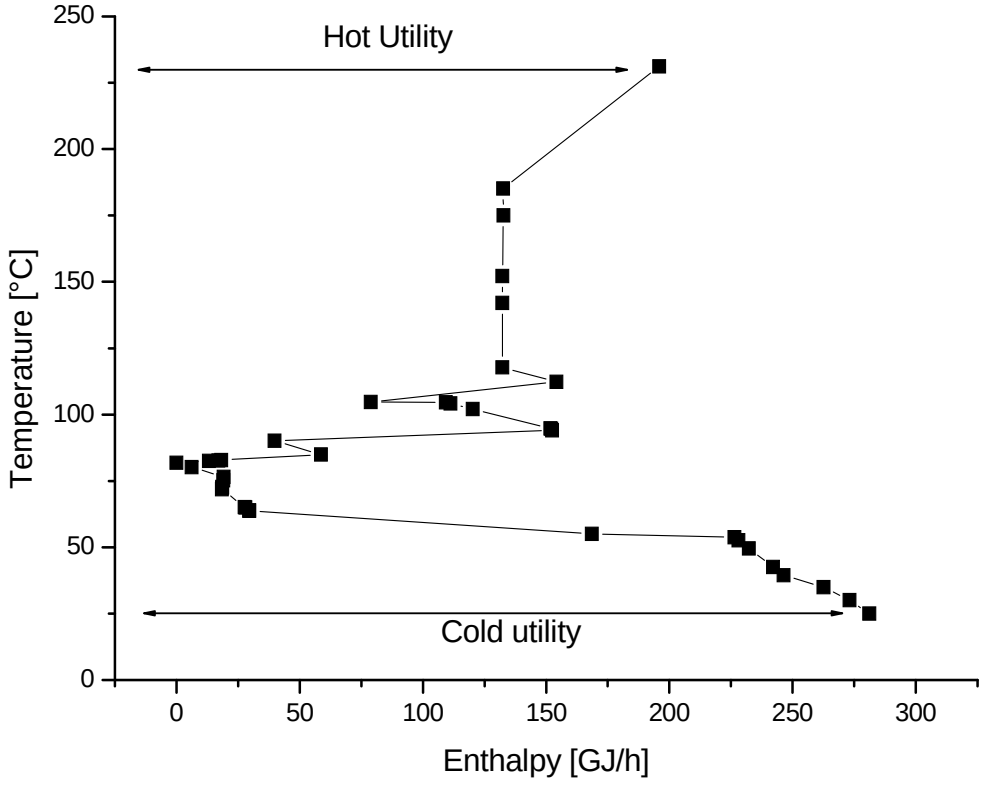

Figure 2.3 *EHF process: grand composite curve.*

The analysis shows that 23 heat exchangers (evaporators included) are needed. The composite curve analysis (basically confirmed by a successive simulation) shows that, after the pre-treatment and fermentation steps, about 196 GJ/h need to be supplied to the process, while about 281 GJ/h should be removed. Supplementary water and steam are needed in the power production section. Global utilities consumption (including steam for the pre-treatment step) is calculated as 3.8 kg of 13 bar steam/L EtOH (of which 1.2 kg/L EtOH for product recovery), 3.0 kg of 4 bar steam/L EtOH, 294.1 kg of cold water/L EtOH. The steam consumption in the molecular sieves was estimated to be equal to 1.1 MJ/L EtOH (Jacques et al., 2003). The total energy consumption is therefore 8.5 MJ/L EtOH. Table 2.3 summarises the energy demand of the most energy intensive operations. Simulation results significantly improve the estimation of energy needs reported in the literature so far (Table 2.3), demonstrating the effectiveness of the optimised design.

Table 2.3 *EHF process: energy requirements [MJ/L EtOH] reported in literature.*

Stage	This case	Cardona and Sanchez (2006)	Lynd et al., 1996	Hamelinck et al. (2005)	Hinman et al. (1992)
Pre-treatment	4.69	4.23	2.46	2.46	9.95
Distillation	2.39	27.89	5	5	
Dehydration	1.11				
Evaporation	4.34	4.35			

2.5 The EHF process: heat and power production

The transformation of lignocellulose into ethanol is energy self-sufficient. In fact, the solid residues exhibit a heating value of about 29.54 MJ/kg (Cardona and Sànchez, 2006). The solid residues together with the concentrated syrup from the evaporators are burnt in a fluidized-bed combustor. The moisture of the combined feed is 55% and its average heating value is 9.54 MJ/kg. Additionally, through the anaerobic treatment of the columns stillage biogas (60% methane; heating value: 20 MJ/m^3) is obtained.

The solid residues and biogas energy content are exploited to produce steam for a turbine system, as in Wooley et al (1999a). A 62% energy efficiency is assumed for the boiler. Calculations show that 2.60 kg/kg dry wood of superheated (510 °C, 104.5 bar) steam can be obtained in the boiler. The simulation of a multiple-stage steam turbine demonstrates that for the plant being considered about 37.9 MW of electricity can be generated (operation assumptions are reported in Table 2.4). Considering that the overall electric power demand is estimated as 32 MW (Wooley et al. 1999b), about 250 MJ of electricity surplus per ton of dry wood is eventually obtained.

Table 2.4 *EHF process: multistage turbine operating conditions and performances.*

Stage	Pressure out [bar]	$\eta_{isoentropic}$	Steam [kg/h]	Power [MW$_e$]
1	13	0.90	101200	33.1
2	4.4	0.38	80784	2.9
3	0.1	0.30	38016	1.9

To summarise, for the process being considered, about 420 MW as biomass heating value produce 156 MW of ethanol and about 5.9 MW of electric power, i.e. 0.39 energy units are obtained for one energy unit of lignocellulosic biomass.

2.6 The EHF process: process sensitivity analysis

Current research focuses on different strategies for improving the performances and the economics of bioethanol production. In particular, a big effort is put on producing biotechnological advancements for high productivity enzymes (stable at higher temperature so as to increase the reaction rate, and tolerant to higher concentrations of products). A sensitivity analysis can be performed to evaluate the impact of a general progress on the process performances. Two potential future scenarios are discussed. Assuming that the yield in the conversion reactor will increase over the years, mid-term and long-term scenarios are simulated. Main assumptions are reported in Table 2.5 (Lynd et al., 1996) and (Hamelinck et al., 2005).

Table 2.5 *EHF process: yields characterising different scenarios.*

	Hemicellulose hydrolysis	**Cellulose Hydrolysis**	**Hexoses fermentation**	**Pentoses fermentation**	**Concentration of broth [w%]**
Mid-term scenario	0.825	0.880	0.950	0.935	7.0
Long-term scenario	0.865	0.920	0.970	0.970	10.0

Simulation results show that according to the mid-term scenario, the amount of ethanol can be increased up to 362 L/ton of dry biomass; the long-term scenario foresees a potential of about 390 L of ethanol per ton of dry biomass.

Product concentration in the fermentation broth sensibly affects the utilities demand, too. According to the mid-term scenario, LP and HP steam consumptions are reduced by 4% and 5%, respectively; with concern to the long-term scenario, a decrease of 12% and 15% is obtained for LP and HP steam consumptions. One direct result is that for the case being investigated the net electric output increases from 5.9 MW up to 6.6 MW (270 MJ/ton of dry wood) for the mid-term scenario and up to 7.7 MW (315 MJ/ton of dry wood) for the long-term scenario, because less duty is required to separate a more concentrated mixture. There is also a reduction in cooling water demand: 8% and 13% for the mid- and long-term scenarios, respectively.

2.7 The EHF process: financial analysis

The process design study has been used to predict production cost and to assess its market potential. The process flow and balances were used to size equipments, and assess variable and fixed costs. The only products considered in this study are ethanol and electricity. For comparisons with gasoline a base of 70 $/bbl of oil is assumed; the gasoline production cost is roughly 0.50 €/L.

2.7.1. Equipment sizing and cost estimation

Equipment sizing follows from the simulation models (heat exchangers, columns, compressors) and from literature data (Wooley et al., 1999a). The total annual investment is calculated by a factored estimation, based on knowledge of major items of equipment (as found by direct sizing and cost correlation) and indexed to the year of interest using the Chemical Engineering Index (Chem. Eng. 144 , 2007). The installation investment costs for separate units are added up. A simplified investment model (Douglas, 1988) is used to estimate the total project investment (TPI). Main estimated costs are reported in Table 2.6.

Table 2.6 *EHF process: equipments and total investment cost.*

	Installation costs [M$]	**Source**	
Pretreatment	31.52	Wooley et al. (1999a)	
Heat exchangers	10.87	Calc	
Stills	4.27	Calc	
Fermentation section	12.86	Wooley et al. (1999a)	
Compressors	0.31	Calc.	
Steam turbine	44.5	Calc.	
WWT	10.40	Wooley et al. (1999a)	
		TPI [M$]	TPI [M€]
Onsite	114.74	270.78	203.44
+30%	149.16	352.02	264.47

The ethanol production cost is calculated by dividing the total annual costs (annual investment, operating and maintenance, raw materials, electricity supply/demand) by the produced amount of fuel. Operational costs are given as a percentage of TCI (Total Cost of Investment) and are derived from literature as well as consumables' purchase cost (Hamelinck et al., 2005). For the base case a 54 €/t dry biomass ton is considered. Table 2.7 summarises cost component allocation (a 5-year depreciation time is assumed).

Table 2.7 *Production cost components (TPC is the Total Production Cost)*

	€ per year (× 10^{-5})	**€/L**
Biomass	366	0.173
Other raw materials	563	0.266
Utilities	25	0.012
Labour	95	0.044
Waste disposal	7	0.003
Depreciation (5 years)	291	0.138
Electricity credit	-16	-0.011
TPC	1321	0.556
TPC (excl. depreciation)	821	0.487

If a depreciation time of 10 years is taken into account, the ethanol production cost decreases to 0.56 €/L. However, for a new production in a very changing (and risky) market and with rapidly evolving technologies, we think it is more sensible to shorten the depreciation time.
The crude oil price should be at around 90 $/bbl to have comparable costs of production. If a 10-year depreciation time is considered, similar costs are obtained for a crude oil price of about 80 $/bbl.

2.7.2. Payback analysis

The financial analysis is carried out by means of a number of profitability indexes. The following hypotheses are assumed
– interest rate: 10%;
– load: 8000 h;
– investment path: 20% in first year, 30% in second and 50% in last year;
– working capital: 15% of TCI;
– electricity price (supply and demand): 0.05 €/kWh;
– fractional income tax rate: 35%.
The double declining balance depreciation method is adopted. Based on the above assumptions two different scenarios are taken into account. The first one (PB10) considers a technical life time for the plant of 15 years, depreciation time and a payback time of 10 years; the second one assumes a 10-year life time and 5 years for both the depreciation and the payback times.
The product selling price is determined as the one allowing the defined payback period. This results as 0.68 €/L for PB10 and 0.80 €/L for PB5, which are sensibly higher than the current market price for ethanol at about 0.58 €/L (note that such price is usually further reduced in the case of long-term supply contracts as is usually the case in the ethanol industry (Solomon et al., 2007)).

A cash flow analysis is carried out for both instances. From Table 2.8, it can be seen that the Net Present Value (NPV) is negative for PB10 and is positive (about 9.4 M€) for PB5. That means that with the price allowing a 10-year payback period, at the end of plant life, the project adds no monetary value: not necessarily the consequence is that the project is unprofitable; however, it stresses that the investment may be risky and the decision whether to invest or not should take into account a deeper product market analysis as well as a more detailed cost estimation analysis. On the other hand in a PB5 scenario, the project will be in the status of cash inflow at the end of plant life. However, ethanol needs selling at a very high price: presently, that does not seem viable unless relying on some forms of government subsidies.

Table 2.8 *EHF process: economic indexes for the PB10 and PB5 scenarios.*

	NPV [M€]	**IRR [%]**	**ROI [%]**
PB10	-22.1	8.16	20.5
PB5	22.7	11.0	32.5

Other profitability indexes are here estimated (Table 2.8): these are the ROI (Return Of Investment, defined as the ratio of profit to investment) and the IRR (Internal Rate of Return, defined as the discount rate that results in a NPV of zero of a series of cash flows). The IRR is possibly the most meaningful index due to its discounted nature. In general, a project is a good investment proposition if its IRR is greater than the rate of return that could be earned by alternative investments. Thus, the IRR should be compared to an alternative cost of capital including an appropriate risk premium. For a project involving a rather high risk level the suggested IRR is usually 15% (Douglas, 1988). Calculated values for ethanol plant are well below this threshold limit, resulting in a poorly profitable investment choice. Furthermore, note that the analysis is based on the possibility of selling ethanol at the prices indicated above. That would be possible either in case of peaking of oil prices (in order to have the same selling price per energy unit, crude oil price should be at about 100 $/bbl for the PB10 instance and about 110 $/bbl for the PB5 case) or through some government intervention in terms of financial subsidies (that, in fact, could even allow a higher selling price).
Furthermore, IRR is determined for the case with ethanol price set at 0.58 €/L, in order to assess process profitability in the actual market conditions. For a 15-year plant life the IRR index is slightly positive (1.7%) and for a 10-year plant it is even negative (−2.6%). This last value, meaningless from the economic point of view, suggests that the investment, with the product price imposed by current market laws, is definitely not profitable.

2.7.3. Product cost sensitivity

The effect of different parameters on ethanol selling price is investigated. It is assumed that the power generation is not sensitive to the variation of such parameters. Although not strictly correct, the assumption is justified by the fact that power generation capital costs are not significantly affected and profits from electricity sold to the grid are a minor contribution (unless government subsidies as the EU Green Credits are taken into the balance).
One of the most important variable is the feedstock cost, which accounts for about 35.5% of the total product cost (excluding depreciation). Table 2.9 summarises the results based on such sensitivity analysis. It can be seen that with a feedstock cost of 36 €/ton of dry biomass a reduction in cost production of more than 10% of that associated with the base case would occur. This decrease also affects the ethanol selling price, determining a reduction of about 8–9% in both the PB5 and PB10 instances.

Table 2.9 *EHF process: ethanol price sensitivity to feedstock cost.*

Feedstock cost [€/dry ton biomass]	TPC10 [€/L EtOH]	TPC5 [€/L EtOH]	PB10 [€/L EtOH]	PB5 [€/L EtOH]
63	0.59	0.65	0.71	0.83
54	0.56	0.63	0.68	0.80
45	0.53	0.60	0.65	0.77
36	0.50	0.57	0.62	0.74

Cellulase is another component cost which plays a decisive role in determining the product cost. Its average charge is estimated from literature data (Hamelinck et al., 2005). Assuming that its cost may decrease with time, a sensitivity analysis is carried out. Table 2.10 summarises the effects on the ethanol price. The case with cellulase production performed in seed reactors is also investigated. This case involves reduced operational costs, but, on the other hand, a decrease in ethanol production (because a biomass fraction is channelled to the seed reactors) and a significant increase in the capital investment (Wooley et al., 1999a). This last aspect strongly affects prices, in particular if a short payback is desired.

Table 2.10 *EHF process: ethanol price sensitivity to cellulase cost.*

Cellulase cost [€/L EtOH]	TPC10 [€/L EtOH]	TPC5 [€/L EtOH]	Price payback 10 [€/L EtOH]	Price payback 5 [€/L EtOH]
0.13	0.56	0.63	0.68	0.80
0.10	0.52	0.59	0.65	0.77
0.07	0.50	0.56	0.62	0.74
Own production	0.46	0.54	0.62	0.76

The technological advancements previously discussed are here assessed in financial terms: as can be seen from Table 2.11, higher conversion yields and broth concentration result in a significantly lower ethanol selling price.

Table 2.11 *EHF process: ethanol cost sensitivity to conversion yields*

Case	TPC10 [€/L EtOH]	TPC5 [€/L EtOH]	Price payback 10 [€/L EtOH]	Price payback 5 [€/L EtOH]
Base case	0.56	0.63	0.68	0.80
Mid-term scenario	0.46	0.52	0.57	0.68
Long-term scenario	0.41	0.47	0.42	0.60

2.8 The GF process: modelling

Thermochemical gasification is the conversion by partial oxidation at elevated temperature of a carbonaceous feedstock into a gas product. The partial oxidation can be carried out using air, oxygen, steam, or a combination of these. Gasification occurs in sequential steps: drying (to evaporate feedstock moisture), pyrolysis (to give gas, vaporized tars and a solid char residue), gasification (or partial oxidation of the solid char, pyrolysis tars and pyrolysis gases).

Numerous models (e.g. Varhegyi et al., (1997) and Rostami et al. (2004)) have been developed so far to describe the pyrolysis of biomass by taking into account kinetics, heat and/or mass transport. However, in a general-purpose analysis as the one in this paper, such models are of little use since parameters and results are very much dependent on the specific pyrolysis conditions and reactors. On the other hand, also models based on thermodynamic equilibrium calculations (e.g. Gueret et al. (1997) and Lee and Sanchez (1997)) are not suitable to describe pyrolysis as equilibrium is not usually reached. For this reason the treatment of the pyrolysis step was simplified and modelled by setting the yield of different products according to literature experimental data (Zanzi et al., 1996). The outlet composition in terms of CO, CO_2, CH_4, H_2, C_2H_4, char (whose physical and chemical properties are assumed to be the same as carbon graphite) and tars (described as anthracene) is reported in Table 2.12. The experimental data refer to a moisture content of 5.0%, which, in general, is obtainable only through a ventilated drying house. For the process being considered that could be practically achieved by using exhausted fumes from the power generation system and, therefore, it is not going to affect the overall energy balance in a significant way. In general, the effect of water in the gasification is to increase the H_2 fraction with respect to CO. Therefore, being CO the most important reactant for the biological fermentation into ethanol,

dry biomass is a benefit. If natural ventilation is used for biomass drying, the final moisture content is usually around 10–15%, which does not represent an issue.

Table 2.12 *GF process: pyrolysis products distribution.*

Tars	0.2
Chars	5.6
Gas	83
Product gas composition (dry)	
CO	45.7
CO_2	7.5
H_2	34
CH_4	11.7
C_6H_6	0.6
C_2+	0.5

Pyrolysis products react with the oxidizing agent to give permanent gases (CO, CO_2, H_2) and a lesser quantity of hydrocarbon gases. Char gasification is the interactive combination of several gas–solid and gas–gas reactions in which solid carbon is oxidized to carbon monoxide and carbon dioxide, and hydrogen is generated through the water–gas shift reaction (Bridgwater, 1995): equilibrium conditions are more likely to occur because of the higher temperature and the "less heterogeneous" reaction conditions.

An equilibrium model of the gasification process is therefore developed and validated by comparison with experimental data (Bridgwater, 1995). Oxygen is considered as the oxidizing agent; experimental data as well as the system thermodynamics show that the gasification should be run at a high temperature, i.e. at least 1000 °C. The composition of the biomass in terms of the constituting elements is summarised in Table 2.13 (Zanzi et al., 1996).

Table 2.13 *GF process: biomass elemental analysis and LHV.*

w% C	48.4
w% N	0.2
w% H	5.6
w% O	45.8
LHV [MJ/kg dry]	18.7

The outlet composition is obtained by minimising the Gibbs energy at T = 1000 °C. Ratios of 0.3 kg of O_2 per kg of dry biomass are typical values, reported for different gasification processes (Hamelinck and Faaij., 2001). The gasifier yield (kmol gas/ton of dry biomass) is equal to 66.6, while the cold gas efficiency is equal to 0.70. Results are summarised in Table 2.14 where they are also compared to a typical gas composition for an oxygen-blown gasifier (Klass, 1991).

Table 2.14 *GF process: comparison between typical experimental gas composition and simulation results.*

Dry gas composition (mol%)	Exp. data	Calc. data
H_2	32	39.2
CO	48	45.4
CH_4	2	0.6
CO_2	15	14.7
C_2	-	-

The main deviations from the expected value concern the hydrogen and methane compositions. This may be related to a different biomass water content and/or to a number of non-equilibrium conditions that may establish because of temperature gradients in the heterogeneous phase (Kilpinen et al., 1991). In fact, by considering pseudo-equilibria in the system (Prins et al., 2007) we indeed verified a better agreement with the reported experimental data. However, once again, since there exists a significant variability in the experimental data reported in the literature, we considered it more "reasonable" to represent a general behaviour rather than tuning the results on some specific data.

Since syngas composition may vary a lot accordingly to feedstock and gasifier configuration, a preliminary sensitivity analysis was carried out to investigate the effect of gas composition on the ethanol yield by considering a rather common range of variability in the experimental data published in the literature (for pure oxygen fed gasifiers operating in similar conditions). Experimental data demonstrate that most variability in the gas composition is related to hydrogen, which is significantly less important in the final ethanol yield. CO is less sensitive and furthermore its variations are somehow balanced by an opposite variation in the hydrogen production. In general, it was verified that some variability in the syngas composition does not affect the analysis significantly: we think it is fair to assume about a 15% error in the potential yield calculated in the base case.

The outlet gas stream is cooled down (by producing steam) and then fed to the fermentation tank. Literature (e.g. Spath and Dayton (2003); Mississippi Ethanol LCC Final report (2002); Clausen, 2006) is not consistent about product gas conversion yields. In this work, it was decided to rely on data derived from. (Mississippi Ethanol LCC Final report (2002)), which

represents the most complete study on the topic published so far. The fermentation is carried out by bacterium *C. ljungdahlii* at 39 °C and atmospheric pressure. The conversion yield of CO is set to 53.1% with respect to ethanol and 4% with respect to acetic acid; as regards H_2 it is assumed that 18.8% will convert to ethanol, while 1.4% will turn into acetic acid. Ethanol concentration in the broth is set to 2.4% in weight and acetic acid concentration is 0.4%.
The recovery section (illustrated in Fig. 2.4) is once again defined according to multi-effect scheme: a pressure stripper operating at 2.1 bar through direct steam injection and a pressure rectifier operating at 1 bar.

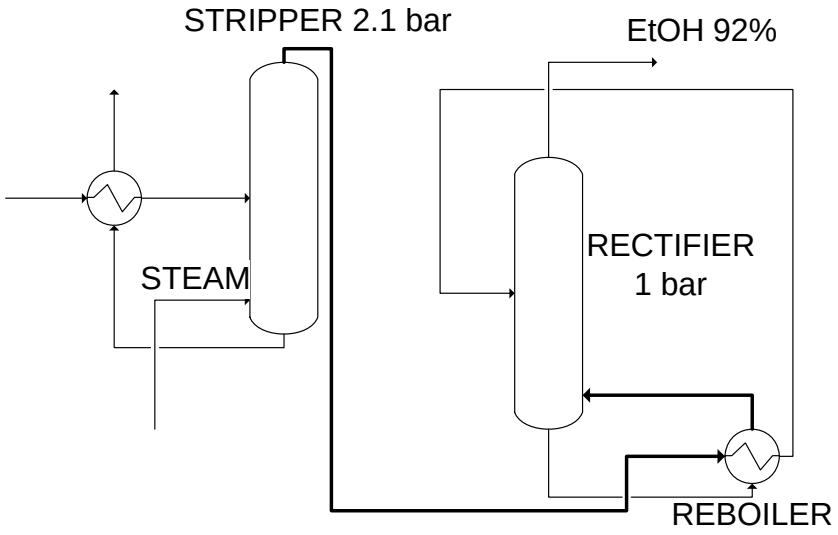

Figure 2.4 *GF Product recovery scheme. (the bold line represents the hot stream)*

Although an optimisation procedure through PTA was carried out in this case, too, the results show that due to the very low ethanol concentration tolerated in the fermentation broth, the product recovery remains a very energy intensive operation. The optimisation shows that 5.4 kg steam/L EtOH are required.
The outlet gas from the fermentation unit is fed to a burner and fuel gases are used to generate superheated steam in a boiler.
The process overall material balance is reported in Table 2.15. It can be seen that 203.5 L of ethanol per ton of dry biomass are obtained.

Table 2.15 *GF process: gasifier-fermenter material balance.*

	INPUT [kg/h]	OUTPUT [kg/h]
Dried Biomass	84670	
Oxygen	25400	
Outlet from gasifier		111243
Ethanol		13611
Acetic acid		2002

2.9 The GF process: heat and power production

The co-generation system consists of a combustor, a number of heat exchangers and a multistage steam turbine (Magnusson, 2005). In the burner exhausted gases from the fermentation tank are burnt with preheated air (250 °C). The air flow is set in order to obtain a ratio of oxygen in the flue gases with respect to the inlet air equal to 0.6: this is done to limit the maximum temperature to 1110 °C.

Feed water (143 t/h) enters the steam boiler and in the economiser is heated to about 25 °C below saturation temperature (330 °C). It is then fed into the evaporator where saturated steam is raised at 150 bar. Finally, in the superheater, steam is pushed to turbine inlet conditions: 540 °C and 140 bar. The specifications for steam turbine system are reported in Table 2.16. Note that also the steam generated in the cooling of the gasifier output stream (46 t/h of steam at 25 bar and 316.6 °C) enters the second stage of the turbine. After the third stage 89 t/h of 4 bar steam are separated and conveyed to the distillation needs.

Table 2.16 *GF process: cogeneration process features and performances.*

Stage	Pressure out [bar]	$\eta_{isoentropic}$	Power [MW_e]
1	25	0.90	19.2
2	6	0.89	15.4
3	4	0.38	1.6
4	0.5	0.33	3.2

The process is self-sufficient from an energetic point of view. About 39.4 MW can be generated. Considering that the process power demand is about 14 MW (Bioengineering Resources Inc (2006)), and power demand for oxygen production 259 kWh/ton of O_2 (Hamelinck and Faaij., 2001), a significant power surplus (18.9 MW) is available and can be sold to the grid: about 780 MJ of electricity surplus per ton of dry wood can be sold to the grid.

To summarise, from about 420 MW of biomass, about 101 MW of ethanol and 18.9 MW of excess electricity can be obtained in this process, i.e. 0.29 energy units are obtained for one energy unit of lignocellulosic biomass (significantly less than in the EHF process).

2.10 The GF process: sensitivity analysis

A critical parameter in assessing the process performance concerns the conversions in the fermentation reactions. Other references suggest that sensibly higher conversions can be obtained in the fermentation reactor (for instance, Spath and Dayton (2003)) declare that 90% of CO and 70% of H_2 can be converted into ethanol on lab-scale facilities). Such conversions, if confirmed, would obviously change the overall technology potential. In this study, it was decided to consider the effect of a 15% and 50% conversion increase in both CO and H_2 with respect to the base case. These improvements are categorised as mid- and long-term scenarios and are summarised in Table 2.17 (the possibility of a higher broth concentration is also assumed).

Table 2.17 *GF process: hypotheses for the mid and long term scenarios.*

Case	Yield EtOH/CO	Yield EtOH/H_2	Concentration
Base case	53.10	18.80	2.4%
Mid-term scenario	61.10	21.60	3.0%
Long-term scenario	80.0	28.00	5.0%

Simulation results show for the mid- and long-term scenarios an increase in the ethanol production up to 228 L and 282 L per ton of dry biomass, respectively; conversely, electric energy surplus is reduced to about 650 MJ and 270 MJ per ton of dry biomass, respectively.
In terms of energy balance (ethanol heating value plus electricity sold to the grid), the mid- and long-term scenarios show an overall increase up to about 113 MW and 139 MW, respectively.

2.11 The GF process: financial analysis

Similar to what was done for the EHF, process equipments size and installation cost are assessed through direct factored estimation or from literature sources (Hamelinck and Faaij., 2001). Table 2.18 summarises the estimated installation costs.

Table 2.18 *GF process: equipments and total investment costs.*

	Installation costs [M$]	Source	
Pretreatment	38.2	(Douglas , 1988)	
Gasifier	73	(Douglas , 1988)	
Cyclones	1.8	(Douglas , 1988)	
Fermentation vessels	12.87	(Douglas , 1988)	
Stills	2.68	Calc.	
Heat exchangers	9.45	Calc.	
O_2 plant	27.63	(Douglas , 1988)	
Steam turbine	53.83	(Douglas , 1988)	
		TCI [M$]	TCI [M€]
Onsite	219.46	517.93	389.12
+30%	285.30	673.31	505.86

2.11.1 Cost estimation

The cost of the product is determined from the annual production cost. Calculations do not consider the biocatalyst cost, which is presently not available on market. Table 2.19 outlines cost allocations (a 5-year depreciation time is assumed).

Table 2.19 *GF process: production cost components.*

	€ per year ($\times 10^{-5}$)	€/L
Biomass	366	0.265
Other raw materials	1.5	0.001
Utilities	1	0.001
Labour	25	0.181
Depreciation (5 years)	711	0.516
Electricity credit	-78	-0.055
Total production cost	1251	0.908
TPC excluded depreciation	543	0.394

Same calculations for a 10-year depreciation time give a total product cost of 0.65 €/L. In the GF process the burden of the capital cost is very important.

For the GF process the difference between the energy cost of ethanol when compared to gasoline is even higher than that in the EHF process. Crude oil price should be at around 125

$/bbl to have comparable costs of production. Even if a 10-year depreciation time is considered, similar costs are obtained for a crude oil price of about 95 $/bbl.

2.11.2 Payback analysis

The PB5 and PB10 instances based on the same hypotheses assumed for the EHF process are assessed. Main economic indexes are summarised in Table 2.20. Results are not so different from the EHF process. The IRR index is well below the recommended 15% value, even if a very high ethanol selling price could be imposed to the fuel market (and in this case a significant income also derives from the selling of electricity).

Table 2.20 *Economic indexes for GF process.*

Case	Ethanol Price [€/L EtOH]	NPV [M€]	IRR [%]	ROI [%]
PB10	0.89	-48.9	7.7	20.2
PB5	1.20	5.9	10.4	31.9

If the present market price of ethanol (0.58 €/L) is assumed, the IRR index for PB5 and PB10 results respectively in 0.3 and −4.1%: these values are symptomatic of a definitely unprofitable project investment.

Note that in order to have the same selling price per unit of energy, the price of crude oil should rise to about 120 $/bbl in the case of the PB10 scenario and about 160 $/bbl in the case of the PB5 case.

2.11.3 Product cost sensitivity

The effect of different parameters on ethanol selling price is investigated. As before, one of the most important variable is the feedstock cost, which accounts for 67% of the total product cost (without depreciation). Table 2.21 summarises the results based on such sensitivity analysis. A feedstock available at 36 €/dry ton would determine a reduction (with respect to the base case) on the production cost of about 11% (TPC10) and 8% (TPC5). However, the ethanol selling price is reduced of only 7.8% for PB10 and 5% for PB5.

Table 2.21 *GF process: effect feedstock cost on production cost and ethanol selling price.*

Feedstock cost [€/dry ton biomass]	TPC 10 [€/L EtOH]	TPC 5 [€/L EtOH]	PB10 [€/L EtOH]	PB5 [€/L EtOH]
63	0.71	0.98	0.96	1.28
54	0.65	0.91	0.89	1.20
45	0.62	0.89	0.87	1.19
36	0.58	0.84	0.82	1.14

The effect of fermentation reaction conversion yields on product price is assessed for the mid- and long-term scenarios previously discussed. Results are summarised in Table 2.22.

Table 2.22 *GF process: effect of fermentation yields on production cost and ethanol selling price.*

Case	TPC 10 [€/L EtOH]	TPC 5 [€/L EtOH]	PB 10 [€/L EtOH]	PB 5 [€/L EtOH]
Base case	0.65	0.91	0.89	1.20
Mid-term scenario	0.59	0.82	0.80	1.08
Long-term scenario	0.50	0.68	0.72	0.94

2.11.4 Additional comments on the GF process

The GF process appears to be a less mature technology than the EHF process, at least from the information available in the scientific literature. One major challenge that needs tackling is how to increase the H_2 and CO conversion in the fermentation reactor. On the one side, a higher conversion would require more efficient micro-organisms for the fermentation reactions. On the other side, a critical issue is to enhance the mass transfer between the gas phase (reactants) and the liquid biological broth. For some aspects, this is a typical chemical engineering issue, which had to be dealt with in several traditional processes. However, although several technological solutions can be taken from elsewhere, biological systems do present some peculiar challenges: for instance, any novel reactor design should take into account the effect of mixing and shear stress on the cell growth and on the fermentation kinetics. Additionally, it is important to assess whether a higher mass transfer may cause a higher concentration of pollutants and inhibitors in the broth, so that a more expensive upstream gas cleaning technology may be necessary. Finally, some biotechnological advancement is advocated to guarantee a suitable selectivity in the fermentation process and to improve the bacteria resistance to ethanol concentration in the broth: that would allow processing more concentrated solutions and decreasing the energy cost for ethanol recovery.

2.12 Final remarks

In this analysis two conversion technologies for the lignocellulose conversion into ethanol have been assessed in terms of yield and profitability.

The first technology is the enzymatic hydrolysis and fermentation (EHF) process. A further improvement in the recovery design in order to reduce the process energy consumption has been demonstrated. The improved design and a comprehensive use of information from previous works have allowed to better assess the present process profitability and the effect of critical process and finance parameters. Although the production cost of ethanol is not so far from the production cost of gasoline (just before submitting this paper crude oil hit a new record at over 80 $/bbl), the complexity of the fuel market advocates for an investment payback of not more than 5 years; as a result the high capital cost causes the ethanol selling price to be set at about 0.80 €/L, which is quite beyond the present market value of fuel-grade ethanol. Furthermore, even if such price were presently viable, the IRR index still signals that the investment would still be rather risky and might not be the best business on the market. The analysis shows that still substantial technological improvements are needed to allow the lowering of the selling price in a significant way and make the technology attractive on a large-scale business.

The second technology investigated is the gasification and fermentation (GF) process. Much less material has been published so far on this technology and one important contribution of this work has been to deliver a first comprehensive process analysis and to assess it versus the EHF process. Although quite an impressive yield could theoretically be achieved if some of the lab results were achievable industrially, the present state of the art of the technology does not seem to be mature enough for an attractive business. In fact, the burdens of large capital cost, energy expensive recovery and a moderate final yield determine a very high production cost and the need of a very high ethanol selling price (about 1.20 €/L) in order to obtain a short-term payback of the investment. Only substantial technological improvements can decrease the ethanol selling price and make the technology a sensible alternative to the EHF process. Nonetheless, it is important to highlight that the GF process exhibits quite a potential in electric power generation (significantly more than the EHF process): that could be an important advantage in countries where electricity is particularly expensive or where power generation from renewable sources is somehow subsidised (as is the case in many European countries through the Green Credits scheme). Also note that a potential technological advantage for the GF process is the use of gasification: although running biomass gasification in a reliable and consistent way is still a rather complex issue, it is a very flexible technology (much more than the pre-treatment and hydrolysis steps in the EHF process).

One important index to assess the performance of energy processes is the Energy Return on Investment (EROI), i.e. the ratio between the gross energy output (ethanol and electricity in our case) and the gross energy input (farming energy costs, transport, process, etc.) according

to the definition given by Hammerschlag (2006). Although its calculation (and its very definition) is often very questionable (Mulder and Hagens, 2008), some approximated estimation (based on the gross energy input suggested by Lynd and Wang, (2004) has been carried out; an EROI of about 3.8 was obtained for the EHF process, whereas the EROI value for the GF process was calculated to be equal to 2.6. The EROI values are consistent with the simulation results and indicate a lower energy efficiency for the GF process.

Chapter 3

Experimental investigation of enzyme adsorption on SO_2 steam-pretreated materials

Lignocellulose hydrolysis is a complex key unit operation in lignocellulosic ethanol: extensive research has been made to identify the many parameters that determine the rate of reaction. The rate limiting factors in enzymatic hydrolysis of lignocellulose can be divided in two main categories. These factors are either related to the substrate or to the enzyme. The substrate related factors, which have been suggested to impact the process kinetic are cristallinity, accessible surface area, particle size, lignin distribution. Enzyme related factors are end-product inhibition, thermal and shear force inactivation, extent of productive and unproductive adsorption of enzymes. An overview of these different aspects is presented in the first part of the Chapter[1]. To tackle the problem in its complexity we decided to focus on the role of a limited number of parameters. Enzymatic catalysis of cellulose is known to be an heterogeneous process and enzyme adsorption on the substrate is the key prerequisite mechanism (Ryu et al., 1984). Enzyme adsorption is a surface phenomenon and hence likely to be related to substrate morphological features. For this reason we chose to characterize substrates through their accessible surface area and pores distribution. The essential emphasis on "real" process substrates led to considerations on the different pretreatment options, which have a strong impact on the morphological features of the materials: thus the effect of different pretreatment conditions on two different lignocellulosic substrates (spruce and wheat straw) has been assessed. Finally the relationship between substrates features and enzyme adsorption and the final hydrolysis kinetic has been investigated.

[1] Portions of this Chapter have been published in Piccolo et al. (2010).

3.1 Enzymatic hydrolysis of lignocellulose

3.1.1 Enzymes related rate limiting factors

The original hypothesis on the mechanism of cellulose hydrolysis by Reese (Reese et al., 1950; Reese and Mandels 1971; Reese, 1956), involves phenomena of physical disruption of insoluble cellulose in addition to endo- and exo-acting enzymes. The importance of such disruption, as well as the cellulase components responsible for it, is still not entirely clear. Coughlan (1985) used the term "amorphogenesis" to describe physical changes (i.e., swelling, segmentation, or destratification of cellulose) that enhance enzymatic hydrolysis and render crystalline cellulose more accessible to cellulase. When cellulase enzyme systems act in vitro on insoluble cellulosic substrates, three processes occur simultaneously: 1) chemical and physical changes in the residual (not yet solubilised) solid-phase cellulose; 2) primary hydrolysis, involving the release of soluble intermediates from the surface of reacting cellulose molecules; and 3) secondary hydrolysis, involving hydrolysis of soluble intermediates to lower molecular weight intermediates, and ultimately to glucose.

3.1.1.1 Enzyme mixtures activities

The biochemical analysis of cellulase systems from aerobic and anaerobic bacteria and fungi has been comprehensively reviewed during the past two decades. Components of cellulase systems were first classified based on their mode of catalytic action and have more recently been classified based on structural properties (Henrissat et al., 1998b). Three major types of enzymatic activities are found: endoglucanases, exoglucanases and β-glucosidases. Endoglucanases cut at random at internal amorphous sites in the cellulose polysaccharide chain, generating oligosaccharides of various lengths and consequently new chain ends. Exoglucanases act in a *processive* manner on reducing or nonreducing ends of cellulose polysaccharide chains, liberating either glucose (glucanohydrolases) or cellobiose (cellobiohydrolase) as major products. Exoglucanases can also act on microcrystalline cellulose, presumably peeling cellulose chains from the microcrystalline structure (Teeri, 1997). β-Glucosidases hydrolyze soluble oligosaccharides and cellobiose to glucose. The insoluble, recalcitrant nature of cellulose represents a challenge for cellulase systems. A general feature of most cellulases is a modular structure often including both catalytic and carbohydrate-binding modules (CBMs). The CBM effects binding to the cellulose surface, presumably to facilitate cellulose hydrolysis by bringing the catalytic domain in close proximity to the substrate, insoluble cellulose. The presence of CBMs is particularly important for the initiation and processivity of exoglucanases (Teeri et al., 1998a). Revisiting the original model of cellulose degradation proposed by Reese et al. (1950), a possible additional noncatalytic role for CBMs in cellulose hydrolysis was proposed: the "sloughing

off" of cellulose fragments from cellulosic surfaces of, e.g., cotton fibres, thereby enhancing cellulose hydrolysis (Din et al., 1994). Cellulases from aerobic fungi have received more study than have those of any other physiological group, and fungal cellulases currently dominate the industrial applications of cellulases (Gusakov and Sinitsyn, 1992; Nieves et al., 1998; Sheehan and Himmel, 1999).

In particular, the cellulase system of *T. reesei* has been the focus of research for 50 years (Mandels and Reese, 1957; Reese, 1956; Reese and Mandels, 1971; Reese et al., 1950). *T. reesei* produces at least two exoglucanases (CBHI and CBHII), five endoglucanases (EGI, EGII, EGIII, EGIV, and EGV), and two β-glucosidases (BGLI and BGLII (Kubicek and Pentillä, 1998; Nogawa et al., 2001; Takashima et al., 1999). The necessity for the two exoglucanases (cellobiohydrolases) has been attributed to their particular preferences for the reducing (CBHI) and nonreducing (CBHII) ends of cellulose chains of microcrystalline cellulose. This notion has also been supported by the exo-exo synergy observed between these two enzymes (Henrissat et al., 1985; Medve et al., 1994; Nidetzky et al., 1994a). Crystallography has elucidated the three-dimensional structures of the two cellobiohydrolases (Divne et al., 1994; Rouvinen et al., 1990). CBHI contains four surface loops that give rise to a tunnel with a length of 50 Å; CBHII contains two surface loops that give rise to a tunnel of 20 Å. These tunnels proved to be essential to the cellobiohydrolases for the processive cleavage of cellulose chains from the reducing or nonreducing ends. The three-dimensional (3-D) structure of CBHI confirmed that cellobiose is the major hydrolytic product as the cellulose chain passes through the tunnel. Occasionally, cellotriose or glucose is released during initial stages of hydrolysis (Divne et al., 1994). The structure of EGI (structurally related to CBHII) also has been resolved (Kleywegt et al., 1997) to reveal the presence of shorter loops that create a groove rather than a tunnel. The groove presumably allows entry of the cellulose chain for subsequent cleavage. A similar groove was shown for the structure of EGIII (Sandgren et al., 2000), an endoglucanase that lacks a CBM. Cellobiohydrolase activity is essential for the hydrolysis of microcrystalline cellulose. CBHI and CBHII are the principal components of the *T. reesei* cellulase system, representing 60 and 20%, respectively, of the total cellulase protein produced by the fungus on a mass basis (Wood, 1992). The important role of CBMs for both enzymes to ensure binding and processivity has been shown clearly (Palonen et al., 1999). However, both the cellobiohydrolases are very slow at decreasing the degree of polymerization of cellulose. Endoglucanases are thought to be primarily responsible for decreasing degree of polymerization by internally cleaving cellulose chains at relatively amorphous regions, thereby generating new cellulose chain ends susceptible to the action of cellobiohydrolases (Teeri et al., 1998a). The need for five endoglucanase species in the *T. reesei* cellulase system has not been clearly explained, particularly considering that endoglucanases (with EGI and EGII as major species) represent less than 20% of the total cellulase protein of *T. reesei*. Cellobiose, the major product of CBHI and CHBII activity,

inhibits the activity of the cellobiohydrolases and endoglucanases (Holtzapple et al., 1990; Medve et al., 1998; Mosier et al., 1999). The production of at least two β-glucosidases by *T. reesei* facilitates the hydrolysis of cellobiose and small oligosaccharides to glucose. Both BGLI and BGLII have been isolated from culture supernatants, but a large fraction of these enzymes remains cell wall bound (Messner et al., 1990; Usami et al., 1990). *T. reesei* produces β-glucosidases at low levels compared to other fungi such as *Aspergillus* species (Reczey et al., 1998). Furthermore, the β-glucosidases of *T. reesei* are subject to product (glucose) inhibition (Messner et al., 1990; Gong et al., 1977; Glick and Pasternak, 1989) whereas those of *Aspergillus* species are more glucose tolerant (Decker et al., 2000; Gunata and Vallier, 1999; Watanabe et al., 1992; Yan and Lin, 1997). *T. reesei* cellulase preparations, supplemented with *Aspergillus* β-glucosidase, are considered most often for cellulose saccharification on an industrial scale (Reczey et al., 1998; Sternberg et al., 1977).

3.1.1.2 Synergism

Cellulase systems exhibit higher collective activity than the sum of the activities of individual enzymes, a phenomenon known as synergism. Four forms of synergism have been reported: (i) endo-exo synergy between endoglucanases and exoglucanases, (ii) exo-exo synergy between exoglucanases processing from the reducing and non-reducing ends of cellulose chains, (iii) synergy between exoglucanases and β-glucosidases that remove cellobiose (and cellodextrins) as end products of the first two enzymes, and (iv) intramolecular synergy between catalytic domains and CBMs (Din et al., 1994; Teeri, 1997).
Synergism between endoglucanases and cellobiohydrolases has been shown for EGI (Väljamäe et al., 1998), and EGII (Medve et al., 1998), and EGIII (Nidetzky, 1994a). However, synergism between endoglucanases has not been clearly demonstrated.

3.1.1.3 Inhibition

The rate of enzyme-mediated hydrolysis of cellulose is inhibited by products of hydrolysis and is also potentially inhibited by fermentation products if hydrolysis and fermentation are carried out at the same time. As reviewed elsewhere (Mosier et al., 1999; Philippidis et al., 1993), cellulose hydrolysis is inhibited by cellobiose and to a much lesser extent by glucose for cellulase from both *Trichoderma* spp. and *C. thermocellum*. β-Glucosidase in *T. reesei* is highly sensitive to inhibition by glucose. Whether inhibition by soluble hydrolysis products is important for microbial cellulose utilization depends on whether such products accumulate in the microenvironments in which hydrolysis occurs. Inhibition of the hydrolysis rate by soluble products has been incorporated into a substantial number of models. Competitive inhibition is the most common mechanism in the literature, but other uncompetitive and noncompetitive mechanisms have also been proposed (Zhang and Lynd, 2004). Both the

structural information (Davies et al., 1997; Teeri et al., 1998a, 1998b) and a considerable body of experimental data indicate that individual cellulase enzymes are inhibited competitively by cellobiose and glucose. However, it appears that mixtures of cellulase components can exhibit behaviour consistent with mechanisms other than competitive inhibition under some conditions (Gusakov et al., 1985a, 1985b; Gusakov and Sinitsyn, 1992; Holtzapple et al., 1984, 1990). The mechanistic basis for this phenomenon is not fully understood and has received little if any examination in the light of structural information gleaned during the 1990s.

3.1.1.4 Adsorption

The first step in cellulose hydrolysis is thus the binding of the cellulase enzymes on the surface of cellulose fibrils. It has been shown that the rate of adsorption is rapid compared to the actual hydrolytic activity of the enzymes, thus making the amount of adsorbed cellulase an important factor in the effectiveness of the reaction (Steiner et al., 1988). The mechanism of enzyme adsorption on *pure* cellulose has been widely studied, using either purified enzymes (Medve et al., 1997; Medve et al., 1998; Wood et al., 1989) or commercial mixtures (van Tilbeurgh et al., 1985; Chanzy and Henrissat, 1985; Henrissat et al., 1985). Enzymes can bind to the solid surface either specifically or non-specifically, by e.g. hydrogen bonding, electrostatic or hydrophobic interactions (Brash and Horbett, 1995). Other adsorbed proteins, as well as low-molecular weight ions in the interfacial region, may affect the adsorption. Electrostatic forces contribute to the binding, but they do not dominate proteins adsorption in all conditions (Norde and Haynes, 1995).

Working with 26 cellulase preparations, 10 of them highly purified, Klyosov (1990) showed a strong correlation between hydrolysis rates and values of the adsorption equilibrium constant. Quantitative description of the adsorption of cellulase(s) to cellulose generally involves expressing the concentration of a cellulose-enzyme complex as a function of a vector of variables relevant to cellulase adsorption that describe the state of the system. In most adsorption models, such "state variables" include the total amount of cellulase present, the total amount of substrate present, substrate-specific and enzyme-specific parameters that impact adsorption (e.g., affinity and capacity), and variables that describe the physical and chemical environment (e.g., temperature and ionic strength). Experimental determination of the concentration of cellulose enzyme complex, [*CE*], is usually carried out by taking the difference between total cellulase present and unabsorbed cellulase, e.g. for a substrate containing only cellulose:

$$[CE]=[E]-[E_f] \tag{3.1}$$

where [E] is the total concentration of binding sites on the enzyme and [E_f] is the concentration of binding sites on the enzyme not adsorbed to cellulose. Techniques for direct measurement of adsorbed enzyme would be desirable but are seldom employed (Mansfield et al., 1999). Equilibrium is assumed in many adsorption models. The equilibrium assumption is often justified by the observation that the time required for adsorbed cellulase to reach a constant value is short relative to the time required for hydrolysis. Most studies find that adsorbed cellulase reaches a constant value in 90 minutes, and many studies have found 30 min to be sufficient (Boussaid and Saddler, 1999; Chernoglazov et al., 1988; Kim et al., 1998, 1994 and 1992, Lee and Woodward, 1989; Ooshima et al., 1983; Rabinovich et al., 1983; Singh et al., 1991; Strobel et al., 1995; Stutzenberger and Lintz, 1986), whereas complete hydrolysis of cellulose usually requires a day or more. The simplest representation of adsorption equilibrium is via an equilibrium constant, K_d:

$$K_d = \frac{[E_f][C]}{[CE]} \tag{3.2}$$

where [C] is the concentration of accessible binding sites on cellulose not adsorbed to enzyme. K_d, [E_f], [C], and [CE] are taken here to have units of micromoles per litre. Other internally consistent units can also be used, and the use of units other than micromoles per litre for K_d is considered below. As an alternative to equilibrium models, some models (Converse et al., 1988; Nidetzky and Steiner, 1993, Nidetzky et al., 1994b) employ a dynamic description of adsorption such as

$$\frac{\mathrm{d}[CE]}{\mathrm{d}t} = k_f[E_f][C] - k_r[CE] \tag{3.3}$$

where $k_r/k_f = K_d$.

Studies by Rabinovich et al. (described in Klyosov, 1990) involving various cellulases and cellulose samples indicate that once a cellulase-cellulose complex is formed, the enzyme stays bound to the cellulose for a significant period (e.g., 30 min or more), during which hundreds of catalytic events occur.

3.1.2 Substrates related rate limiting factors

Important substrate parameters affecting enzymes adsorption and the overall hydrolysis process include the material crystallinity, the accessible surface area, the particle (chip) size and the lignin distribution (Chang and Holtzapple, 2000; Mooney et al., 1998; Ramos et al., 1993; Grethlein, 1985; Fan et al., 1980; Fan et al., 1981).

3.1.2.1 Crystallinity Index (CrI)

Crystallinity has often been thought of as providing an indication of substrate reactivity, and is prominently featured in the model of Wood (1975) as well as in other models. The crystallinity of dried cellulose samples can be quantitatively measured from the wide-range X-ray diffraction pattern (Krassig, 1993). Cellulose hydrolysis rates mediated by fungal cellulases are typically 3–30 times faster for amorphous cellulose as compared to high crystalline cellulose (Lynd et al., 2002). This observation led investigators in the 1980s to postulate a model for cellulose structure consisting of amorphous and crystalline fractions (Fan et al., 1980, 1981; Lee et al., 1983). If this hypothesis were correct, it would be expected that crystallinity should increase over the course of cellulose hydrolysis as a result of preferential reaction of amorphous cellulose (Betrabet and Paralikar, 1977; Ooshima et al., 1983). However, several studies have found that crystallinity does not increase during enzymatic hydrolysis (Lenze et al., 1990; Ohmine et al., 1983; Puls and Wood, 1991; Schurz et al., 1985; Sinitsyn et al., 1989). Several treatments that decrease crystallinity also increase surface area, and it has been suggested that the increased hydrolysis rates observed with substrates arising from such treatments may be due to increasing adsorptive capacity rather than substrate reactivity (Caulfield and Moore, 1974; Howell and Stuck, 1975; Lee and Fan, 1982). Comparing the hydrolysis rates on various sources of model cellulosic substrates, Fierobe et al. (2002) concluded that accessibility of cellulose is a more important factor than crystallinity index in determining the hydrolysis rate.

3.1.2.2 Degree of Polymerization

The DP of cellulosic substrates determines the relative abundance of terminal and interior h-glucosidic bonds, and of substrates for exo-acting and endo-acting enzymes, respectively.
Measurement of DP begins with dissolution of cellulose using a technique that does not alter chain length. DP can be measured with different techniques: membrane or vapor pressure osmometry, cryoscopy, ebullioscopy, determination of reducing end concentration, or electron microscopy (Krassig, 1993). The weight average polymerisation degree (DPW) can be measured based on light scattering, sedimentation equilibrium, and X-ray small angle scattering, and the viscosity average polymerisation degree (DPV) is measured based on viscosity. The distribution of DPs among a population of cellulose molecules can be measured by size exclusion chromatography (Yau et al., 1979). Cellulose solubility decreases drastically with increasing DP due to intermolecular hydrogen bonds. The DP of cellulosic substrates varies greatly, from <100 to >15000, depending on substrate origin and preparation.

3.1.2.3 Lignin

Clearly, the composition of the raw material as such will influence the cellulase adsorption. The removal or redistribution of lignin has been shown to influence the degradability of

lignocellulose substrates (Converse and Optekar, 1993; Lynd et al., 2002). The negative influence of lignin on enzymatic hydrolysis has several explanations. For a representative lignocellulosic substrate, cellulases have been found to adsorb both to the cellulosic and lignin components of the substrate (Sutcliffe and Saddler, 1986). This implies that lignin could have a negative effect on the hydrolysis, since there would be a competitive unproductive adsorption of cellulase on the lignin (Sutcliffe and Saddler, 1986; Bernardez et al., 1993; Ooshima et al., 1990; Eriksson et al., 2002). In addition, it has been suggested that residual lignin can act as a steric hindrance to cellulolytic enzymes, thus preventing the effective binding to cellulose chains (Mandfield et al., 1999).

3.1.2.4 Accessibility

The 3D structure of substrate particles (including microstructure) in combination with the size and shape of the cellulase enzymes under consideration determine whether β-glucosidic bonds are or are not accessible to enzymatic attack. Cellulosic particles have both external and internal surfaces. In general, the internal surface area of cellulose is 1–2 orders higher than the external surface area (Chang et al., 1981), but this is not always the case, for example, in the case of bacterial cellulose. The internal surface area can be measured by small angle X-ray scattering (SAXS), mercury porosimetry, water vapor sorption, and size exclusion (Grethlein, 1985; Neuman and Walker, 1992; Stone et al., 1969). The internal surface area of porous cellulose particles depends on the capillary structure and includes intraparticulate pores (1–10 nm) as well as interparticulate voids (>5 Å) (Marshall and Sixsmith, 1974). Grethlein (1985) found linear correlations between the initial hydrolysis rate of pretreated biomass and the pore size accessible to a molecule with a diameter of 51 Å, similar to the size of *T. reesei* cellulase components. But the surface exposed to dextran cannot distinguish the specific active cellulose surface area at which enzymatic hydrolysis occurs from the surface area which is not a site for enzymatic attack (Chanzy et al., 1984; Gilkes et al., 1992; Lehtio et al., 2003), resulting in potential overestimation of effective cellulaseaccessible area. External surface area is closely related to shape and particle size, and can be estimated by microscopic observation (Gilkes et al., 1992; Henrissat et al., 1988a; Reinikainen et al., 1995; Weimer et al., 1990; White and Brown, 1981). For example, the external surface area of Avicel is 0.3 m^2/g (Weimer et al., 1990). Increasing cellulase adsorption and cellulose reactivity with decreasing particle size has been reported (Kim et al., 1992; Mandels et al., 1971). However, this may be due to causes other than increased external area, perhaps decreasing mass transfer resistance, since external surface is thought to be a small fraction of overall surface area for most substrates. The gross cellulose accessibility is generally measured by the sorption of nitrogen, argon or water vapor, dimensional change or weight gain by swelling in water or organic liquids, and exchange of H to D atoms with D_2H. The most widely used procedure for specific surface area (SSA) is the Brunauer-Emmett-Teller (BET) method using nitrogen

adsorption. Due to variations in the experimental conditions such as adsorption time, vacuum time and vacuum pressure (Marshall and Sixsmith, 1974), sample preparation (Grethlein, 1985; Lee et al., 1983), and sample origin and features (Marshall and Sixsmith, 1974; Weimer et al., 1990), a wide range of gross area values have been reported in the literature even for the same substrate. The typical SSA values for Avicel span the range 1.8–22 m^2/g (Fan et al., 1980; Lee et al., 1983; Marshall and Sixsmith, 1974). Because a nitrogen molecule is much smaller than cellulase, it has access to pores and cavities on the fiber surface that cellulase cannot enter. Therefore, there is limited basis to infer that SSA measured using the BET method is a key determinant of enzymatic hydrolysis rate (Mansfield et al., 1999). Recently, new semiquantitative procedures (Modified Simons'staining technique and water retention values measurements) have been developed and effectively used to assess the accessibility of lignocellulosic substrates (pine) after different pretreatment methods and operating conditions (Chandra et al., 2008; Chandra et al., 2009).

3.2 Motivations for the experimental investigation

In view of above, it is clear that the pretreatment of lignocellulosic material is an important step to improve enzymatic hydrolysis of the polymeric carbohydrates into simple sugars, which is necessary for e.g. conversion of lignocellulose to ethanol or other products by fermentation. The rate of hydrolysis and the cost of the enzymatic degradation step are still quite substantial, although much progress has been made in decreasing the cost of enzymes (Himmel et al., 1999; Gregg et al., 1998). Optimization of pretreatment methods, such as acid catalyzed steam explosion, is to a large extent done by empirical methods based on direct measurements of the digestibility of obtained material. An increased understanding of the desired properties of the pretreated material leading to an efficient enzymatic hydrolysis would, however, clearly be beneficial, allowing for both new leads for pretreatment development and *a priori* predictions of degradability of pretreated materials, and may also facilitate the development of better enzymes.

Formation of enzyme-cellulose complexes is a prerequisite for cellulose hydrolysis, and such complexes are a central feature of most conceptual and quantitative models for cellulose hydrolysis. Enzyme adsorption is therefore a crucial phenomenon and, as it acts as a typical surface phenomenon, it is likely that surface properties have a huge effect on its mechanism, rate and extent. Unfortunately, the description of the system and the identification of the phenomena affecting the process become significantly more complicated as soon as a "real" lignocellulosic material is treated. In general, there are surprisingly few reports on the effect of directly measured specific surface area on the hydrolysis rate in lignocellulosic materials (Grethlein, 1985; Wong et al., 1988; Converse et al., 1990; Sinitsyn et al. 1991; Thompson et al., 1992). The choice of pretreatment conditions will furthermore most certainly affect the

surface area – and thereby the available surface area for enzyme adsorption - but may also change the ratio between accessible lignin and cellulose surface areas. The objective of the study was to investigate enzyme adsorption and hydrolysis of pretreated spruce and wheat straw and relate these to the morphological effects caused by the treatment. Avicel cellulose was included in the study as a model substrate. Enzyme adsorption measurements were made using three different methods; direct protein adsorption measurements by the Bradford method, assessment of Filter Paper Activity (FPA), which returns a "total" cellulase adsorption, and assessment of hydroxyethylcellulose (HEC) hydrolysis, which gives a measurement of adsorbed endoglucanases. The pretreated materials were analyzed for their carbohydrate and lignin contents, and the total specific surface area and the pore size distributions were determined using BET. The pretreated materials were also studied using SEM. The correlation between enzyme adsorption properties, hydrolysis, and the material morphology is discussed.

3.3 Materials & Methods

3.3.1 Substrates

A comparative study was carried out on seven different substrates: Avicel, taken as substrate reference, spruce pre-treated at two different conditions and wheat straw pre-treated at four different conditions. Avicel PH-101 (i.e. microcrystalline cellulose) was purchased from Fluka. Product number: 11363 (EC No. 2326749. Spruce hydrolyzates were prepared by steam explosion in a batch reactor with SO_2 impregnation at the department of Chemical Engineering, Lund University using a 10 L reactor (previously described by Stenberg et al., 1998). Two different pretreatment conditions were used for the same spruce material: *a)* temperature 210°C, SO_2 content 2.5% (w/w) and residence time 5 min (denoted S1 in the following), *b)* temperature 190°C, residence time 10 min, same SO_2 content as before (S2). The first pretreatment condition was chosen based on previous experience to produce a hydrolyzate, which was well suited for enzymatic degradation without a too large degradation of formed monomeric sugars from the hemicellulose. Four different pretreatments were explored for wheat straw. In all cases a sulphuric acid soaking at 0.2% (w/w) was made of the straw material, which was followed by pretreatment at different conditions. The mildest conditions were at a temperature of 190°C and residence time of 2 min (denoted WS1 in the following). The second conditions were at a temperature of 190°C and a residence time of 5 min (WS2). Thirdly a temperature of 190°C, and a residence time 10 min was used (WS3), and finally a temperature of 210°C with a residence time of 10 min was tested (WS4). In the case of wheat straw, the conditions which are reported to give the best overall process performances, i.e. a good enzymatic hydrolysis without a too large degradation of monomeric

sugars from the hemicellulose, are the third conditions (WS3). All pretreated substrates were washed with distilled water and stored at 4°C. The compositional analysis of the materials was made using NREL (National Renewable Energy Laboratories) standard procedures (Sluiter et al., 2008; Ruiz and Ehrman, 1996). The results are reported in Table 3.1 and 3.2, for the solid and the liquid fraction, respectively.

Table 3.1 *Composition of the solid fractions in % on a dry weight basis of the steam pretreated substrates studied. S1 and S2 refer to pretreated spruce material, whereas WS1, WS2, WS3 and WS4 refer to pretreated wheat straw material.*

Material	WIS [%]	Glucan [%]	Mannan [%]	Xylan [%]	Galactan [%]	Arabinan [%]	AIL [%]
Spruce, S1	14.9	46.7	1.9	1.6	1.2	1.2	42.0
S2	13.4	48.6	2.9	2.1	1.2	1.2	35.7
Wheat straw, WS1	14.9	37.8	1.8	9.1	0.0	1.7	29.2
WS2	16.0	38.7	0.0	8.2	0.0	1.4	29.2
WS3	13.4	41.4	0.0	1.4	0.0	1.0	32.2
WS4	10.0	47.4	1.5	0.0	0.0	1.1	30.9

AIL = Acid insoluble lignin

Table 3.2 *Composition of the liquid fractions obtained after steam pretreatment of the substrates studied. S1 and S2 refer to pretreated spruce material, whereas WS1, WS2, WS3 and WS4 refer to pretreated wheat straw material.*

	Glucose[g/L]	Xylose g/L]	Galactose g/L]	Arabinose[g/L	Mannose g/L]
Spruce, S1	12.20	8.71	3.21	2.07	19.48
S2	9.17	10.10	3.58	2.38	23.04
Wheat straw, WS1	5.195	46.971	4.931	8.396	0.000
WS2	5.727	48.555	5.139	8.098	0.000
WS3	5.275	41.844	4.465	5.165	1.824
WS4	3.584	18.475	2.216	2.397	1.307

3.3.2 Enzymes

A commercial cellulase mixture (Celluclast 1.5L provided by Novozymes A/S, Bagsvaerd, Denmark) was used in the experiments. The cellulase enzyme had an activity of 46.8 FPU/mL. No extra β-glucosidase was supplemented in the experiments.

3.3.3 BET measurements

The Brunauer-Emmett-Teller (BET) method - often used for the determination of the specific surface area of inorganic catalysts - is based on nitrogen adsorption onto the material surface at different pressures. Surface area, total pore volumes, at a relative pressure of about 0.994, and pore size distributions were determined on a Micromeritics ASAP 2400 after outgassing for 10 days at 40°C. Before degassing, the materials were dried. Different drying conditions were chosen in order to investigate the impact on the biomass structure of the dewatering process. Some samples were dried for 48 h in an oven at 105°C, whilst other samples were dried for 5 days at room temperature (20°C). Avicel, stored at room temperature, was not further dried before degassing.

3.3.4 Adsorption isotherms studies

Adsorption isotherms studies for the pretreated substrates whose BET surface had been assessed were conducted at a chosen adsorption time of 90 min and at constant temperature using different enzyme-substrate ratios. It has been widely observed that the time required for adsorbed cellulase to reach a constant value is short relative to the time required for hydrolysis. Different concentrations of enzyme solution were added to the substrate in 50 mL plastic Falcon test tubes at a final dry matter loading of 10 g/L. The pH was adjusted at 4.8 by addition of NaOH. After 90 minutes of incubation at the selected temperature, the supernatant was collected, centrifuged for 5 minutes at 3500 rpm and filtered through low protein binding syringe filters (DISMIC® 10 – 13 CP, Cellulose Acetate, pore size 0.20 μm). The residual cellulase content or activity in the liquid fraction was assessed using three different assays: the Bradford method for overall protein content determination, the Filter Paper Activity (FPA) assay for the overall CBHs and EGs activity, and finally the hydroxyethylcellulose (HEC) assay for the determination of the endoglucanase activity. The experiments were first performed at 4°C to avoid changes in substrate properties due to extensive hydrolysis. Afterwards, a temperature of 30°C, which corresponds to the temperature of the hydrolysis experiments, was chosen. With concern to the enzyme preparations, we investigated a range of dilutions between 10% v/v enzyme (5.4 mg protein/ml) to 0.03% v/v enzyme (0.02 mg protein/ml).

The filtrate was analyzed with the three assays mentioned above, according to the procedures described by Ghose (1987) and Bradford (1976). The amount of bound cellulase at a given time point was calculated as the difference between the initial cellulase activity (or protein concentration) and the measured cellulase activity (or protein concentration) in the liquid fraction at that time.

3.3.5 Hydrolysis studies

Hydrolysis experiments were performed in 300 mL baffled Erlenmeyer flasks, at a pH value of 4.8 and a temperature of 30°C, in distilled deionised water, using Avicel, the two differently pretreated spruce samples, and the four differently pretreated wheat straw samples as substrates. The WIS (Water Insoluble Solids) content was 10 g/L (i.e. about 1% w/v) and the total volume was 200 mL. Two different enzyme loads were tested: 2 mL and 0.067 mL, corresponding to 47 FPU/g WIS and 1.6 FPU/g WIS, respectively. The experiments started by pipetting the commercial enzyme solutions (Celluclast 1.5) into the substrate solutions. To ensure proper mixing, the flasks were put in a temperature controlled shaker. The incubation time was 30 h and samples were withdrawn after 1, 2, 3, 4, 6, 8, 10, 20, 30 h to monitor hydrolysis. The experiments were carried out without ensuring sterile conditions and without addition of antibiotics as the incubation time was too short to allow for significant contamination effects. Duplicates experiments were made in all cases. Each sample was first centrifuged, than filtered through a small syringe filter (DISMIC® 13 – 13 CP, Cellulose Acetate, pore size 0.20 μm) to remove particles. The filtrate, without any further pretreatment, was analyzed by HPLC (Shimazdu, Kyoto, Japan) to measure hydrolysis product (glucose and cellobiose). The HPLC was equipped with a refractive index detector (RID-10A). The column was a Biorad Aminex HPX-87P (Hercules, CA, USA) with de-ashing refill cartridges prior to the main column. The eluent was purified water at a flow of 0.6 mL/min and the temperature was 85°C. The cellulose conversion, x, was calculated using equation 1:

$$X = \frac{0.9G + 0.95G_2}{[C]_0} \tag{3.4}$$

where $[C]_0$ is the initial cellulose concentration, $[G_2]$ is the concentration of cellobiose and $[G]$ is the concentration of glucose, all in (g/L).

3.3.6 Scanning Electron Microscopy

Pretreated material for SEM were washed with deionized water and then dried at 30°C for at least 24 h. A sample of each material was mounted on a stub (d = 10 mm) using double-coated tape. They were then coated with gold in a Balzers SCD004 sputter coater and finally examined in a JEOL JSM 6700F (FegSEM) microscope, operating at an accelerating voltage of 5 kV and an average working distance of 8 mm.

3.4 Results

3.4.1 BET measurements of surface area and pore size distribution

Since the first step in hydrolysis will involve an interaction between the endoglucanases and cellobiohydrolases adsorbing onto the cellulose surface, the specific surface area as well as the pore size distribution is likely to play a significant role for at least the initial rate of hydrolysis. The internal surface area of porous cellulose particles depends on the capillary structure and includes intraparticle pores (1–10 nm) as well as interparticle voids (>5 Å) (Marshall and Sixsmith, 1974). The pores size distribution is important in determining the fraction of pores accessible to the enzymes. The pretreated materials as well as the Avicel material were subjected to BET analysis, providing information about the specific surface area (Table 3.3) as well as pore size distribution (Figure 3.1).

Table 3.3 *Measured specific surface area (SSA) by BET for the seven substrates considered in the study.*

Substrate	Room temperature drying [m^2/g]	Oven drying (105 °C) [m^2/g]
Avicel	1.1±0.0	**N.A**
Spruce, S1	2.0±0.1	2.4±0.1
S2	1.6±0.1	1.2±0.0
Wheat straw, WS1	1.9±0.2	2.5±0.1
WS2	2.1±0.3	3.0±0.3
WS3	2.8±0.2	3.3±0.1
WS4	3.1±0.0	4.1±0.2

N.A. = Not analyzed

*Error of measurement ± 0.9%

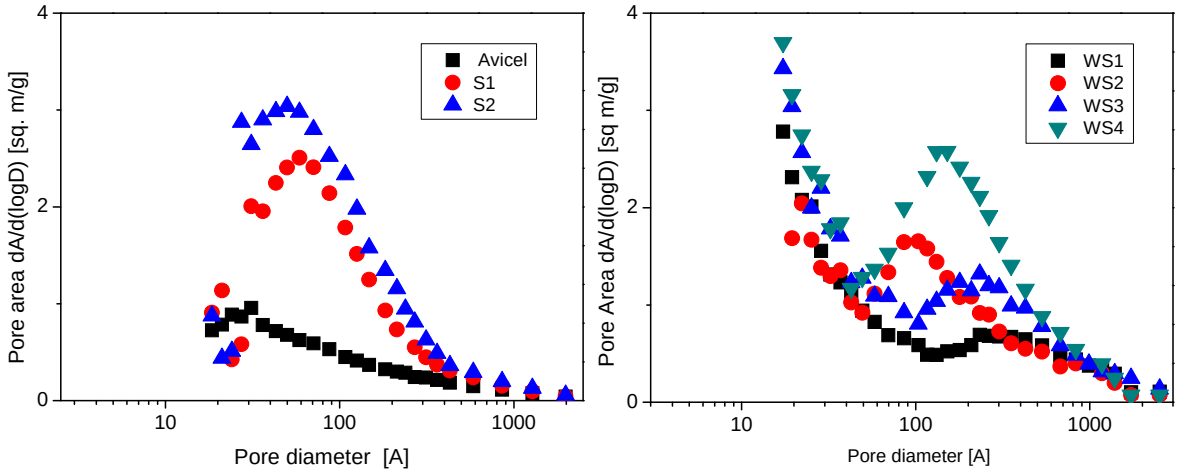

(a) (b)

Figure 3.1 *Pore area distribution from BET measurements. (a) Pretreated spruce and (b) Pretreated wheat straw.*

The pretreated spruce materials, S1 and S2, have rather similar pore size distribution patterns, with a peak at 80-100 Å (Figure 3.1a), whereas the wheat straw materials have their maximum at larger pore areas (Figure 3.1b). Avicel is characterized by a more flat distribution with a weak maximum at 30 Å. The fraction of the total surface accessible to enzymes for each substrate, assuming a minimum required pore size of 54 Å, was calculated from the distributions (Table 3.4). With the exception of (untreated) Avicel and the mildest pretreated wheat straw (WS1), the accessible fraction was relatively similar for the different materials (about 65% of the total specific surface area).

Table 3.4 *Calculated fraction of accessible SSA for the seven substrates considered in the study.*

Substrate	Room temperature drying	Oven drying (105 °C)
Avicel	0.43	**N.A.**
Spruce, S1	0.67	0.69
S2	0.64	0.68
Wheat straw, WS1	0.55	0.48
WS2	0.67	0.60
WS3	0.67	0.59
WS4	0.66	0.66

N.A. = Not analyzed

The drying procedure was expected to affect the materials, and to assess the magnitude of these effects drying at two different temperatures – room temperature and 105 ºC (i.e. standard oven drying) - were tested for all the pretreated materials (Table 3.3-3.4 and Figure

3.2). The fraction of pores smaller than 200 Å tended to increase of for substrates dried in the oven, especially for the wheat straw materials (cf. Figure 3.2c-f).

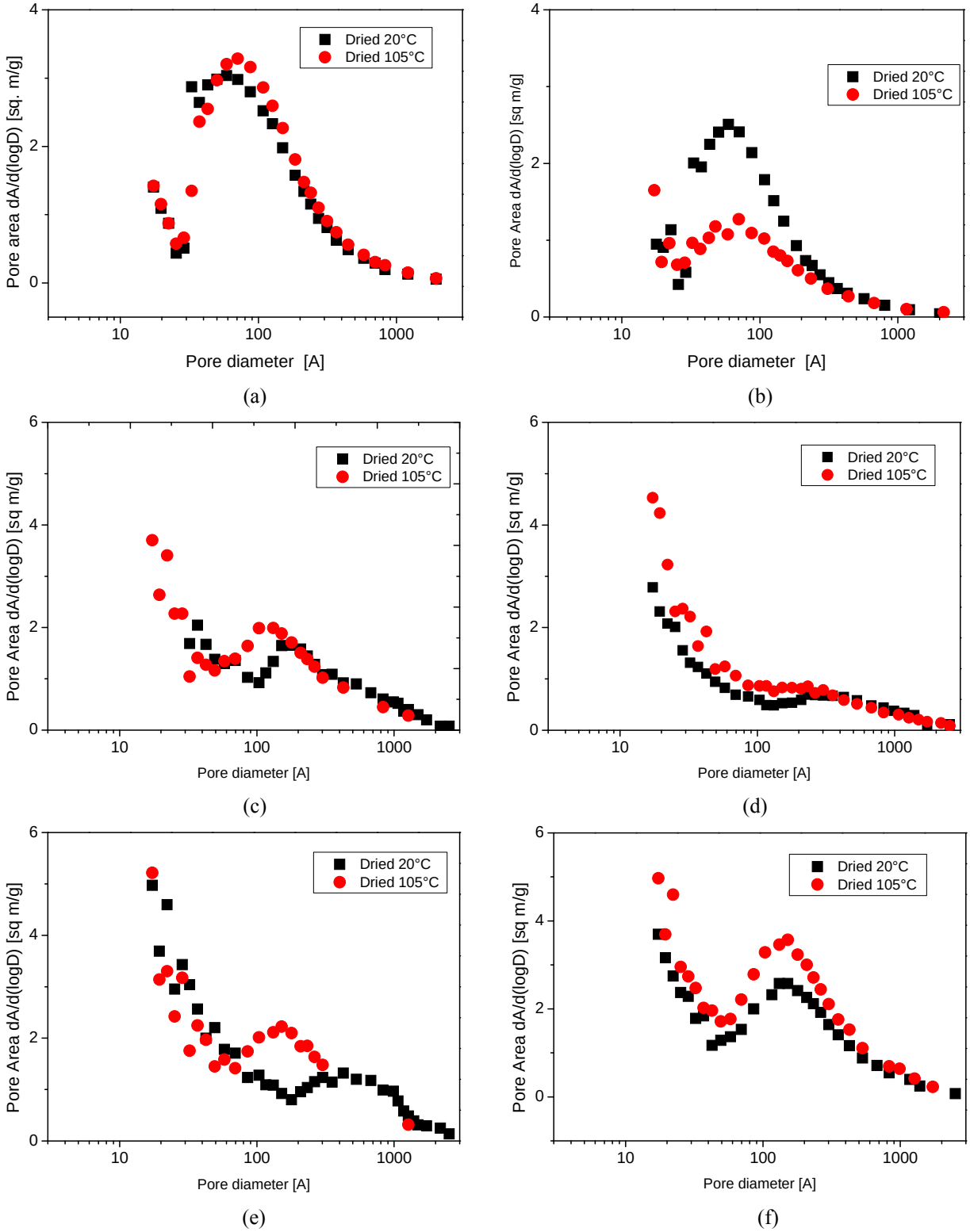

Figure 3.2 *Effect of drying temperature on pore area distribution from BET measurements. (a) S1, (b) S2, (c) WS1, (d) WS2, (e) WS3 and (f) WS4.*

3.4.2 Adsorption experiments

Following the determination of surface area characteristics, the adsorption properties of the materials were assessed. The protein concentration, as well as the hydrolytic activity on reference substrates (filter paper and HEC) in the liquid phase were determined after incubation of various amounts of cellulase enzymes with a fixed amount of substrate, giving the adsorption isotherms - i.e. the relation between the amount of adsorbed enzyme (or activity) and the amount of added enzyme (or activity) (Figure 3.3-3.5). As to be expected, the different macromolecular compositions of the substrates spruce and wheat resulted in qualitatively different adsorption properties of these materials when using the Bradford protein assay. By comparing the isotherms for Avicel, and the two spruce materials (S1 and S2) (Figure 3.3a) it can be concluded that the extent of adsorption follows the measured BET areas. This was also seen for the different wheat straw material (Figure 3.3b).

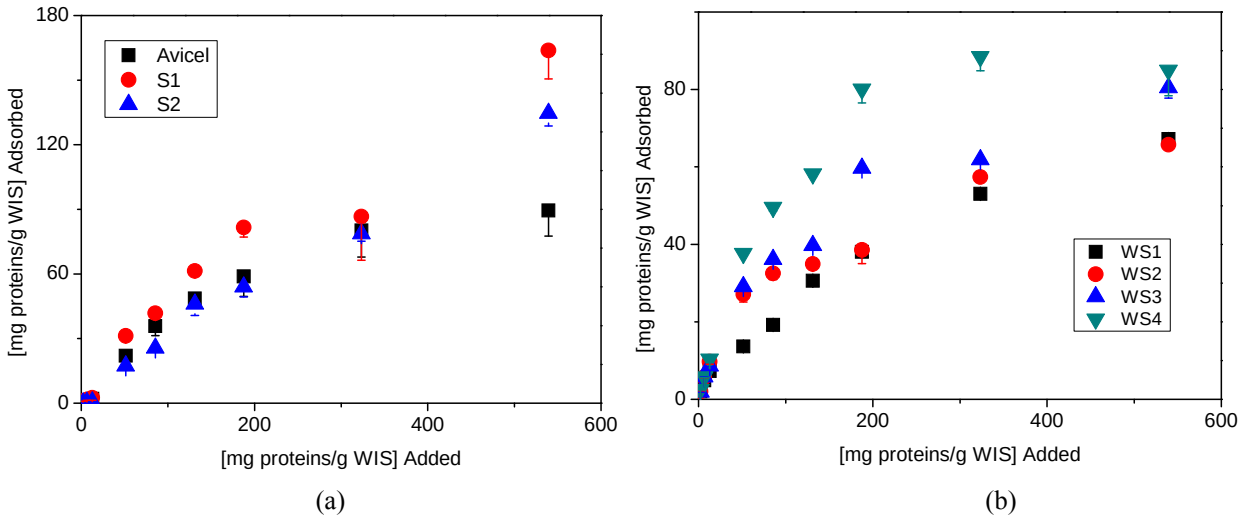

Figure 3.3 *Adsorption isotherms at 4°C using the Bradford protein assay. (a) Pretreated spruce: S1, S2 and Avicel. (b) Pretreated wheat straw: WS1, WS2, WS3, WS4 and Avicel. The standard deviations are given only on one side of the data points in order to facilitate reading. (Note that (a) and (b) have a different y-axis scale)*

By comparing the isotherms, based on FPA, it can be concluded that the extent of adsorption follows the available specific surface area very well with S1 giving higher adsorption than S2 and Avicel, and a consistently positive correlation between adsorption and available specific surface area for the wheat straw materials. The wheat straws also show higher adsorption than the spruce materials (Figure 3.4). A different behaviour is, however, seen when the HEC assay was used. The adsorption isotherm for Avicel is higher than for S2 and most of the wheat straw materials.

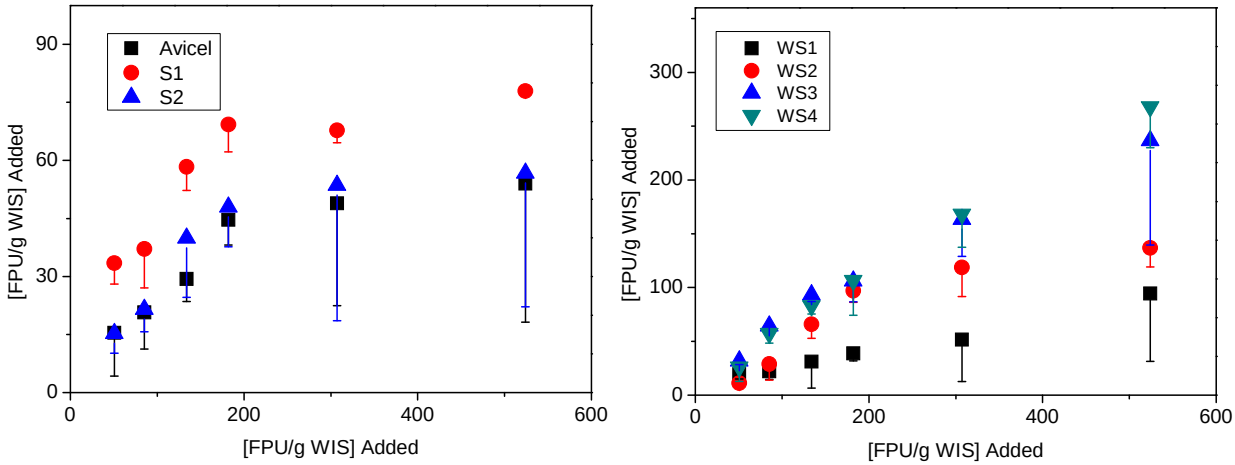

(a) (b)

Figure 3.4 *Adsorption isotherms at 4°C using the FPA assay. (a) Pretreated spruce: S1, S2 and Avicel. (b) Pretreated wheat straw: WS1, WS2, WS3, WS4 and Avicel. The standard deviations are given only on one side of the data points in order to facilitate reading. (Note that (a) and (b) have a different y-axis scale)*

In addition, when considering the available specific surface area the pretreated wheat straw materials have relatively low adsorption compared to the spruce materials and WS1 and WS2 have practically no EG adsorption at all (Figure 3.5). This may be explained by a different behaviour of the endoglucanases in a lignocellulosic matrix.

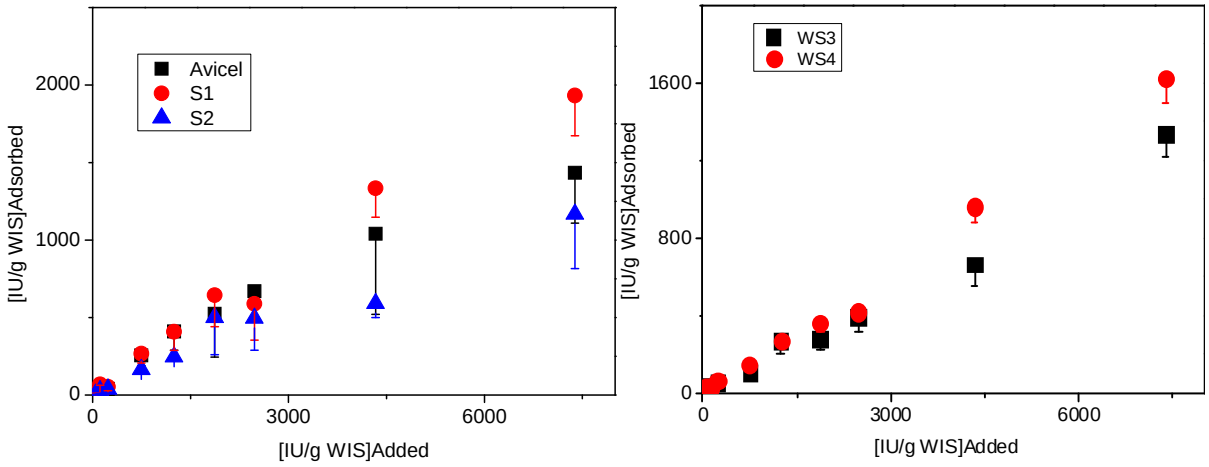

(a) (b)

Figure 3.5 *Adsorption isotherms at 4°C using the HEC assay. (a) Pretreated spruce: S1, S2 and Avicel. (b) Pretreated wheat straw: WS1, WS2, WS3, WS4 and Avicel. The standard deviations are given only on one side of the data points in order to facilitate reading. (Note that (a) and (b) have a different y-axis scale)*

The effect of temperature on protein adsorption was investigated by running the adsorption experiments on S1, S2 and Avicel also at 30°C (Figure 3.6). However, no significant changes in the amounts adsorbed could be found as a result of different temperature in this study (cf. Figure 3.7) indicating that the enzyme adsorption can be discussed and related to the hydrolysis experiments.

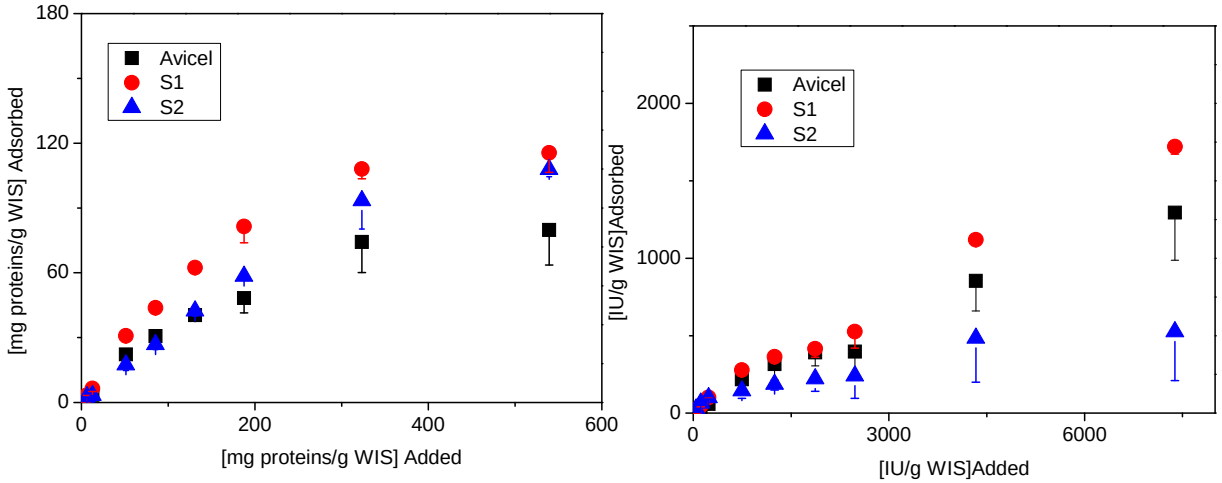

(a) (b)

Figure 3.6 *Adsorption Experiments. Ratio between the amount of enzyme adsorbed vs. the amount of enzyme added for different substrates at 30°C determined through Bradford method (a) and HEC assay (b). The error bar has been reported only below the experimental point to facilitate the reading; obviously, error is symmetrical.*

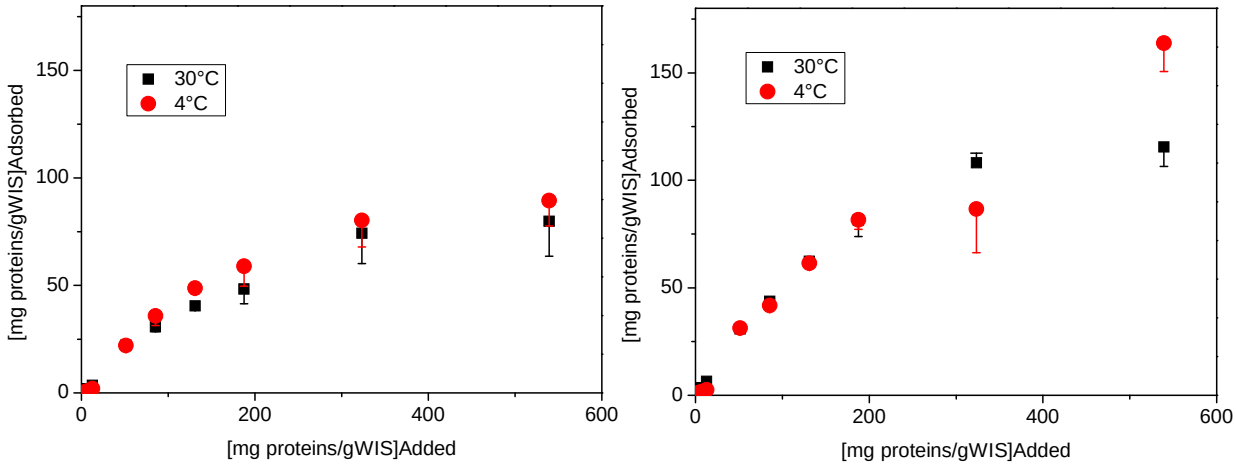

(a) (b)

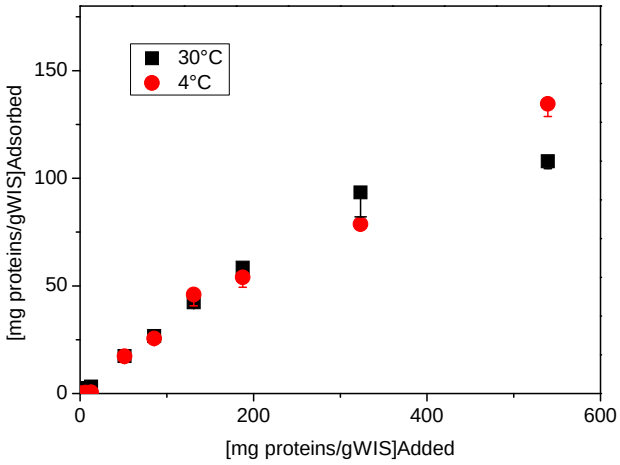

(c)

Figure 3.7 *Effect of temperature on the adsorption isotherms for pretreated spruce using the Bradford protein assay. (a) Avicel, (b) S1 and (c) S2. Adsorption experiments were run at 4°C and 30°C.The standard deviations are given only on one side of the data points in order to facilitate reading.*

There are conflicting reports on the effect of temperature on the adsorption of cellulases. It has been observed that an increase in temperature may cause either a decrease (Kim et al., 1992; Ooshima et al., 1983) or an increase (Kyriacou et al., 1988) in the adsorption of cellulases. Other studies (Tomme et al., 1990; Lee et al., 1982) have reported only a small effect of the temperature on the adsorption even when changing the temperature from 4°C to 50°C.

3.4.3 Hydrolysis experiments

Enzymatic hydrolysis studies were performed to assess the relation between the amount of enzyme adsorbed and the rate of hydrolysis. Glucose and cellobiose concentrations were measured during the first 30 h of hydrolysis for high (47 FPU/g WIS) (Figure 3.8 and 3.9) and low (1.6 FPU/g WIS) enzyme dosages (Figure 3.9 and 3.10).

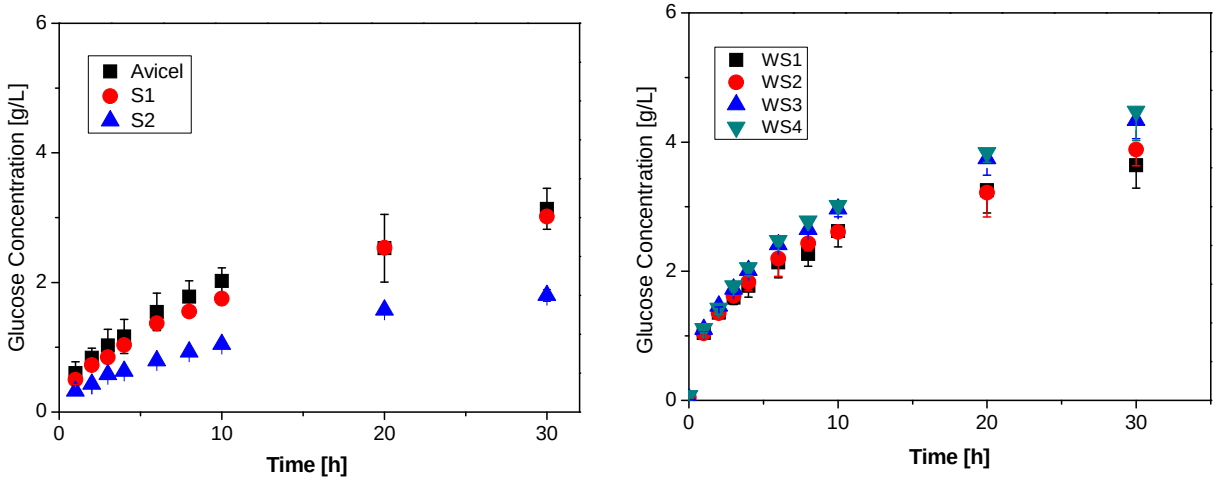

(a) (b)

Figure 3.8 *Sugar release during enzymatic hydrolysis using at high enzyme loading. (a) shows glucose concentration profile, respectively, for S1, S2 and Avicel. And (b) shows glucose concentration profile, respectively, for WS1, WS2, WS3, WS4. The standard deviations are given only on one side of the data points in order to facilitate reading.*

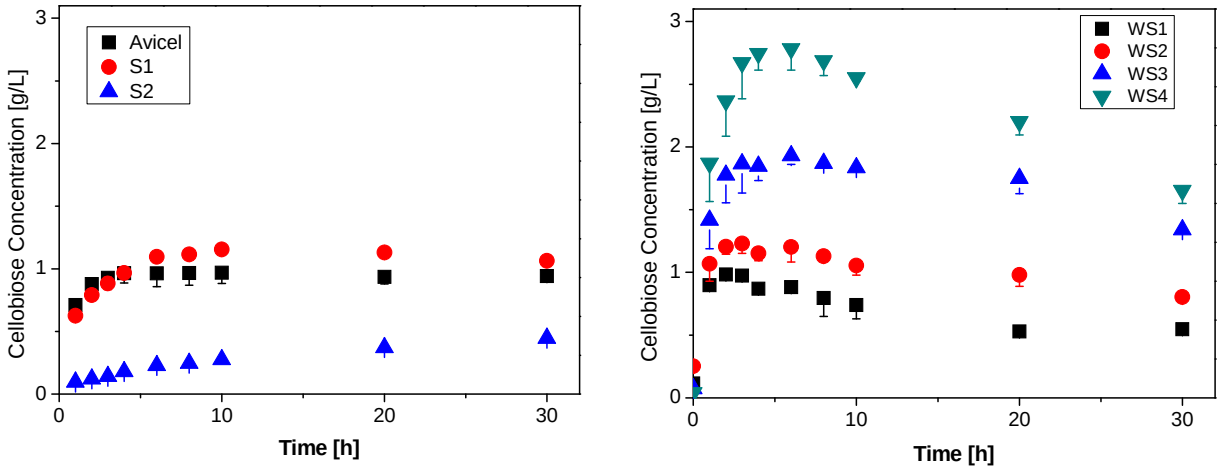

(a) (b)

Figure 3.9 *Sugar release during enzymatic hydrolysis using at high enzyme loading. (a) shows cellobiose concentration profile, respectively, for S1, S2 and Avicel. And (b) shows cellobiose concentration profile, respectively, for WS1, WS2, WS3, WS4. The standard deviations are given only on one side of the data points in order to facilitate reading.*

Interestingly, the glucose profiles for Avicel and S1 nearly overlap. The rate of hydrolysis is significantly lower for the S2 material, in agreement with the specific surface area and adsorption isotherms. Also for wheat straw, a higher specific surface area gives a higher rate of hydrolysis although the glucose profiles are close to each other. The conversion after 4 h

(Table 3.5) is higher for S1 than for Avicel and S2, at both high and low enzyme dosage. The initial reactivity of wheat straw samples is much higher compared to the spruce materials, and increases from WS1 to WS4, as pretreatment severity increases, in the case of high enzyme load.

Table 3.5 *Cellulose conversion after 4 hours hydrolysis for the seven substrates considered in the study.*

Substrate	Conversion at high enzyme dosage [%]	Conversion at low enzyme dosage [%]
Avicel	19.7	1.9
Spruce, S1	39.6	3.3
S2	15.6	2.3
Wheat straw, WS1	64.2	9.2
WS2	70.9	7.7
WS3	84.0	8.0
WS4	91.8	6.1

The difference in conversion is partly maintained also after 30 h (Table 3.6). However, at the higher enzyme load the conversion for all the wheat straw substrates is almost complete for all differently pretreated materials, with the exception of WS1. At the lower enzyme dosage the conversion is rather similar for the different straw materials, but surprisingly slightly lower for WS4.

Table 3.6 *Cellulose conversion after 30 hours hydrolysis for the seven substrates considered in the study.*

Substrate	Conversion at high enzyme dosage [%]	Conversion at low enzyme dosage [%]
Avicel	37	4.6
Spruce, S1	80	6.7
S2	42	4.0
Wheat straw, WS1	96.8	25.6
WS2	100	24.1
WS3	100	23.6
WS4	100	19.4

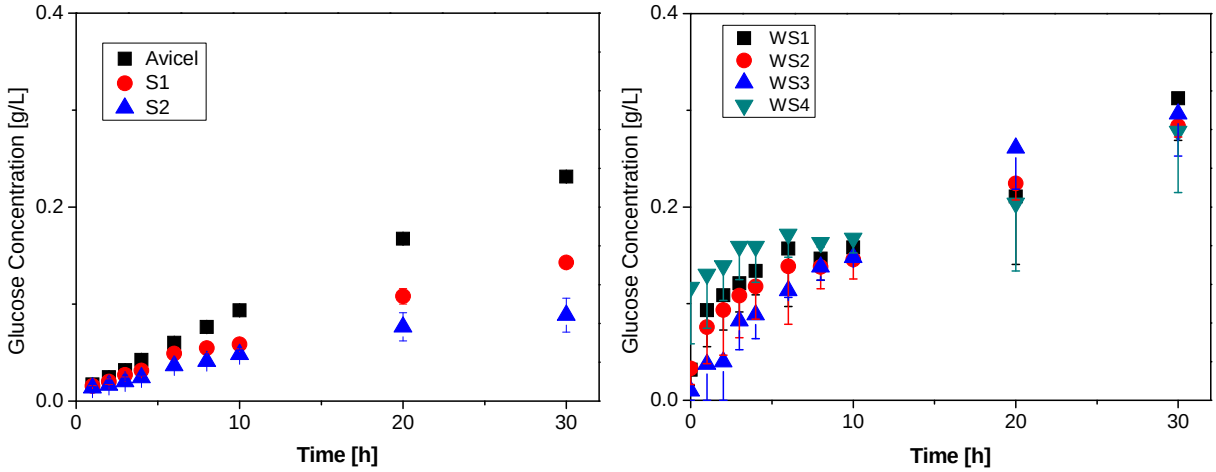

(a) (b)

Figure 3.10 *Sugar release during enzymatic hydrolysis using at low enzyme loading. (a) shows glucose concentration profile, respectively, for S1, S2 and Avicel. And (b) shows glucose concentration profile, respectively, for WS1, WS2, WS3, WS4. The standard deviations are given only on one side of the data points in order to facilitate reading.*

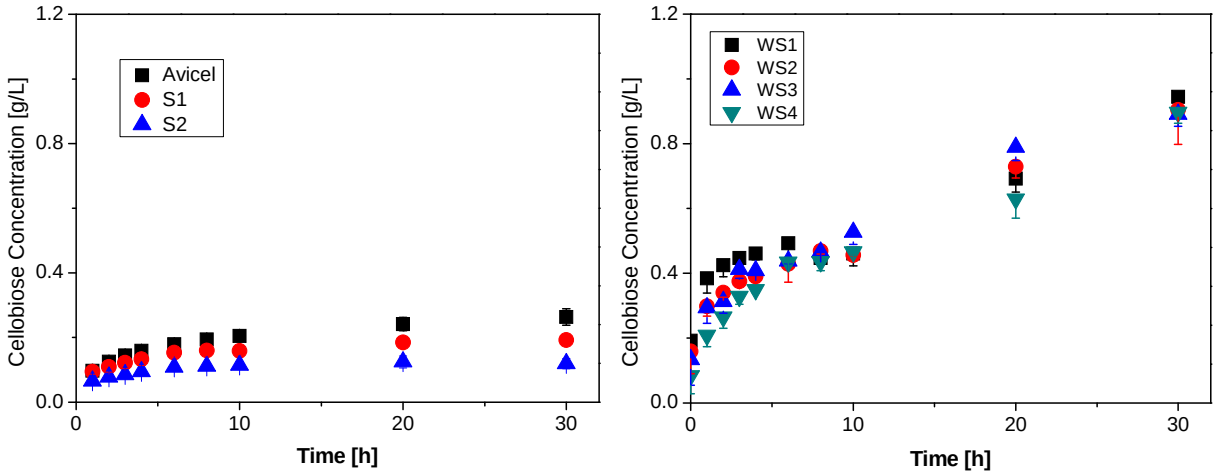

(a) (b)

Figure 3.11 *Sugar release during enzymatic hydrolysis using at low enzyme loading. (a) shows cellobiose concentration profile, respectively, for S1, S2 and Avicel. And (b) shows cellobiose concentration profile, respectively, for WS1, WS2, WS3, WS4. The standard deviations are given only on one side of the data points in order to facilitate reading.*

3.4.4 SEM pictures analysis

The pretreated materials were analyzed with SEM to get an appreciation of the morphological changes. During pretreatment, the natural structures of lignocellulose are broken-up, leaving a highly heterogeneous solid fraction (Brownell and Saddler, 1987; Donaldson et al., 1988; Zeng et al., 2007; Kristensen et al., 2008). Several spots were therefore studied in each material. The results from the SEM analysis illustrate the typical changes in structure of steam-exploded wheat straw (Figure 3.12) and spruce (Figure 3.13) at different pretreatment severities. In the wheat straw samples the individual fibres and cell types are partially separated (Figure 3.12A, D, G and J). Fragments of broken cell-walls also seem to have been produced to some extent in all pretreatments of wheat straw. At higher magnification the surface of the individual fibres can be examined (Figure 3.12B, E, H and K). Already at the mildest pretreatment condition some deposited cell-wall fragments can be seen on the fibres (Figure 3.12B). However, this gets more accentuated at harsher pretreatment conditions (Figure 3.12E, H and K). At more severe pretreatment, the outer lignin-rich cell-wall structures appear to be extensively disrupted, exposing the inner layers of the cell-wall (Figure 3.12H and K).

Interestingly, harsher pretreatment seems to result in a more porous surface, as seen at the highest magnification (cf. Figure 3.12C, F, I and L), which has not been illustrated with SEM before. Possibly, lignin is more extensively re-distributed at more severe pretreatments. At the highest magnification droplet-like structures can be seen which may be condensed lignin (Brownell and Saddler, 1987; Donaldson et al., 1988; Kristensen et al., 2008). The uneven surfaces seen in Figure 3.12I and 3.12L could also be a result of hemicellulose removal since WS3 and WS4 contain significantly less hemicellulose (Table 3.1). These results agree satisfactorily with, and may explain, the higher specific surface area from the BET analysis.

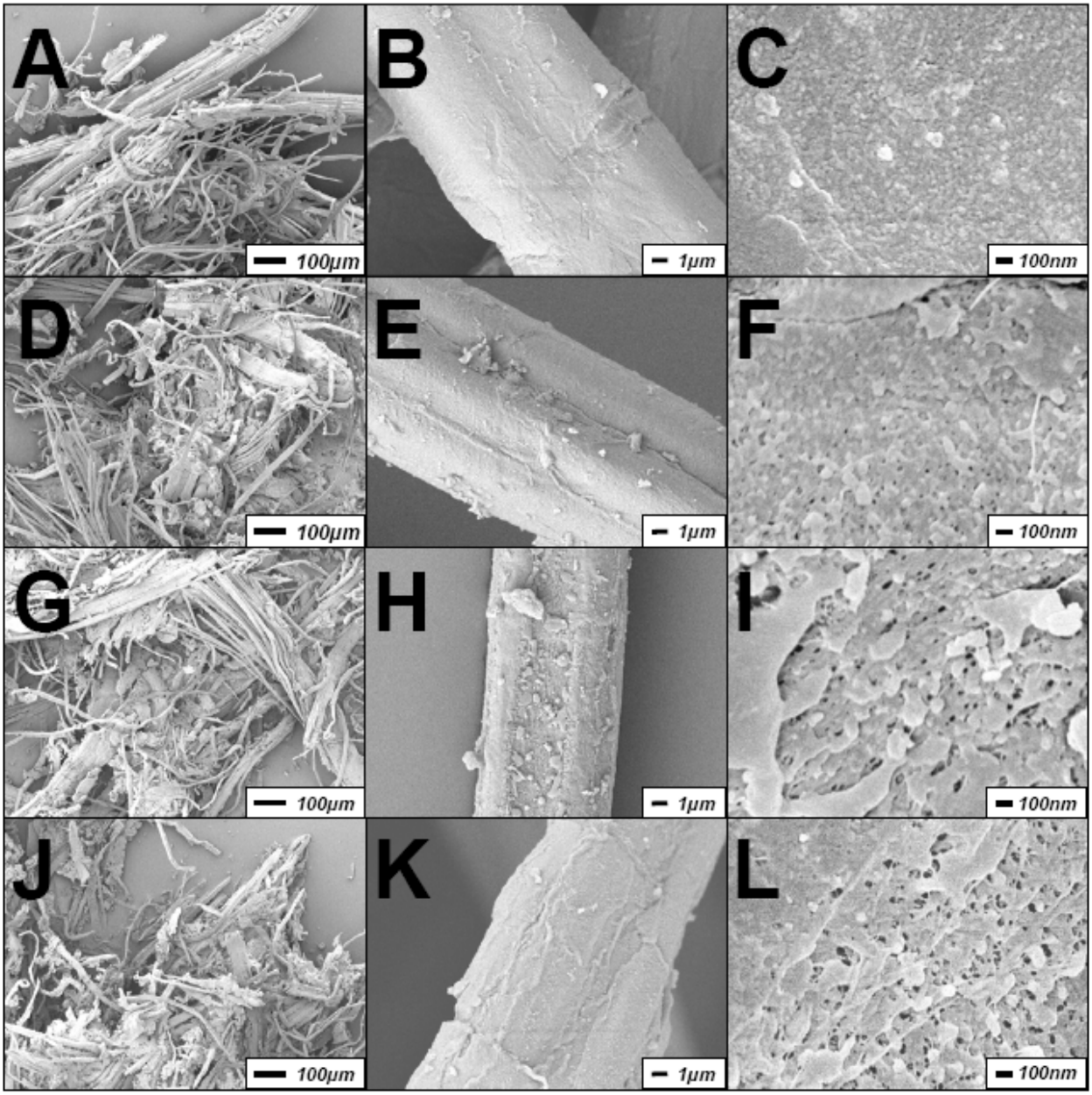

Figure 3.12 *SEM pictures of pretreated wheat straw. The first, second and third column represents 100X, 5000X and 50000X magnifications, respectively. WS1: (A-C), WS2: (D-F), WS3: (G-I) and WS4: (J-L).*

Except from the fiber separation, similar effects of steam-explosion were seen also on the pretreated spruce materials although the latter materials were even more heterogeneous. In the spruce samples the most obvious difference between S1 and S2 was the more extensive rupture and fragmentation in S1 (cf. Figure 3.13A and D). However, Figure 3.13C and F suggest that the higher specific surface area of S1 may be explained by a higher porosity, although this was not fully conclusive due to the material heterogeneity.

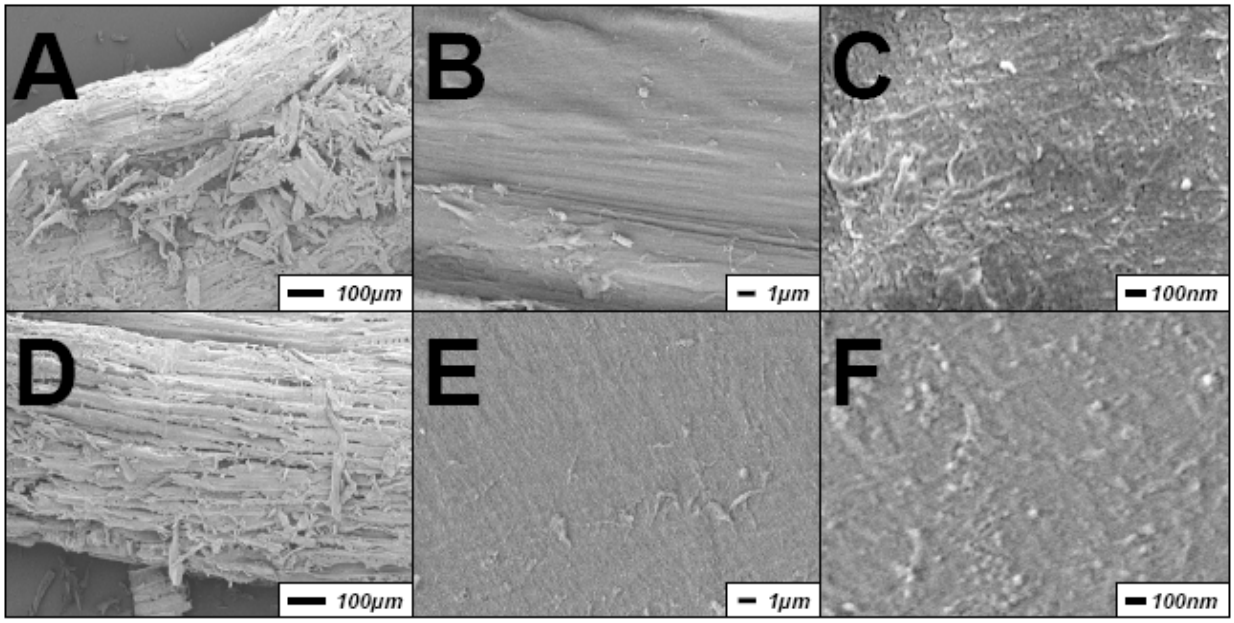

Figure 3.13 *SEM pictures of pretreated spruce. First, second and third columns represent 100X, 5000X and 50000X magnifications, respectively. S1: (a-c) and S2: (d-f).*

3.5 Discussion

A fundamental problem in enzymatic lignocellulose conversion, to ethanol or any other carbohydrate based fermentative product, is the low rate of hydrolysis of the cellulose. A pretreatment, e.g. steam pretreatment, speeds up this process significantly, most certainly due to several different effects. From the heterogeneous nature of enzymatic degradation, one might expect that the increase in specific surface area – and the changed distribution of pore volume size – brought about by the pretreatment would be important. A higher specific area should lead to a faster rate of hydrolysis – at least initially – provided that the surface is indeed accessible to enzyme adsorption. This may not be the case due to either steric hindrance (e.g. too small pore sizes) or the chemical composition of the free surface area. The purpose of the study was to simultaneously assess the changes in specific surface area, surface morphology, enzyme adsorption and enzymatic hydrolysis caused by varying the pretreatment conditions in SO_2 catalyzed steam pretreatment of wheat straw and spruce. Measuring the specific surface area of this kind of materials is non-trivial. For measurement of the specific surface area we used the BET method, which is widely used in assessing specific surface areas of ceramic support material for traditional catalysts. Not only the surface area, but also the pore area or pore volume distribution can be obtained by this method. A problem when using BET is that it requires dry samples. By comparing materials dried at different temperatures in the investigation, it was indeed confirmed that some changes in the material

result from the drying procedure (cf. Figure 3.2 and Table 3.3). The absolute values of the specific surface areas are therefore not the same as the actual area in real pretreatment slurries. Solvent drying procedures can be used to better maintain the fine capillary structure (Grethlein, 1985). However, for the purpose of comparing surface areas from different pretreatment, the method is useful. BET areas for pretreated spruce and wheat straw have not been previously reported, to the best of the authors´ knowledge. However, dilute acid pretreated silvergrass has been assessed using BET and the obtained areas were correlated with the sugar yield in the pretreatment (Guo et al., 2008). The reported BET areas were in the same range (1.5 – 4.5 m^2/g) as the areas obtained experimentally (Table 3.3). Compared to when solute exclusion techniques have been used, the BET method results in relatively low specific surface areas for pretreated lignocellulose. It has however been reported that results from nitrogen adsorption (dry samples) are proportional to results based on adsorptions of dyes (wet samples) (Chandra et al., 2008; Yu and Atalla, 1998).

In the current study, a more severe pretreatment was found to give a larger specific surface area for both spruce and wheat straw (Table 3.3). For wheat straw, the specific surface area increased with more than 50% from the mildest to the harshest conditions. This was also illustrated by the SEM study (Figure 3.12 and 3.13) in which cell-walls were ruptured to different extents, as could be seen already at the lowest magnification, which is in agreement with previous works (Donaldson et al., 1988 and Kristensen et al., 2008). At the highest magnification an increased porosity was observed as a result of increased pretreatment severity, especially in the wheat straw samples (Figure 3.12C, F, I and L). Pore formation has previously been reported for pretreated softwood (Donaldson et al., 1988), but in a recent study on pretreated wheat straw these structures were not observed (Kristensen et al., 2008). Interestingly, the pore size distribution (in the available range) for both spruce and wheat straw (Figure 3.1) peaks at about the same pore diameter as the pores seen in the SEM pictures. Thus, the increased porosity at harsher pretreatments, observed by SEM, is possibly responsible for the higher rates of hydrolysis in these samples. Most likely the specific surface area would increase even more when increasing the pretreatment severity further, however, at the expense of degradation of formed monosaccharides from the hemicellulose hydrolysis (Mosier et al., 2005). A significant degradation of xylose is for instance apparent in the liquid fraction analysis for WS4 (Table 3.2). The accessible fraction of the surface area (assuming a pore size > 54 Å is required) increased somewhat between WS1 and WS2, but was then approximately constant at 65%. The available surface area has been suggested as the most important factor for the rate of hydrolysis of cellulosic materials (Fierobe, 2002) and positive correlations between degradability and pore accessibility/pore volume have been reported in several studies (Grethlein, 1985; Wong et al., 1988; Sinitsyn et al., 1991; Thompson et al., 1991; Chandra et al., 2008; Weimer et al., 1990; Burns et al., 1989; Grethlein et al., 1984). Grethlein (1985) obtained a nearly perfect linear relation between available specific surface

area (i.e. above 51Å size pore diameter) and the initial glucose yield for different, dilute acid pretreated, lignocellulosic materials. Other studies where the initial rate of hydrolysis shows a positive correlation to the available specific area include Wong et al. (1988) (Pinus radiata), Thompson et al. (1992) (mixed hardwood) and Sinitsyn et al. (1991) (sugar cane bagasse). Initial cellulose conversion has also been correlated with the amount of adsorbed dye on different lignocellulosic materials (Chandra et al., 2008). In addition, kinetic parameters for the hydrolysing reactions have shown strong positive correlation with specific surface area of pure cellulose (Lee et al., 1983). It was evident that a larger surface area – for each material - gave a higher adsorption of cellulase protein as assessed by the Bradford method and also by the FPA assay (Table 3.3 and Figure 3.3-3.4). However, the difference in material properties distorted a direct correlation between amounts of adsorbed enzyme and accessible specific surface area across different materials. A higher total protein adsorption was found for spruce than for wheat straw, despite a lower accessible specific surface area (cf. Figure 3.3). One well-known factor, which most likely is highly important here, is the difference in lignin content (Gharpuray et al., 1983; Schwald et al., 1988). The lignin has been shown to give unspecific adsorption of cellulase enzymes (Eriksson et al., 2002) and the lower lignin content of wheat straw (Table 3.1) may therefore affect the adsorption. However, not only the amount of lignin *per se*, but also the distribution and composition of the lignin will matter (Mooney et al., 1998; Wong et al, 1988; Ooshima et al., 1990) which complicates explanation of the adsorption patterns, especially between the spruce and wheat straw samples. Interestingly, the HEC assay, which shows binding of endoglucanases, showed virtually no adsorption on either WS1 or WS2 (Figure 3.5b), although these materials had a high FPA adsorption.

This would indicate a high binding of CBHs, but only little binding of EGs. Previous studies have shown that the cellulose binding domain of the CenA endoglucanase of *Cellulumonas fimi* adsorbs strongly to crystalline cellulose (Gilkes et al., 1992), while the catalytic domain of CBH has been shown to bind to amorphous regions preferentially (Ståhlberg, 1991). From this perspective, the different behaviour in the HEC assay may be explained by considering the different affinity towards crystalline and amorphous fractions by EGs and CBHs, respectively. An alternative explanation of the different bindings of EGs may be the distinct variation in xylan content between WS1-2 and WS3-4. CHBs and EGs have been reported to adsorb differently to also to lignins, which may explain the differences (Palonen et al., 2004). In line with the FPA analysis, (but in contrast to the total protein adsorption), the initial rate of hydrolysis (4 hour measurement) is higher for the wheat straw material than for the spruce (Table 3.5 and Figure 3.8 and 3.9). The hydrolysis experiments show that the Avicel (100% cellulose) material and S1 (roughly 50% cellulose) behave more similarly than expected based on the protein adsorption. As discussed above unproductive adsorption on lignin is a likely explanation for both these observations. Since the hydrolysis rate is proportional to the extent of the productive binding, the hydrolysis experimental results suggest that S1 and

Avicel exhibit comparable productive surface areas. This result is not surprising if we consider that, on the one side, S1 has a specific surface area which is about twice that of Avicel, but on the other hand, only 50% of the total amount of material is cellulose. Accordingly, only 50% of the total specific surface in S1 is actually "productive". At the lower enzyme dosage the hydrolysis pattern of the different materials changes, and the rates of hydrolysis are no longer clearly related to the specific surface areas (Table 3.5, Figure 3.10 and 3.11). A possible explanation is that at very low enzyme concentration, nearly all the enzyme is adsorbed to the fibers, and available area becomes unimportant within the range. In this situation characteristics such as surface composition and lignin distribution would more strongly affect the hydrolysis. Thus, the fact that Avicel was more readily hydrolysed compared to S1 could possibly be a result of unproductive binding due to the high lignin content in S1. In conclusion, this study shows a clear connection between the specific surface area and the pretreatment severity for the materials studied. This was also illustrated with SEM. The increased surface area gives, for each substrate, an increased overall protein adsorption, and gives a higher initial rate of hydrolysis. Not surprisingly, the difference in chemical composition between wheat, spruce and Avicel prevents a simple comparison between digestibility based only on the accessible surface area. The surface chemistry in terms of e.g. binding on lignin and difference in affinity based on crystallinity will necessarily add to the overall performance.

Chapter 4

Lignocellulose hydrolysis kinetic modelling

Enzymatic hydrolysis is a complex phenomenon. In fact, the full extent of this complexity is not represented in any quantitative model proposed to date. Depending on the purpose at hand, either relatively simple or complex models have been reported. In this Chapter[1], different adsorption and hydrolysis models have been reviewed and classified based on the degree of complexity. This analysis was the starting point to develop a new concept model, characterized, on one hand, by the same structural patterns whose effectiveness in describing phenomena have been proven in literature, and, on the other hand, embedding as critical input parameters, experimentally determined *SSA* and α, substrate features strongly affecting process, as demonstrated by the experimental investigation.
Model parameters have been identified and the sensitivity of the main process variables against different parameters has been assessed. Finally the validity of the model in reproduce experimental profiles has been tested.

4.1 Quantitative description

The rate of an enzymatic reaction depends on a number of different enzyme and substrate properties and reaction conditions. An enzymatic reaction is usually divided into several consecutive steps: adsorption, reaction and desorption. Enzymes are catalysts increasing the reaction rates and/or making new reaction paths available. In homogenous catalysis the reactant and catalyst are in the same phase, for example dissolved in a solution.
The homogenous reaction can be described by a first order reaction rate:

$$r = k[S] \tag{4.1}$$

where k is the rate constant and $[S]$ the substrate concentration.
The heterogeneous reaction involves for example a solid substrate and a catalyst in solution. The reaction rate of this kind of catalysis is often described with a Michaelis-Menten expression, which is based on the following reaction scheme:

[1]Portions of this Chapter have been published in Piccolo et al. (2009).

$$S + E \underset{k_{-1}}{\overset{k_1}{\rightleftarrows}} ES \xrightarrow{k_2} E + B \tag{4.2}$$

The rate of the reaction is described by:

$$r = \frac{k[S]}{K_M + [S]} \tag{4.3}$$

where k is the rate constant and K_M is the Michaelis-Menten constant. The Michaelis-Menten constant is described by:

$$K_M = \frac{k_2 + k_{-1}}{k_1} \tag{4.4}$$

where the different k_1, k_{-1}, *and* k_2 are the adsorption and desorption rates.
One way of describing k in Eq. 4.1 is to include a Michaelis-Menten dependence on cellulase concentration [E]:

$$k = k_{max} \frac{[E]e_{reac}}{K_{eq} + [E]e_{reac}} \tag{4.5}$$

where k_{max} is the maximum specific reaction rate (h^{-1}), e_{reac} is the specific activity of the enzyme (activity/g of enzyme) and K_{eq} is enzyme saturation constant (activity/L).
However most models for the rate of enzymatic catalysis are based on the mathematical product of the concentration of the enzyme substrate complex and a proportionality factor relating this concentration to the reaction rate:

$$r_C = k[CE] \tag{4.6}$$

where r_C is the cellulose hydrolysis rate (substrate units/[volume*time]) and k is the rate constant, a proportionality factor between the concentration of the enzyme-substrate complex [CE] and r_C (units as needed for dimensional consistency). An adsorption model is used to describe quantity [CE].

4.1.1 Adsorption modelling: review

The most common description of cellulase adsorption is the Langmuir isotherm, derived assuming that adsorption can be described by a single adsorption equilibrium constant and a specified adsorption capacity. In contrast to Michaelis-Menten, the Langmuir equation does not assume that the substrate is in excess relative to the enzyme, but takes into account that the substrate can be saturated with respect to enzyme. The Langmuir isotherm may be represented as:

$$E_a = \frac{W_{max} K_P E_f}{1 + K_P E_f} \tag{4.7}$$

in which E_a is the adsorbed cellulase (mg or μmol cellulase/L), W_{max} is the maximum cellulase adsorption = ($A_{max}S$) (mg or μmol cellulase/L), A_{max} is the maximum cellulase adsorption per g cellulose (mg or μmol cellulase/g cellulose), S is cellulose concentration (g cellulose/L), E_f is free cellulase (mg or μmol cellulase/L), and K_P is the dissociation constant ($K_P=E_a/(E_f S)$) in terms of L/g cellulose. Lynd et al. (2002) present in their wide review about the microbial cellulose utilization, a compilation of values of adsorption parameters for cellulases isolated from different microorganism and for diverse substrates. In addition to equilibrium adsorption models, a dynamic adsorption model has been used by some investigators (Converse et al., 1988; Converse and Optekar, 1993; Nidetzky and Steiner, 1993; Nidetzky et al., 1994c). The Langmuir equation is widely used because in most cases it provides a good (and often very good) fit to the data, and it represents a simple mechanistic model that can be used to compare kinetic properties of various cellulase–cellulose systems. However it is evident that cellulase binding does not comply with assumptions implicit in the Langmuir model due to one or more of the following: 1) partially irreversible cellulase adsorption (Palonen et al., 1999); 2) interaction among adsorbing cellulase components, especially at high concentrations (Jeoh et al., 2002); 3) multiple types of adsorption sites, even for one cellulase molecule (Linder and Teeri, 1997; Carrard and Linder, 1999); 4) cellulase entrapment by pores of cellulose (Lee et al., 1983); and 5) multicomponent cellulase adsorptions in which each component has different constants (Beldman et al., 1987). In light of these considerations, several equilibrium models representing alternatives to simple Langmuir adsorption have been proposed, including two-sites adsorption models (Linder et al., 1996; Medve et al., 1997; Stålhberg et al., 1991; Woodward et al., 1988a), Freundlich isotherms (Medve et al., 1997), and combined Langmuir Freundlich isotherms (Medve et al., 1997).

4.1.2 Hydrolysis modelling: review

Quantitative description of cellulose hydrolysis is useful in different stages of processing of biomass to fermentable sugars. They span the entire domain of operations, namely enzyme characterization and modification, substrate preparation, reactor design, and optimization of operational policies.

There are two types of modelling approaches, empirical and mechanistic modelling. Empirical models relate the factors using mathematical correlations, without any insight into the underlying mechanism. These are easy to develop and useful in enzyme characterization and substrate preparation. Mechanistic models are developed from the reaction mechanisms, mass transfer considerations and other physical parameters that affect the extent of hydrolysis. As these models address the underlying dynamics of the process, they can be extensively used in every stage. Mechanistic models vary in their complexity based on the intended use of the models. These

models are quite useful in describing the reaction mechanisms, mass transfer considerations and other physical parameters that affect the extent of hydrolysis

4.1.2.1 Empirical models

Nonmechanistic models in the literature provide correlations for either fractional conversion or the rate of reaction as a function of various factors. Factors incorporated into models with conversion as the output include enzyme loading and substrate concentration (Sattler et al., 1989) as well as pretreated biomass properties (Chang and Holtzapple, 2000; Gharpuray et al., 1983; Koullas et al., 1992). Factors incorporated into models with rate as the output include hydrolysis time (Karrer et al., 1925; Miyamoto and Nisozawa, 1945), enzyme loading (Miyamoto and Nisozawa, 1945), and cellulose conversion (Ooshima et al., 1982). A few nonmechanistic models are considered here by way of example. Nonmechanistic models developed prior to the early 1980s are considered in detail in the reviews of Lee et al. (1980) and Ladisch et al. (1981). An example of a model with conversion extent as an output is that proposed by Gharpuray et al. (1983). Those authors used regression to develop an exponential model to describe the influence of characteristics of pretreated wheat straw on the conversion of cellulose X measured after 8 h:

$$X = 2.044(SSA)^{0.998}(100 - CrI)^{0.257}(L)^{-0.388} \tag{4.8}$$

in which SSA is measured by BET, and L is residual lignin content. Their results indicated that an increase in surface area and a decrease in the crystallinity and lignin content enhance hydrolysis, with specific surface area as the most influential of the structural features, followed by the lignin content. Chang and Holtzapple (2000) reported a model to correlate maximum conversion in relation to residual lignin, crystallinity index, and acetyl content. They found that lignin content and CrI have the greatest impact on final conversion, whereas acetyl content had a smaller effect. Koullas et al. (1992) also attempted to relate maximum conversion with CrI and degree of delignification, and obtained a similar conclusion about CrI and lignin effects. Sattler et al. (1989) developed the following equation to describe final fractional conversion after enzymatic hydrolysis of pretreated poplar in relation to cellulase loading:

$$\frac{Y}{[C]_0} = \frac{Y_{max}}{[C]_0}\frac{[E]}{K + [E]} \tag{4.9}$$

where $Y/[C]_0$ gives the fraction of substrate hydrolyzed; $[E]$ is given in FPU/g initially added substrate (FPU/g substrate); and $Y_{max}/[C]_0$ is the fraction of substrate which could maximally be hydrolyzed at an infinite enzyme loading, i.e., maximum digestibility. Later, Adney et al. (1994) applied this model to describe hydrolysis of cellulose such as Sigmacell 50 and various pretreated wood-powders. An example of a model with reaction rate (V) as an output is that proposed by Holtzapple et al. (1984c):

$$V = \frac{(X_{max} - X)^2}{t_{1/2} X_{max}} \tag{4.10}$$

where X_{max} is the maximum conversion, X is conversion, and $t_{1/2}$ is the time after which is reached $0.5*X_{max}$. Prompted by the observation that rate declines with increasing conversion, Ooshima et al. (1982) proposed the relationship:

$$\frac{\mathrm{d}V}{\mathrm{d}X} = -kV \tag{4.11}$$

where V is the hydrolysis rate and X is conversion.

4.1.2.2 Mechanistic Models

Zhang and Lynd (2004) reviewed in detail the works concerning the modelling of cellulose hydrolysis and pointed out that most of the proposed models for the design of industrial systems fall in the category of mechanistic models, i.e. models taking into account the substrate concentration or one of the enzymatic activities as a state variable. These models meet the requirement of including the minimum of necessary information for the description of the process. Mechanistic models can be used for data correlation but also for reactor design and identification of important characteristics. These models are based on the reaction paths shown in Figure 4.1.

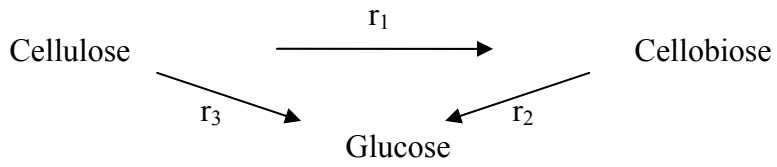

Figure 4.1 *Hydrolysis reaction rates.*

Some models only include reaction r_3, i.e. the direct path from cellulose to glucose; others also consider the intermediate cellobiose and thus include reactions r_1 and r_2 as well. Reactions r_1 and r_3 are examples of heterogeneous catalysis reactions and thus the reaction rates are described by Eq. 4.6; r_2, which is a homogenous reaction, is described by Eq. 4.1. The two equations (4.1 and 4.6) are the foundation in all mechanistic models but they have been modified to describe different aspects, such as end-product inhibition, changed substrate reactivity and enzyme deactivation, into account.

Mechanistic models with respect to substrate and enzyme are based on an adsorption model but use a single variable to describe the state of the substrate and describe the action of cellulase in terms of a single solubilizing activity. A representative model in this category is the *HCH-1 model* developed by Holtzapple et al. (1984a, 1984b), which describes the initial rate of hydrolysis by:

$$V = \frac{k[S][E]i}{(\varphi + [S] + e[E])} \tag{4.12}$$

in which k is a rate constant; φ, a lumped affinity constant; e, the number of cellulose sites covered by an adsorbed enzyme molecule, and i the fraction of total enzyme which is not inhibited by product. The quantity i represents inhibition by glucose [G] and cellobiose [G_2] according to:

$$i = 1/(1 + [G]/K_{I1} + [G_2]/K_{I2}) \tag{4.13}$$

in which K_{I1} and K_{I2} are inhibition constants. This model was used to simulate a total of 50 different hydrolysis conditions with a 10-fold range in enzyme concentration and a 30-fold range in cellulose concentration. Agreement with experimental data was rather good, and appeared better than some older models (Howell and Stuck, 1975; Huang, 1975).

Mechanistic models with respect to enzyme only involve variables in addition to concentration to describe the state of the substrate. The widely observed trend of declining rate with increasing conversion appears to be a central motivation for many models in this category. Models describing an assumed change in shape and surface area over the course of hydrolysis have been proposed (Converse and Grethlein, 1987; Converse et al., 1988; Luo et al., 1999; Oh et al., 2001; Philippidis et al., 1992, 1993). However, none of these models have been tested against experimental data to our knowledge.

Several ‘‘two-substrate’’ models have been proposed that partition cellulose into a less reactive highly crystalline fraction, and a more reactive amorphous fraction (Fan and Lee, 1983; Gonzalez et al., 1989; Gusakov et al., 1985a,b; Nidetzky and Steiner, 1993; Peitersen and Ross, 1979; Ryu and Lee, 1982; Scheiding et al., 1984). Although such models have met with some success in terms of correlating data, the trend of increasing *CrI* with increasing conversion—which would be expected if amorphous cellulose in fact reacts first—has not been conclusively confirmed by experimental data. An example of a two-substrates model is that of Wald et al. (1984), which includes shrinking cellulose spheres with an amorphous shell and a shrinking core as well as inhibition of cellulose hydrolysis by cellobiose and liquid-phase hydrolysis of cellobiose by h-glucosidase with inhibition by glucose.

The NREL has funded projects concerning the modelling of biomass-to-ethanol conversion as in the case of continuous SSF of wood performed by South et al. (1995). This study was based on the experimental data obtained in a previous work of these same authors using commercial fungal cellulases (South et al., 1993). In this study, a kinetic model considering the cellulose conversion, the formation and disappearance of cellobiose and glucose, the formation of cells and the biosynthesis of ethanol, was structured. In addition, a Langmuir- type model taking into account the adsorption of cellulases on the solid particles of cellulose and lignin, and expressions describing the dependence of cellulose conversion on the residence time of non-soluble solid particles of biomass were considered.

This last description confers great validity to the model since it provides a better approximation to real processes, which cannot be suitably explained by the traditional models for CSTR considering soluble substances.

South et al. (1995) used a conversion-dependent rate constant to account for declining specific activity of cellulase–cellulose complexes over the course of hydrolysis:

$$k(X) = k\left\{(1-X)^n + c\right\} \tag{4.14}$$

Those authors found an empirically determined value of *n* equal to 5.3, indicative of the very strong decline in rate with increasing conversion and in general agreement with direct specific activity measurements (Nutor and Converse, 1991; Ooshima et al., 1991).

Mechanistic models with respect to substrate (only) involve concentration as the only substrate state variable and two or more solubilizing activities. Examples of models in this category are based on endoglucanase and exoglucanase. Nidetzky et al. (1994b) described saturation of the hydrolysis rate in terms of the concentration of a particular cellulase component, E_i, as follows:

$$V(E_i) = V_{max}\frac{E_i}{K_{E_i} + E_i} \tag{4.15}$$

in which *i* is either 1 (for exoglucanase) or 2 (for endoglucanase), and K_{Ei} is a half-saturation constant. Based on this relationship, the following equation was proposed for the rate of hydrolysis in the presence of both exoglucanase and endoglucanase:

$$V(E_1, E_2) = V(E_1) + V(E_2) + V_{syn,max}\frac{E_1E_2}{K_{E_1}K_{E_2} + K_{E_1}E_2 + K_{E_2}E_2 + E_1E_2} \tag{4.16}$$

in which $V_{syn,max}$ is the maximum synergistic hydrolytic rate, and K_1,K_2 were the half-saturation constants corresponding to enzyme 1 and 2 in binary combination. The experimental results and model prediction clearly showed that the optimal ratio of exoglucanase to endoglucanase is a function of the total cellulase concentration, with higher enzyme concentrations needing less endoglucanase to achieve the maximum synergistic effect. The model of Beltrame et al. (1984) accounts for exoglucanase, endoglucanase, and β-glucosidase on textile cotton and cellulose pulp at various temperatures. The variable values can be adjusted depending on experimental conditions to fit experimental data well. About half of the mechanistic models cited by Zhang and Lynd (2004) are based on the Michaelis–Menten model, which is valid when the limiting substrate is in excess in relation to the enzyme (Lynd et al., 2002). In light of the small fraction of β-glucosidic bonds accessible to enzymatic attack, this condition is particularly limiting for cellulosic substrates. Excess substrate may be achieved in fundamentally oriented work, e.g., to characterize specific activity under laboratory conditions, but is seldom achieved in applications involving cellulose hydrolysis. Models based on a Langmuir adsorption model do not implicitly assume excess in either

enzyme or substrate, and thus have a considerably broader range of potential application. Although adsorption models other than the Langmuir model have been proposed, few have been incorporated into kinetic models that lead to a prediction of hydrolysis rate. Inhibition of the hydrolysis rate by soluble products has been incorporated into a substantial number of models. Competitive inhibition is the most common mechanism in the literature, but other uncompetitive and noncompetitive mechanisms have also been proposed. Both the structural information (Davies et al., 1997; Teeri et al., 1998a,b) and a considerable body of experimental data indicate that individual cellulase enzymes are inhibited competitively by cellobiose and glucose. However, it appears that mixtures of cellulase components can exhibit behaviour consistent with mechanisms other than competitive inhibition under some conditions (Gusakov et al., 1985a, 1985c; Gusakov and Sinitsyn, 1992; Holtzapple et al., 1984b, 1990). The mechanistic basis for this phenomenon is not fully understood and has received little if any examination in the light of structural information obtained during the 1990s.

4.1.2.3 Functionally and structurally based models

A few functionally based models, involving multiple substrate variables and solubilizing activities, have been proposed in the literature. Moo-Young and co-workers (Okazaki and Moo-Young, 1978; Suga et al., 1975) developed models based on the Michaelis-Menten model and assuming that all β-glucosidic bonds are accessible that incorporated two solubilizing activities (endoglucanase and exoglucanase) as well as β-glucosidase. In addition, these investigators used concentration and DP as substrate variables. The model predicts (Suga et al., 1975) that substrate *DP* changes as a function of time in the presence of endoglucanase, and that exoglucanase and endoglucanase synergism occurs for the degradation of longer chain cellulose molecules. Later, the model of Okazaki and Moo-Young (1978) predicted that the degree of endo-exo synergism is strongly impacted by DP. Converse and Optekar (1993) considered competitive adsorption of exoglucanase and endoglucanase for a limited number of sites, and, using surface area as a substrate state variable, predicted a lower degree of synergism under oversaturating conditions— that is, when cellulase is in substantial excess relative to the substrate, due to competitive adsorption. Fenske et al. (1999) used virtual DP and surface area as substrate state variables in addition to concentration to give insights into inhibition of cellulase activity by insoluble substrates. In the case of three of the four functionally based models listed (Fenske et al., 1999, Okazaki and Moo-Young, 1978, Suga et al., 1975), no comparison to experimental data has been made. Converse and Optekar (1993) compared model results to a single set of experimental data with a focus exclusively on synergism. Recently Zhang and Lynd (2006) have proposed a new functionally based model representing the action of three different enzymes (CBHI, CBHII and EGI) and incorporating two measurable and physically interpretable substrate parameters: the degree of polymerisation (*DP*) and the fraction of β-glucosidic bonds accessible to cellulase F_a (Zhang and Lynd, 2004). However the applicability of the model is limited by the fact that currently there is no rational basis to estimate some of the parameters included.

Finally, models based on structural features of cellulase components and their interaction with their substrates are termed "structurally based models". To a much greater extent than models in other categories, structurally based models are useful for molecular design as well for developing an understanding on the relationship between cellulase structure and function. Derivation of meaningful kinetic models based on structural models cannot be done at this time, and awaits major advances in the general field of inferring protein function from structure.

4.1.3 Declining rate

Although initial rates are often used for biochemical characterization, it is of interest from both fundamental and applied perspectives to understand and describe the enzymatic hydrolysis of cellulose over the entire course of reaction. A near-universal feature of cellulose hydrolysis observed in many studies over several decades is that the rate declines sharply as the reaction proceeds (corresponding to increasing values of X) in a batch hydrolysis. Measurements of rate in conjunction with adsorbed enzyme (Desai and Converse, 1997; Nutor and Converse, 1991; Ooshima et al., 1991) confirm that the phenomenon of declining rate with increasing conversion is observed on a specific (rate per adsorbed enzyme) as well as on an absolute basis. Enzyme inactivation due to thermal effects (Caminal et al., 1985; Gonzàles et al., 1989; Converse et al., 1988), formation of an inactive enzyme-substrate (lignin) complex (Gusakov and Synitsyn, 1992; Ooshima et al., 1990; Sutcliffe and Saddler, 1986), and inhibition by hydrolysis products (Caminal et al., 1985, Gusakov et al., 1985; Lee and Fan, 1983) have been implicated as important factors underlying the decreasing-rate phenomenon. However, it is significant to observe that this phenomenon has been documented in studies in which neither inactivation nor inhibition appears operative (Väljamäe et al., 1998; Zhang et al., 1999). Several studies have attributed declining rates of hydrolysis to a corresponding change in substrate reactivity. One subset of these studies postulates two types of cellulose that differ in their susceptibility to enzymatic attack (Gonzàles et al., 1989; Huang, 1975; Nidetzky and Steiner, 1975; Pietersen and Ross, 1979; Sattler et al.,1989; Wald et al., 1984). While this "two-substrate" hypothesis cannot be rejected based on the literature to date, it also appears that the difference between the more reactive and less reactive substrate fractions is attributable primarily to factors other than crystallinity. If this difference were due to crystallinity, then cellulose crystallinity should increase over the course of reaction. However, relatively constant crystallinity over the course of enzymatic hydrolysis has been observed in studies involving a variety of cellulase systems (Dermoun and Bélaich, 1988; Fan et al., 1980; Gama and Mota, 1997; Lee et al., 1983), although such crystallinity measurements may be due to artifacts (Weimer et al., 1995). A second subset of studies feature a continuous decline in substrate reactivity rather than two distinct substrate types. Working with pretreated poplar and the *T. reesei* system, Nutor and Converse (1991) found that the rate of cellulose hydrolysis per adsorbed cellulase decreased monotonically by 1 to 2 orders of magnitude over the course of reaction. The model proposed by South et al. (1995) Eq. 4.14 represents this declining specific activity of the cellulase-cellulose complex over the course of simultaneous saccharification. Working with purified

cellulase components from *T. fusca*, Zhang et al. (1999) concluded that substrate heterogeneity causes the nonlinear kinetics exhibited during hydrolysis of filter paper whereas product inhibition and enzyme inactivation were rejected as explanations for this phenomenon. The explanation of Ooshima et al. (1991) is that synergistic interaction between cellulase components becomes less effective with increasing conversion. Väljamäe et al. (1998) attribute the rate decline to steric hindrance due to nonproductive cellulose binding in combination with surface erosion.

Most kinetic models do not consider the changes in the hydrolysis rate during the course of the reaction, and that those models that do this, are based mainly on empirically adjusted parameters and not on a mechanistic approach. For instance, the model of SSF process developed for the case of unpretreated wastepaper using commercial cellulases and *S. cerevisiae* for both batch and two-stage continuous regimes (Philippidis and Hatzis, 1997) made use of an exponential decay term to describe the time-dependent decline in the rate of cellulose hydrolysis. With the help of an exhaustive sensitivity analysis, the model showed the digestibility of substrate (as a result of pretreatment), cellulase dosage, specific activity, and composition have a great effect on ethanol yield. This confirms that major research efforts should be oriented to the development of more effective pretreatment methods and production of cellulases with higher specific activity.

4.2 Modelling approach

4.2.1 Adsorption model

The focus of the study was not to propose a new phenomenological adsorption model but rather to present a model structure which can be properly identified, given the actual information potential of experimental data.

Accordingly, the structure of the Langmuir equation, which is widely used because it provides a good (or often very good) fit to experimental data and represents a simple mechanistic model that can be used to compare kinetic properties of various cellulase–cellulose systems, was maintained. Specific surface areas and a measure of pore accessibility were embedded in the model.

$$E_a = \frac{W_{max} K_P E_f}{1 + K_P E_f} \tag{4.17}$$

Variables and parameters on Eq. 4.17 are thus changed as follows: E_a is the adsorbed cellulase (mg cellulase/g WIS); W_{max} is the maximum cellulase adsorption (mg cellulase/g WIS) defined as:

$$W_{max} = A_{max}(SSA)\alpha \tag{4.18}$$

with A_{max} the maximum cellulase adsorption/m^2 on the substrate (mg cellulase/m^2 substrate), *SSA* the substrate specific area (m^2/g WIS) and α is the fraction of pores accessible to enzyme as

calculated from pores size distribution; E_f is the free cellulase (mg cellulase/L); and K_P is the dissociation constant.

4.2.2 Hydrolysis model

The adsorption model has been embedded in an overall hydrolysis model. Referring to the three reaction rates reported in Figure 4.1 the model consist of the material balances:

$$\frac{dC}{dt} = -r_1 - r_3 \tag{4.19}$$

$$\frac{dG}{dt} = 1.111 r_3 + 1.053 r_2 \tag{4.20}$$

$$\frac{dG_2}{dt} = 1.056 r_1 - r_2 \tag{4.21}$$

Where C, G, G_2 are the concentration [g/L] of cellulose, glucose and cellobiose, r_2 is the homogeneous reaction rate expressed through a Michaelis-Menten scheme (Eq. 4.22):

$$r_2 = \frac{k_2 G_2}{K_M + G_2} \tag{4.22}$$

where K_M is the Michaelis-Menten constant [g/L] and k_2 is the lumped specific rate constant, proportional to the effective β-glucosidase concentration:

$$k_2 = k_2^* e_g E \tag{4.23}$$

where k_2^* is the specific cellobiose hydrolysis rate [g/(IU*h)], E is the amount of enzyme supplemented [g] and e_g is the specific β-glucosidase activity of the enzyme supplemented [IU/g].
r_1 and r_3 are heterogeneous reaction rates expressed as:

$$r_i = k_i [EC] C, \; i = 1, 3 \tag{4.24}$$

in which k_i is a kinetic constant, $[EC]$ is an appraisal of the productive binding [mg proteins/g WIS], based on experimental evidences. As discussed in Chapter 3, a comparable hydrolysis rate was observed for Avicel and S1 which suggested that S1 and Avicel exhibit comparable productive surface areas. Since S1 has a specific surface area which is about twice that of Avicel, but on the other hand, only 50% of the total amount of material is cellulose, then only 50% of the total specific surface in S1 is actually "productive". Based on these speculations we considered reasonable to express the extent of productive binding as a function of cellulose fraction f_C.

$$[EC] = E_a f_C \tag{4.25}$$

where E_a is calculated through the Langmuir modified equation (Eq. 4.17) and f_C is the current cellulose fraction.

Overall substrate conversion is given by the conversion X:

$$X = \frac{0.9G + 0.95G_2}{[C]_0} \tag{4.26}$$

where $[C]_0$ is the initial cellulose concentration.
Table 4.1 summarises the parameters and the variables that appear in the model.

Table 4.1 *Parameters and variables of hydrolysis kinetic model.*

Model parameters		Model variables	
A_{max}	Maximum cellulase adsorption	C	Cellulose concentration
K_P	Dissociation constant	G_2	Cellobiose concentration
k_1	Kinetic constant	G	Glucose concentration
k_3	Kinetic constant	E	Enzyme concentration
k_2^*	Specific cellobiose hydrolysis rate	E_a	Bound enzyme concentration
e_g	Total β-glucosidase activity of the enzyme	$[EC]$	Concentration of the enzyme-cellulose complex
K_M	Michaelis-Menten constant		
SSA	Substrate Specific surface area	r_1	Reaction rate
α	Fraction of accessible surface	r_2	Reaction rate
f_C	Cellulose fraction	k_2	Lumped kinetic constant
		r_3	Reaction rate
		X	Conversion

Before the model can be used to simulate and optimise the operation of the reactor, all parameters that appear in it must be assigned a fixed value. Some of these, namely SSA, α, f_C and e_g are considered as input parameters information and are experimentally determine. The remaining parameters should be identified through an estimation procedure, using experimental data.
As the experimental investigation described in Chapter 3 did not take into account β-glucosidase supplementation and activity, the available experimental data provide no information about the specific enzyme kinetic. For this reason we decided to assume for parameters k_2^* and K_M the values from Philippidis et al. (1993).
Eventually the subset of parameters we aimed at identifying was:

$$\theta = [k_1, k_3, K_P, A_{max}]$$

4.3 Model identification

The model implementation, simulation and identification, based on statistical methods, are performed in gPROMS® 3.2 modelling environment (Process System Enterprise Ltd., 2009).
The value of kinetic parameters were estimated using experimental data. Adsorption experiments and different sets of batch hydrolysis data were examined. The model equations were used to search parameters values by fitting experimental data. A nonlinear parameter identification procedure based on the criteria of maximum likelihood was employed.
The model equations 4.17-4.26 represent a non linear system of differential and algebraic equations (DAE) which can be written as:

$$\begin{cases} f(\dot{\mathbf{x}}, \mathbf{x}, t, \boldsymbol{\theta}) = 0 \\ \mathbf{y} = g(\mathbf{x}, \boldsymbol{\theta}) \end{cases} \tag{4.27}$$

Here **x** is the vector of states variables, t is the time, **θ** represents the vector of model parameters, **y** is the concentration vector that encompasses cellobiose and glucose.
Parameters estimation attempt to determine values for the uncertain physical and variance model parameters, **θ**, that maximize the probability that the mathematical model will predict the measurement values obtained from the experiments. Assuming independent, normally distributed measurement errors, ε_{ijk}, with zero means and standard deviations, σ_{ijk}, the maximum likelihood goal can be captured through the following objective function:

$$\boldsymbol{\Phi} = \frac{N}{2}\ln(2\pi) + \frac{1}{2}\min_{\theta}\left\{\sum_{i=1}^{NE}\sum_{j=1}^{NV_i}\sum_{k=1}^{NM_{ij}}[\ln(\sigma_{ijk}^2) + \frac{(\hat{y}_{ijk} - y_{ijk})^2}{\sigma_{ijk}^2}]\right\} \tag{4.28}$$

where N is the total number of measurements taken during all the experiments, NE is the number of experiments performed, NV_i is the number of variables measured in the i^{th} experiment, NM_{ij} is the number of measurements of the j^{th} variable in the i^{th} experiment, σ_{ijk} is the variance of the k^{th} measurement of variable j in experiment i (this is determined by the measured variable's variance model), $\hat{y}_{ijk}$ is k^{th} measured value of variable j in experiment i and y_{ijk} is k^{th} predicted value of variable j in experiment i.
The maximum likelihood objective function gives the flexibility for several types of variance model to be specified by the user.
gPROMS® allows defining three different variance models:

- a *constant variance* model, in which the measurement error has a constant standard deviation ω.

$$\sigma^2 = \omega^2 \tag{4.29}$$

- a *constant relative* variance model in which the measurement error depends on the magnitude of the predicted or measured values, mathematically represented respectively by:

$$\sigma^2 = \omega^2(y^2 + \varepsilon) \tag{4.30}$$

or

$$\sigma^2 = \omega^2(\hat{y}^2 + \varepsilon) \tag{4.31}$$

- a *heteroscedastic* variance model in which the measurement error depends on the measured or predicted values but is proportional to $y^{\gamma/2}$ or $\hat{y}^{\gamma/2}$, respectively

$$\sigma^2 = \omega^2(y^2 + \varepsilon)^{\gamma} \tag{4.32}$$

or

$$\sigma^2 = \omega^2(\hat{y}^2 + \varepsilon)^{\gamma} \tag{4.33}$$

Where ω is a proportionality factor, γ is the heteroscedasticity parameter, ε is a very small but non-zero number calculated by the software, which ensures that the variance has a meaningful definition for measured or predicted values that are close or equal to zero.
As the estimation of the parameters and the statistical analysis of the results depend strongly on the given or estimated standard deviations of the measurement errors, attention should be paid to the formulation of the variance model and the values of the respective variance model parameters.

4.3.1 Parameters estimation run

Given the the highly specific behaviour of different biomass substrates detected during experimental activity, a direct correlation between amounts of adsorbed enzyme and accessible specific surface area across different materials. For this reason the set of model parameters
$\theta = [k_1, k_3, K_P, A_{max}]$
have been specifically estimated for each substrate taken into account.
The variance model which reasonably reproduces the variance of experimental data is a constant relative variance model with ω equal to 0.1.
The mean value of different parameters resulting from the parameters estimation session together with different measures of the uncertainty of the parameters estimates are reported in Table 4.2 for pretreated spruce model and in Table 4.3 for wheat straw model.

Table 4.2 *Results of the parameters estimation run and statistical significance for pretreated spruce model [t_{ref}=1.6499].*

Parameter	Optimal Estimate	95% CI	95% t-value	Standard Deviation
k_1	0.001199	0.000065	18.5178	0.000033
k_3	0.002961	0.000137	21.5999	0.000070
K_P	0.000267	0.000057	4.7351	0.000029
A_{max}	203.61	32.47	6.2715	16.47

Table 4.3 *Results of the parameters estimation run for pretreated wheat straw model [t_{ref}=1.6499].*

Parameter	Optimal Estimate	95% CI	95% t-value	Standard Deviation
k_1	0.004582	0.000386	11.8668	0.000196
k_3	0.006150	0.000137	14.0015	0.000223
K_P	0.001751	0.000486	3.6028	0.000247
A_{max}	50.60	6.47	7.8253	3.29

The 95% confidence intervals (CI) are reported. A 95% confidence region means that if we repeat the experiments and estimate the parameters out of the repeated experimental data, the value of the estimated parameters will lie in the confidence region with a 95% probability. The smaller the confidence intervals, the more accurate is the parameter estimate. Each parameter reported in Table 4.2 and 4.3 presents a CI sufficiently low to consider the parameter, statistically identifiable.

The 95% t-values show the percentage accuracy of the estimated parameters with respect to the 95% confidence intervals. The t-values associated to each parameter θ_i are compared with the reference 95% t-value, which is again calculated using internal statistical functions. A t-value larger than the reference t-value indicates that the corresponding parameter has been accurately estimated (i.e. the standard deviation and the confidence intervals are small compared to the value of the estimated parameter. 95% t-values higher than the reference value are associated to the estimates provided for the parameters set of each material considered, with a lower absolute value for parameters A_{max} and K_P.

The identifiability methodology is fulfilled with an analysis of the sensitivity of the model variables to the parameters, used to screen parameters significance and detect issues of correlation between parameters.

4.3.2 Sensitivity Analysis

Parametric sensitivity analysis studies how variation in the model output can be apportioned to the variation of different parameters.

Absolute sensitivity index of the j^{th} parameter can be given as:

$$Q_{a,ij} = \frac{\partial y_i}{\partial \theta_j} \tag{4.34}$$

The individual parameter sensitivity indices are estimated over the whole experiment time horizon.

Relative sensitivity to parameters (Eq. 4.35) is useful to compare different parameters dynamic profiles, because it is normalized and clearly shows where maxima and minima occur for different sensitivity coefficient.

$$Q_{r,ij} = \frac{\partial y_i}{\partial \theta_j} \frac{\theta_j}{sc_j} \tag{4.35}$$

where sc_j is the scaling factor for the parameter θ_j (in this case as scaling factors is assumed the maximum value of $Q_{a,ij}$ in the time horizon considered).

A 1% variation of the estimated value has been considered for each parameter.

The dynamic sensitivity coefficient profiles obtained for S1 are reported in Figure 4.2 and 4.3 and for WS3 in Figure 4.4 and 4.5 calculated for a high (2mL) enzyme load hydrolysis experiment.

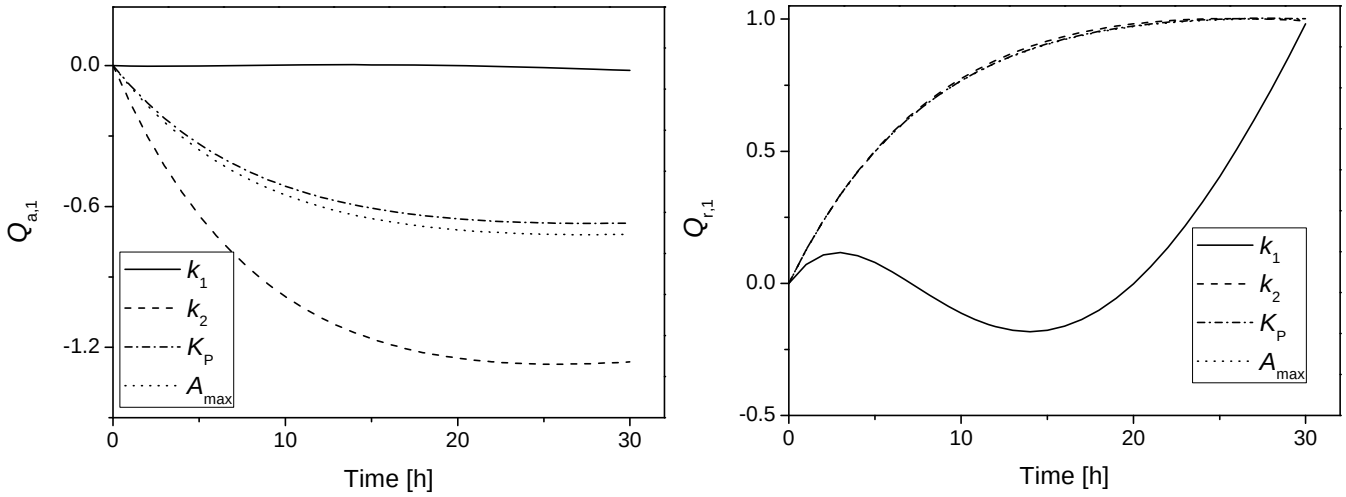

Figure 4.2 *Absolute (a) and relative (b) sensitivity dynamic coefficients of glucose concentration for S1 hydrolysis, calculated at the estimated values of parameters.*

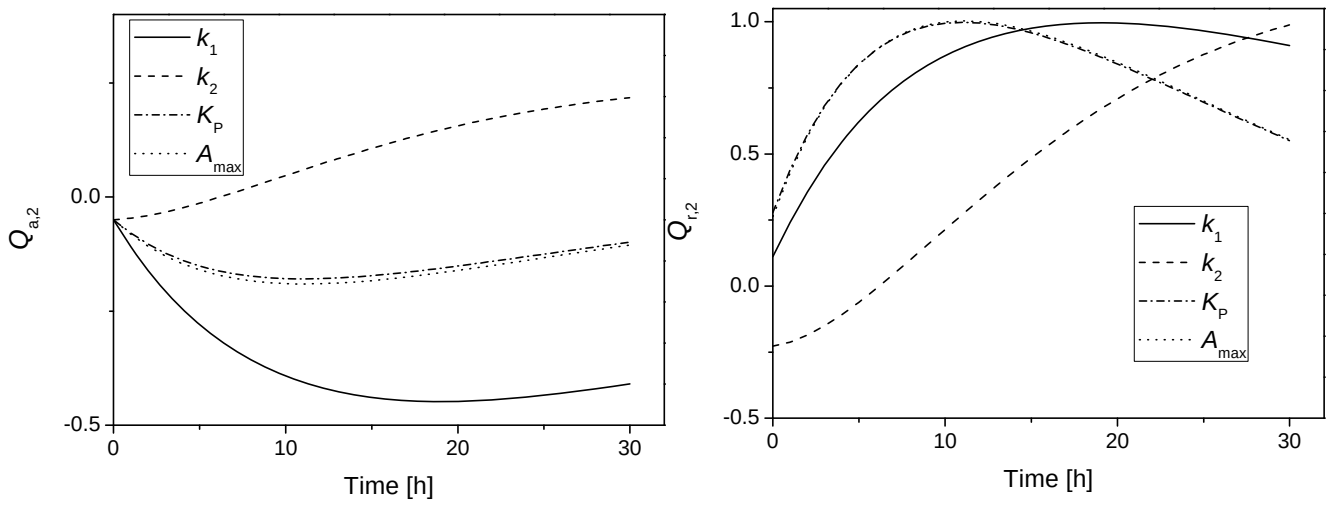

(a) (b)

Figure 4.3 *Absolute (a) and relative (b) sensitivity dynamic coefficients of cellobiose concentration for S1 hydrolysis, calculated at the estimated values of parameters.*

Even with some differences between different profiles calculated, a high correlation between K_P and A_{max} is clearly observed. In the case of S1 hydrolysis kinetic constant k_1 strongly affects glucose concentration and, on the other hand, the cellobiose is more dependent on k_3. Sensitivity coefficients dynamic (easily traceable in the case of relative sensitivities) is similar for three (k_3, K_P, A_{max}) over four parameters for $Q_{r,1}$ (glucose concentration sensitivity to parameters), with the maximum reached at the end of the experiment, and is similar for k_1, K_P, A_{max} in the case of $Q_{r,2}$ (cellobiose concentration sensitivity to parameters), with a maximum reached at about 10 hours from the beginning of the experiment. These observations can be useful to re-design more informative experiments, since they provide hints to optimise sampling intervals.

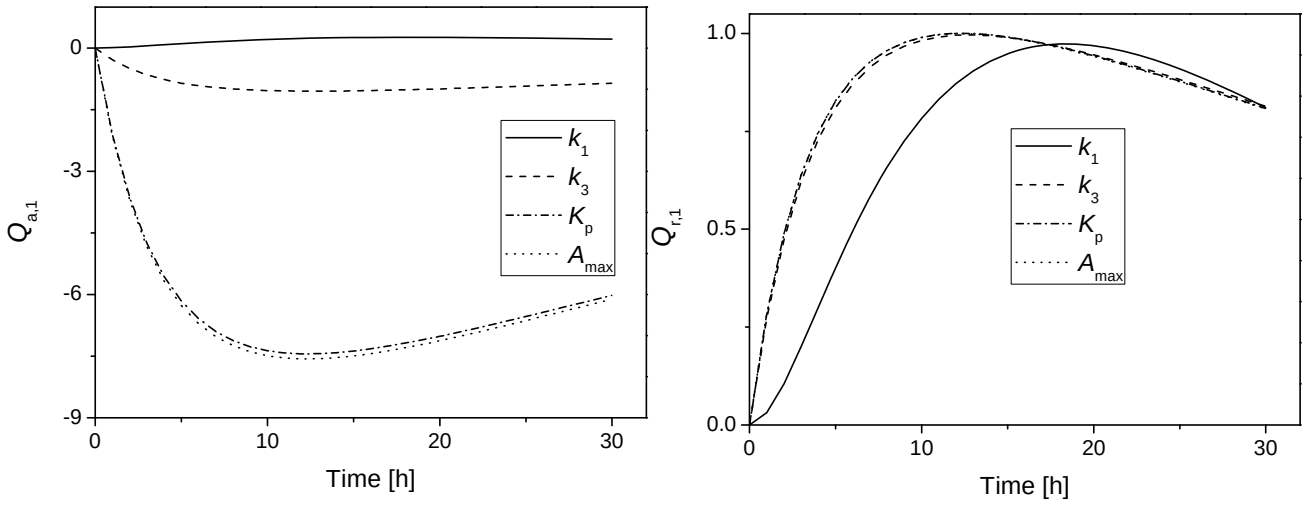

(a) (b)

Figure 4.4 *Absolute (a) and relative (b) sensitivity dynamic coefficients of glucose concentration for WS3 hydrolysis, calculated at the estimated values of parameters.*

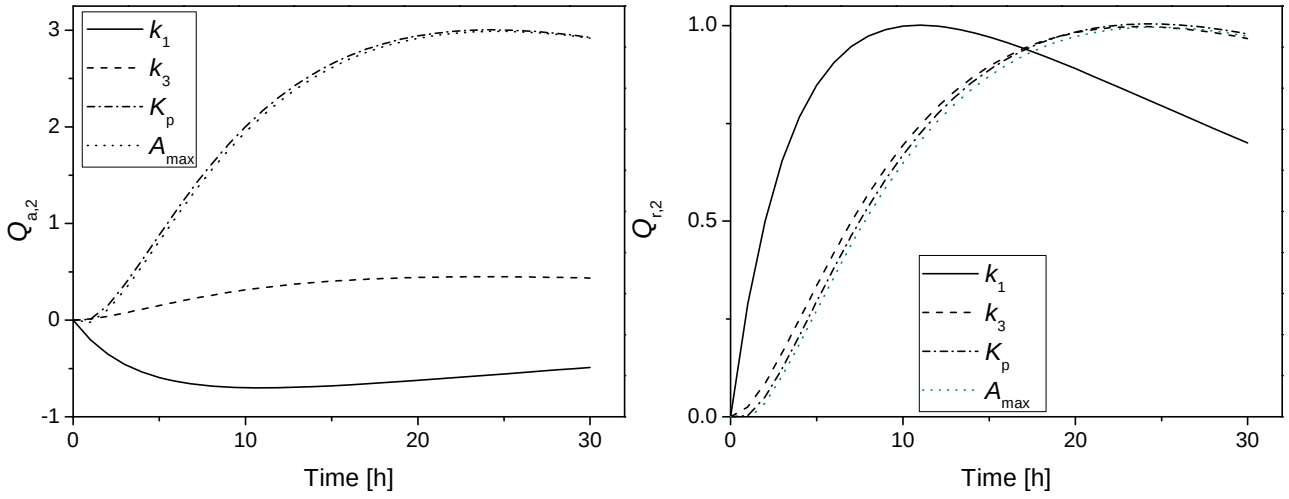

(a) (b)

Figure 4.5 *Absolute (a) and relative (b) sensitivity dynamic coefficients of cellobiose concentration for WS3 hydrolysis calculated at the estimated values of parameters.*

Glucose and cellobiose concentration in WS3 hydrolysis are strongly impacted by adsorption parameters K_P and A_{max} which show the same high correlation observed for S1. Parameters k_3, K_P and A_{max} present the same dynamic profile, with a maximum reached by $Q_{r,1}$ at about 10 hours and by $Q_{r,2}$ at about 25 hours.

4.3.3 Model riparametrisation

The preliminary sensitivity analysis showed a strong correlation between the adsorption parameters K_P and $A_{\max}$. This means that any change in one parameter could be compensate by a change in the other one, hence making it extremely difficult to find a unique estimate for these correlated parameters. This correlation stems for the model structure itself (Sin et al., 2009, Okazaki and Moo-Young, 1978, Gan et al., 2003, Kadam et al., 2004). There are several ways to reduce the correlation: 1) modify the model structure, 2) increase the information content of experimental data by proper design of experiments, and 3) search for a parameter subset that can be reliably estimated from the given data (Sin et al., 2009). In this study we tried to doodge parameters identification procedure choosing a different set of parameters for the estimation procedure.
We introduced a new parameter:

$$P = A_{max} K_P \tag{4.36}$$

and we estimated the new parameters set:

$$\theta = [k_1, k_2, K_P, P]$$

The mean value of the estimated parameters as well as the 95% confidence intervals (CI), 95% t-value and parameters standard deviation are shown in Table 4.4 for spruce model and in Table 4.5 for wheat straw model.
Statistical significance indexes are still satisfactory, as for the original parameters set, and the uncertainty of the estimate of the new parameter P for pretreated spruce model is reduced if compared to the original estimated parameter A_{max}, as testified by the higher 95% t-values. The improvement is not visible for wheat straw model parameters estimation.

Table 4.4 *Results of parameters estimation run and statistical significance for spruce [t_{ref}=1.6499].*

Parameter	Optimal Estimate	95%	95% t-value	Standard Deviation
k_1	0.001199	0.000066	18.271948	0.000033
k_3	0.003003	0.000138	21.727068	0.000070
K_P	0.000246	0.000053	4.620340	0.000027
P	0.053691	0.003356	15.999185	0.001702

Table 4.5 *Results of parameters estimation run and statistical significance for wheat straw [t_{ref}=1.6499].*

Parameter	Optimal Estimate	95%	95% t-value	Standard Deviation
k_1	0.004893	0.000437	11.190040	0.000222
k_3	0.006579	0.000506	13.011238	0.000257
K_P	0.001256	0.000342	3.676676	0.000174
P	0.074812	0.013173	5.679266	0.006693

As a second step of the identificability analysis, the sensitivity analysis was performed to evaluate parameters collinearity. Absolute and relative dynamic sensitivity coefficients were calculated for a 1% variation of the estimated values of parameters. The calculated profiles, obtained in the conditions of a high (2mL) enzyme load hydrolysis experiment, for S1 are reported in Figure 4.6-4.7 and for WS3 in Figure 4.8-4.9.

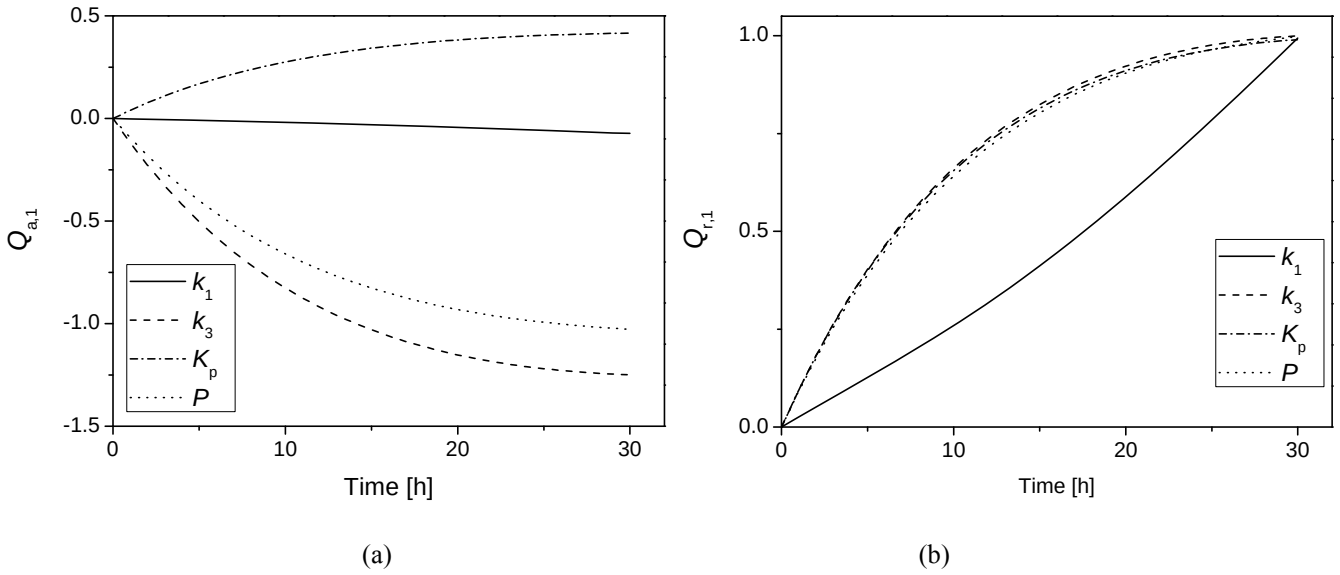

Figure 4.6 *Absolute (a) and relative (b) sensitivity dynamic coefficients of glucose concentration for S1 hydrolysis, calculated at the estimated values of parameters.*

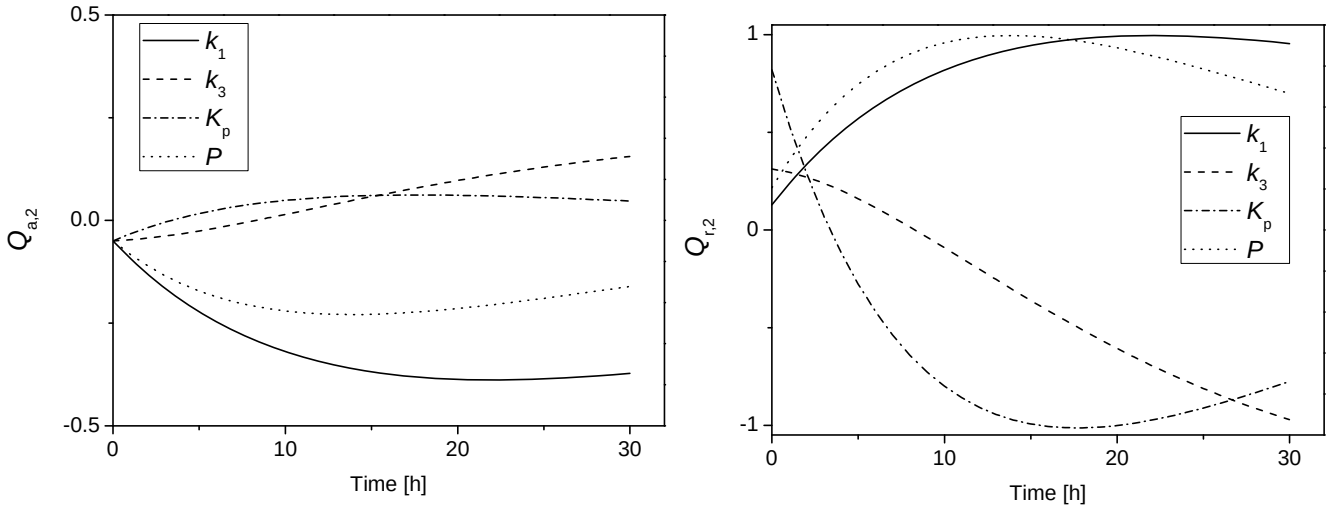

(a) (b)

Figure 4.7 *Absolute (a) and relative (b) sensitivity dynamic coefficients of cellobiose concentration for S1 hydrolysis, calculated at the estimated values of parameters.*

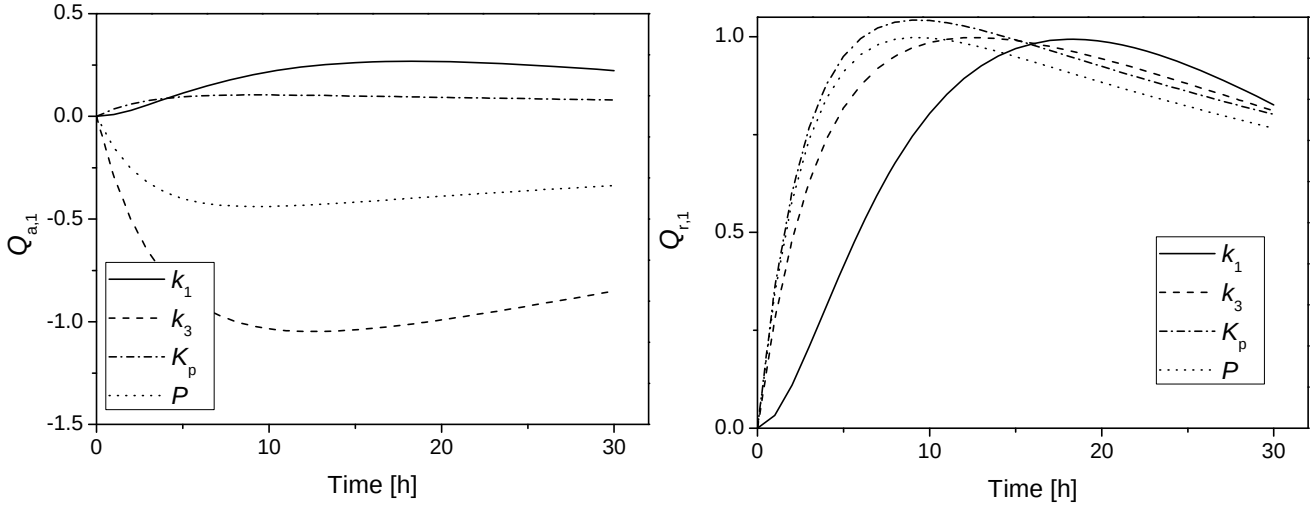

(a) (b)

Figure 4.8 *Absolute (a) and relative (b) sensitivity dynamic coefficients of glucose concentration for WS3 hydrolysis, calculated at the estimated values of parameters.*

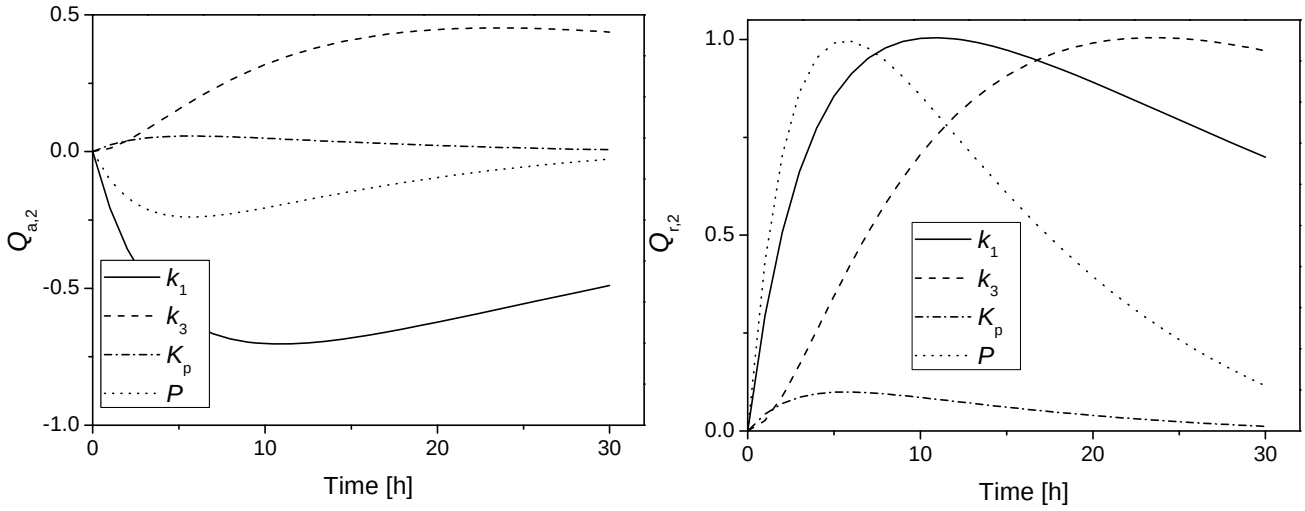

(a) (b)

Figure 4.9 *Absolute (a) and relative (b) sensitivity dynamic coefficients of cellobiose concentration for WS3 hydrolysis, calculated at the estimated values of parameters.*

A general positive effect of riparametrization can be observed: parameters collinearity is strongly reduced for both the spruce and the wheat straw materials. Except for the sensitivity dynamic coefficients of glucose concentration in S1 hydrolysis, presenting three parameters (k_1, k_3, P) characterized by the same dynamics, the other coefficients show a quite distinctive dynamic with maxima and minima distributed during the whole time duration of the experiment.

4.3.4 Correlation matrix

Consideration on parameters collinearity can be done also through the analysis of correlation matrix **R** where R_{ij} are given by:

$$R_{ij} = \frac{V_{ij}}{\sqrt{V_{ii}V_{jj}}}, \quad i \neq j \tag{4.37}$$

$$R_{ij} = 1, \quad i=j \tag{4.38}$$

Where V_{ij} and V_{ii} are calculated from the variance-covariance matrix **V**. This matrix contains the variances and covariances of the estimated process model and variance model parameters. The square root of each diagonal element, $\sqrt{V_{ii}}$, is the approximated standard deviation of the respective estimated parameter. The following approximation to the variance-covariance matrix is used:

$$\mathbf{V} = \mathbf{H}^{*^{-1}}\mathbf{\Gamma\Sigma\Gamma}^T\mathbf{H}^{*^{-1}} \tag{4.39}$$

where

$$\mathbf{H}^{*} = \begin{pmatrix} \dfrac{\partial^2}{\partial \boldsymbol{\theta}^2}\boldsymbol{\Phi} & \dfrac{\partial^2}{\partial \omega_{i,j}\partial \boldsymbol{\theta}}\boldsymbol{\Phi} \\ \dfrac{\partial^2}{\partial \omega_{i,j}\partial \boldsymbol{\theta}}\boldsymbol{\Phi} & \dfrac{\partial^2}{\partial \omega_{i,j}{}^2}\boldsymbol{\Phi} \end{pmatrix} \tag{4.40}$$

$$\boldsymbol{\Gamma} = \begin{pmatrix} \dfrac{\partial^2}{\partial \hat{y}_{i,j,k}\partial \boldsymbol{\theta}}\boldsymbol{\Phi} \\ \dfrac{\partial^2}{\partial \hat{y}_{i,j,k}\partial \omega_{i,j}}\boldsymbol{\Phi} \end{pmatrix} \tag{4.41}$$

and $\boldsymbol{\Sigma} = diag(\sigma_{ijk}^2)$ denotes the variance-covariance matrix of the measurement errors ($\boldsymbol{\Phi}$ is the maximum likelihood objective function defined in Eq. 4.28). The variance-covariance matrix of the estimated parameters, **V**, is of size $\mathbb{R}^{N_p \times N_p}$, where N_p is the number of all estimated parameters (process model parameters $\boldsymbol{\theta}$ and variance model parameters, $\boldsymbol{\omega}$ and $\boldsymbol{\gamma}$) whose values do not lie at one of their respective lower or upper bounds.

R_{ij} coefficient with absolute value close to one in the off-diagonals indicate a high correlation of the corresponding parameters i and j, and vice versa. The correlation matrix for the original parameters set estimated in the case of spruce materials is shown in Table 4.6.

It can be noticed that a high absolute value of the pair of parameters in the correlation matrix is associated to the high correlation between K_p and A_{max}, observed with the preliminary parameters sensitivity analysis.

Table 4.6 *Correlation matrix for the original set of parameters.*

Parameter	Parameter Number	1	2	3	4
A_{max}	**1**	1.0000	0.3992	0.5527	**-0.9809**
k_1	**2**	0.3992	1.0000	0.5340	-0.4821
k_3	**3**	0.5527	0.5340	1.0000	-0.6420
K_P	**4**	**-0.9809**	-0.4821	-0.6420	1.0000

Correlation matrix calculated for the new set of parameters (Table 4.7) shows the positive effect of riparametrisation: correlation coefficients between K_P and P are still quite high but less critical than the values reported for the original set of parameters.

Table 4.7 *Correlation matrix for the new set of parameters.*

Parameter	Parameter Number	1	2	3	4
k_1	**1**	1.0000	0.5306	-0.4815	-0.6010
k_3	**2**	0.5306	1.0000	-0.6480	-0.7583
K_P	**3**	-0.4815	-0.6480	1.0000	**0.8713**
P	**4**	-0.6010	-0.7583	**0.8713**	1.0000

4.4 Data fitting

Model predictive capabilities have been evaluated against experimental data. Data fitting is presented in Figure 4.10-4.11. It appears that the model, as structured still exhibit some issues. If, on the one side, the most critical glucose concentration is usually estimated quite satisfactorily (particularly with wheat straw as in Figure 4.11a-d), the representation of the cellobiose dynamics can be represented only in a qualitative way (especially for S1, WS1 and WS4). It appears that in general exists a faster cellobiose initial dynamics, which the model is unable to grasp. The phenomenon is more emphasized for substrates treated at the most harsh pretreatment conditions (S1 and WS3-4). A possible explanation is the formation of a fraction of soluble cello-oligosaccharides which is easily converted to cellobiose during the initial hydrolysis stage.

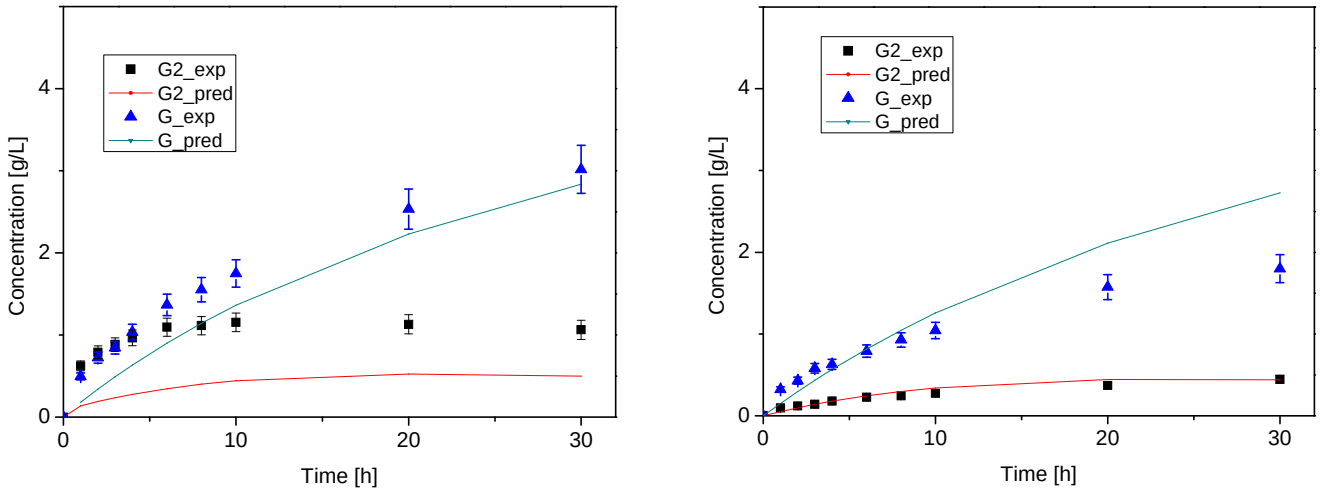

(a) (b)

Figure 4.10 *Comparison between cellobiose (G2) and glucose (G) experimental and predicted profiles for S1 (a) and S2 (b).*

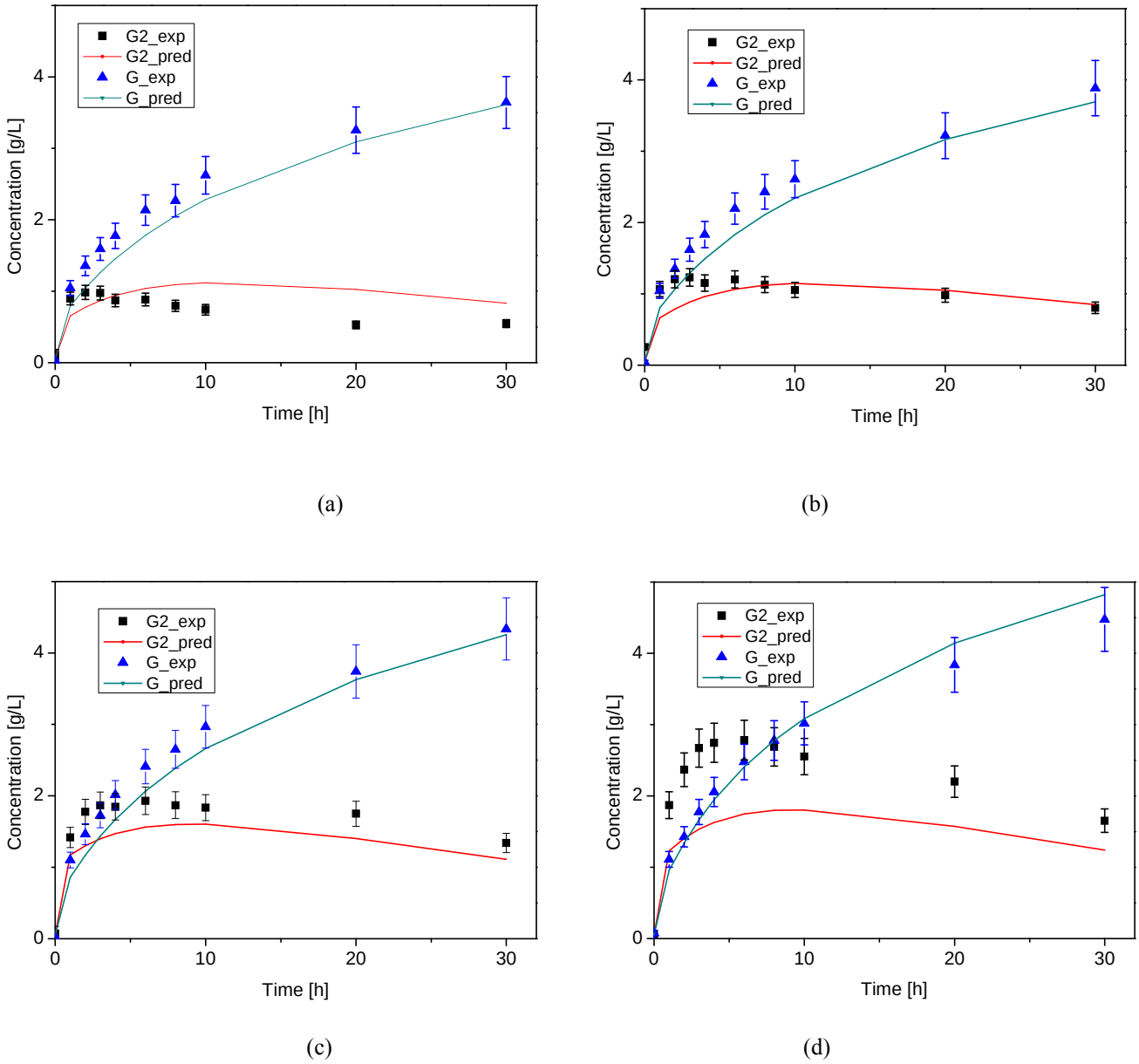

Figure 4.11 *Comparison between cellobiose (G2) and glucose (G) experimental and predicted profiles for WS1 (a), WS2 (b), WS3 (c), WS4 (d).*

The limited predictive potential is to ascribe to the oversimplification of model structure performed in order to tackle identification issues which affect more complex models, which in several studies resulted over-parameterised with respect of available experimental data (Sin et al., 2009; Kadam et al., 2004; Gan et al., 2003).

4.5 Discussion

Starting from the observations on the effect of pretreatment on the morphologic properties of lignocellulosic materials a model for the enzymatic hydrolysis of lignocellulosic materials has been developed. Specific surface area and the fraction of pores accessible to enzyme, experimentally determined, have been embedded as critical input parameter into a modified Langmuir-type adsorption model. Successively the adsorption model has been included in a three reactions hydrolysis model, based on two heterogeneous reaction rates and a Michaelis-Menten type kinetic.
Parameters estimation procedure have been carried out aiming at identifying a subset of parameters (the heterogeneous reactions kinetic constant and the adsorption isotherm parameters) for each of the two substrates considered in the experimental investigation, pretreated spruce and pretreated wheat straw.
The identification procedure provides a set of mean values of estimated parameters as well as the uncertainty of the parameters estimated represented as 95% confidence intervals, 95% t-value and parameter standard deviation. All the parameters are found to have satisfactory statistical significance, with limited confidence bands and standard deviation and 95% t-value higher than the reference value.
However the correlation matrix as well as a preliminary parameters sensitivity analysis put on evidence the strong correlation between the isotherm adsorptions parameters. For this reason we chose to estimate a new parameter P defined ad the product of the adsorption model parameters A_{max} and K_p. The riparametrisation was successful and a new set of new mean values with good statistical significance have been provided. The correlation matrix and the parameters sensitivity analysis showed a decrease in the correlation between the parameter of the new set.
Model fitting to experimental data have been evaluated; however the model capability at representing the cellobiose profile is still quite poor. A likely explanation is the limited number of parameters of the model which disregards fundamentals phenomena such as change in substrate reactivity during hydrolysis, end product inhibition, enzyme deactivation, the impact of substrate morphological features other than the specific surface area. However several studies (Sin et al., 2009; Kadam et al., 2004; Gan et al., 2003) report identification issues for increasing number of parameters, due to the strong correlation between fundamentals parameters that we have already experienced in a very simple model such as the one proposed.
It should be emphasized that more research needs to be done to overcome these identificability issues. For these models to be reliable for process design purposes, the focus on issues such as identification analysis and model structure redefinition are fundamental topics in future research.

.
.

Conclusions and perspectives

There is an increasing interest in many countries in the use of fuel ethanol from renewable biomass as a replacement of fossil fuels for the consideration of environment and energy security. Lignocellulosic biomass is considered one of most promising feedstock for production of fuel ethanol due to its global availability and environmental benefits of its use. Consequently wide varieties of processes for the production of ethanol from lignocellulosic biomass are studied and are currently under development.

For the first time, within this work, two of the most promising process routes for the production of lignocellulosic ethanol, namely the EHF and the GF process, have been compared on the basis of their techno-economic performances.

The final evaluation shows that production costs of fuel ethanol, for both technologies assessed, are still higher than gasoline production costs, although there is a strong influence of factors as the prices of oil and feedstock for ethanol production.

Furthermore some unresolved issues, common to both process options and still hindering their commercialization, have been pointed out:

- further biotechnological advancements are needed to engineer both feedstock and microorganisms utilized in biological steps in order to maximise yields and decrease the cost of enzymes production (EHF process).
- there are design, optimization and scale up problems especially for bioreactors which involve multiphase systems, for the pre-treatment step in EHF process and for the gasifier in the GF process. The problems are emphasized if continuous systems need arranging: biomass has no fixed composition and at the state of the art it is impossible to control the quality of the products coming out the different conversion steps. The development of faster and more reliable methods for biomass composition measurements is another obstacle to tackle.
- there is a need for disposal of energy intensive unit operations, such as distillation in favour of systems such as pervaporation and membrane technologies.

Integrations opportunities should also be explored as a possible approach for reducing investment costs and for improvements of the economic competitiveness of lignocellulosic ethanol production: integration between different unit operations within the same process, integrations between the two different technologies considered and integration between first generation and second generation fuel ethanol processes. Valuable co-products production, other than electricity, should be assessed in a biorefinery perspective, since a better utilization of all substrates fractions and all residues streams increases the revenues and improve the overall economics.

A deeper and aggregated understanding of the EHF process has been achieved through the experimental investigation and the kinetic modelling of lignocellulose hydrolysis step. The effect of pretreatment severity on the morphological properties of the substrate was measured in terms of the

BET surface area and pore size distribution. Another result of the experimental activity is the highly specific behaviour of different biomass substrates since peculiarities in material properties distort a direct correlation between amounts of adsorbed enzyme and accessible specific surface area across different materials. Given the correlation between the specific surface area, the extent of adsorption and the rate of hydrolysis for a specific substrate (pretreated spruce materials and pretreated wheat straw materials), we found reasonable to embed the specific surface area as a critical parameter of a new concept adsorption model. The model was then included in a simple deterministic model of lignocellulose hydrolysis and was identified through experimental data.

Despite its simplicity the model shows an acceptable agreement with experimental data and can be used in further studies to optimize enzyme loads, substrate concentration, and identify some optimal feeding and operational policies.

We acknowledge that many phenomena which are known to impact cellulose hydrolysis are not considered in the model as reported here. Further model improvement could envisage the incorporation of, for instance, competitive or synergistic adsorption, changes in the specific surface area during the course of hydrolysis, products inhibition, cellulase deactivation. Finally, the presence of lignin and hemicellulose give rise to important multiple effects which need to be further investigated and then considered from a modelling point of view. However, as model complexity increases, identificability issues arise and a trade-off between the incorporation of vital information with respect to the reaction mechanism and the unnecessary complication of the model equations should be advocated.

The integration of a kinetic model of enzymatic hydrolysis process with a model of substrates pretreatment step is an important objective for future research, as these steps are the most cost-effective operations in EHF process. A deeper understanding of the effect of different operational variables on biomass degradability and on the final rate of hydrolysis could facilitate the design of optimal pretreatments with a positive effect on the overall process economics.

References

Aden, A., M. Ruth, K. Ibsen, J. Jechura, K. Neeves, J. Sheehan, B. Wallace (2002) *Lignocellulosic biomass to ethanol processing design and economics utilizing co-current dilute acid prehydrolysis and enzymatic hydrolysis for corn stover*. Technical Report NREL/TP-510-32438. National Renewable Energy Laboratory , Golden, CO (U.S.A.).

Aden, A., P. Spath and B. Atherton (2005). *The potential of thermochemical ethanol via mixed alcohols production.* Milestone Completion Report of National Renewable Energy Laboratory, Golden, CO (U.S.A.).

Adney, W.S., C.I. Ehrman, J.O. Baker, S.R. Thomas, M.E. Himmel (1994). Cellulase assays: methods from empirical mathematical models. *ACS Ser*, **566**, 219–235.

Arato, C., E.K. Pye, G. Gjennestad (2005). The Lignol approach to biorefining of woody biomass to produce ethanol and chemicals. *Applied Biochemistry and Biotechnology*, **121–124**, 871–882.

Badger, P.C. (2002). Ethanol from cellulose: a general review. In: *Trends in new crops and new uses*, (J. Janick and A. Whipkey Editors), ASHS Press, Alexandria (VA).

Balat, M. (2007). Global bio-fuel processing and production trends, *Energy Explor Exploit*, **25**, 195–218.

Balat, M. (2009). New biofuel production technologies, *Energy Educ Sci Technol,* **22**, 147–161.

Béguin, P., J.P. Aubert (1994). The biological degradation of cellulose. *FEMS Microbiology Reviews*, **13,** 25–58.

Beldman, G., A.G.J. Voragen, F.M. Rombouts, M.F. Searle-van Leeuwen, and W. Pilnik (1987). Adsorption and kinetic behavior of purified endoglucanases and exoglucanases from *Trichoderma viride. Biotechnol. Bioeng.*, **30,** 251–257.

Beltrame, P.L., P. Carniti, B. Focher, A. Marzetti, V. Sarto (1984). Enzymatic hydrolysis of cellulosic materials: a kinetic study. *Biotechnol Bioeng*, **26**, 1233– 1238.

Bernardez, T.D., K. Lyford, D.A. Hogsett, L.R. Lynd (1993). Adsorption of Clostridium thermocellum cellulase onto pretreated mixed hardwood, Avicel and Lignin. *Biotechnol Bioeng,* **43,** 899–907.

Betrabet, S.M., K.M. Paralikar (1977). Effect of cellulase on the morphology and fine structure of cellulosic substrates. 1. wheat straw pulp. *Cellulose Chem Technol*, **11**, 615–625.

Biofuels for transportation (2007). European Biomass Industry Association (EUBIA), Renewable Energy House, Brussels (Belgium). `http://www.eubia.org`. (last accessed October 2009).

Botello, J.I. M.A. Gilarranz, F. Rodriguez M. Oliet (1999). Preliminary study on products distribution in alcohol pulping of *Eucalyptus globulus. J. Chem. Technol. Biotechnol.*, **74,** 141– 148.

Boussaid, A., J.N. Saddler (1999). Adsorption and activity profiles of cellulases during the hydrolysis of two Douglas-fir pulps. *Enzyme Microbial Technol*, **24,** 138-143.

Bradford, M.M. (1976). A rapid and sensitive method for the quantitation of microgram quantities of protein utilizing the principle of protein-dye binding. *Analytical Biochem*, **72,** 248-254.

Brash, J.L., T.A. Horbett (1995). Proteins at interfaces, an overview. In: *Proteins at interfaces II, Fundamentals and Applications* (Horbett TJ, Brash JL Eds.), ACS Symposium Series 602, American Chemical Society, Washington, DC, (U.S.A.).

Bredwell, M.D., P. Srivastava e R.M. Worden (1999). Reactor design issues for synthesis.gas fermentations. *Biotechnol. Prog*, **15**, 834-844.

Bridgwater, A. V. (1995). The technical and economic feasibility of biomass gasification for power generation. *Fuel*, **74**, 5, 631-653.

Brown, R.C. (2007). Hybrid thermochemical/biological processing. *Applied biochem and biotechnol*. **136-140**, 947-956.

Brown, R.M. (2004). Cellulose structure and biosynthesis : what is in store for the 21st century ?, *Journal of Polymer Science*, **42,** 487-495.

Brownell, H.H., J.N. Saddler (1987). Steam pretreatment of lignocellulosic material for enhanced enzymatic hydrolysis. *Biotechnol Bioeng,* **29,** 228-235.

Bruce, W. (BRI Energy President) (2006). *Testimony in front of United States Senate Natural Resources Committee*, Washington, DC, 1 May.

Bungay, H. and J. Peterson (1992). CMA as a byproduct of the manufacture of fuel ethanol. *Resources, Conservation and Recycling*, **7**, 83–94.

Burns, D.S., H. Ooshima, A.O. Converse (1989). Surface area of pretreated lignocellulosics as a function of the extent of enzymatic hydrolysis. *Appl Biochem Biotechnol,* **20/21**, 79-94.

Caminal, G., J. Lòpez-Santin, and C. Sola (1985). Kinetic modeling of the enzymatic hydrolysis of pretreated cellulose. *Biotechnol. Bioeng.*, **27**, 1282– 1290.

Campbell, G. (2007). *Panorama of transport*. Office for Publications of the European Communities, Luxembourg.

Cardona, C. A., O. J. Sànchez (2006). Energy consumption analysis of integrated flowsheet for production of fuel ethanol from lignocellulosic biomass. *Energy*, **31**, 13, 2447-2459.

Cardona, C.A. and O.J. Sanchez (2007). Fuel ethanol production: process design trends and integration opportunities, *Bioresour Technol*, **98,** 2415–2457.

Cardona, C.A., O.J. Sànchez, (2004). Analysis of integrated flow sheets for biotechnological production of fuel ethanol. In: *PRES 2004-16th International congress of chemical and process engineering (CHISA 2004)*, Prague (Czech Republic).

Carrard, G., M. Linder (1999). Widely different off rates of two closely related cellulose-binding domains from *Trichoderma reesei*. *Eur J Biochem*, **262,** 637– 643.

Caulfield, D.F., W.E. Moore (1974). Effect of varying crystallinity of cellulose on enzyme hydrolysis. *Wood Sci*, **6**, 375– 379.

Chandra, R.P., S.M. Ewanick, C. Hsieh, J.N. Saddler (2008). The characterization of pretreated lignocellulosic subsrates prior to enzymatic hydrolysis, part1: a modified Simon's staining technique. *Biotechnol Prog*, **24**, 1178-1185.

Chandra, R.P., S.M. Ewanick, P.A. Chung, K. Au-Yeung , L. Del Rio, W. Mabee, J.N. Saddler (2009). Comparison of method to assess the enzyme accessibility and hydrolysis of pretreated lignocellulosic substrates. *Biotechnol Lett*, **31**, 1217-1222.

Chandrakant, P., V.S. Bisaria (1998). Simultaneous bioconversion of cellulose and hemicellulose to ethanol. *Critical Reviews in Biotechnology*, **18,** 295–331.

Chang, M.M., T.Y.C. Chou, G.T. Tsao (1981). Structure, pretreatment and hydrolysis of cellulose. *Adv Biochem Eng*, **20**, 15– 42.

Chang, V.S., M.T. Holtzapple (2000). Fundamental factors affecting biomass enzymatic reactivity. *Appl Biochem and Biotechnol*, **84-86**, 5-37.

Chang, V.S., M.T. Holtzapple (2000). Fundamental factors affecting biomass enzymatic reactivity. *Appl Biochem Biotechnol*, **84/86**, 5– 37.

Chanzy, H. and B. Henrissat (1985). Unidirectional degradation of Valonia cellulose microcrystals subjected to cellulase action. *FEBS Lett*, **184,** 285–288.

Chanzy, H., B. Henrissat, R.Vuong (1984). Colloidal gold labeling of 1,4- β-glucan cellobiohydrolase adsorbed on cellulose substrates. *FEBS Lett*, **172,** 193– 196.

Chem Eng **114** (May 2007), p. 96.

Chen, C.S., Y.W. Lai, C.J. Tien (2008). Partitioning of aromatic and oxygenated constituents into water from regular and ethanol-blended gasolines, *Environ Pollut,* **156**, 988–996.

Chernoglazov, V.M., O.V. Ermolova, A.A. Klyosov (1988). Adsorption of high-purity *endo*-1,4-β-glucanases from *Trichoderma reesei* on components of lignocellulosic materials: cellulose, lignin, and xylan. *Enzyme Microb Technol*, **10**, 503–507.

Claassen, P.A.M., J.B. van Lier, A.M. López Contreras, E.W.J. van Niel, L. Sijtsma, A.J.M. Stams, de Vries, S.S. and R.A. Weusthuis (1999). Utilisation of biomass for the supply of energy carriers, *Applied Microbiology and Biotechnology,* **52**, 741–755.

Clausen, E.C. (2006). Personal Communication.

Converse, A.O., H. Ooshima, D.S. Burns (1990). Kinetics of enzymatic hydrolysis of lignocellulose materials based on surface area of cellulose accessible to enzyme and enzyme adsorption on lignin and cellulose. *Appl Biochem and Biotechnol*, **24-25**, 67-73.

Converse, A.O., H.E. Grethlein (1987). On the use of an adsorption model to represent the effect of steam explosion pretreatment on the enzymatic hydrolysis of lignocellulosic substances. *Enzyme Microb Technol,* **9**, 79–82.

Converse, A.O., J.D. Optekar (1993). A synergistic kinetics model for enzymatic cellulose hydrolysis compared to degree-of-synergism experimental results. *Biotechnol Bioeng*, **42,** 145–148.

Converse, A.O., R. Matsuno, M. Tanaka, M. Taniguchi (1988). A model of enzyme adsorption and hydrolysis of microcrystalline cellulose with slow deactivation of the adsorbed enzyme. *Biotechnol Bioeng*, **32**, 38–45.

Converti, A., S. Arni, S. Sato, J.C.M. Carvalho, E. Aquarone (2003). Simplified modeling of fed-batch alcoholic fermentation of sugarcane blackstrap molasses, *Biotechnology and Bioengineering* **84,** 88–95.

Co-production of ethanol and electricity from carbon- based wastes. A report from Bioengineering Resources, Inc. regarding a new technology that addresses multiple energy and waste disposal solutions (2006). Technical report. www.brienergy.com (ultimo accesso: 2009).

Coughlan, M. (1985), The properties of fungal and bacterial cellulases with comment on their production and application.*Biotech. Genet. Eng. Rev,.* **3,** 39–109.

Dale, B.E. (1986). *Method for increasing the reactivity and digestibility of cellulose with ammonia.* US Patent 4,600,590.

Datar, R.P., R.M. Shenkman, B.G. Cateni, R.L. Huhnke e R.S. Lewis (2004). Fermentation biomass-generated producer gas to ethanol. *Biotechnology and Bioengineering*, **86**, 587-594.

Davies, G.J., V. Ducros, R.J. Lewis, T.V. Borchert, M. Schulein (1997). Oligosaccharide specificity of a family 7 endoglucanase: insertion of potential sugar-binding subsites. *J Biotechnol,* **57**, 91–100.

Decker, C.H., J. Visser and P. Schreier (2000). β-Glucosidases from five black *Aspergillus* species: study of their physico-chemical and biocatalytic properties. *J. Agric. Food Chem*. **48**, 4929–4936.

Demirbas, A. (2000). Biomass resources for energy and chemical industry. *Energy Edu Sci Technol*, **5**, 21–45.

Demirbas, A. (2005). Bioethanol from cellulosic materials: a renewable motor fuel from biomass, *Energy Sources Part A,* **27**, 327–337.

Demirbas, A. (2006). Global biofuel strategies, *Energy Educ Sci Technol,* **17**, 33–63.

Demirbas, A. (2007). Producing and using bioethanol as an automotive fuel, *Energy Sources Part B,* **2**, 391–401.

Demirbas, M.F., M. Balat (2006). Recent advances on the production and utilization trends of bio-fuels: a global perspective, *Energy Convers Manage,* **47**, 2371–2381.

Dermoun, Z., and J.P. Bélaïch (1988). Crystalline index change in cellulose during aerobic and anaerobic *Cellulomonas uda* growth. *Appl. Microbiol. Biotechnol*., **27**, 399–404.

Desai, S. G., and A. O. Converse (1997). Substrate reactivity as a function of the extent of reaction in the enzymatic hydrolysis of lignocellulose. *Biotechnol. Bioeng.*, **56**, 650–655.

Detchon (2005). *Biofuels for Our Future: A Primer.* UN Foundation `www.energyfuturecoalition.org/biofuels/BioFuels_FAQ.pdf` (last accessed October 2009).

Deurwaarder, E.P. (2005). *Overview and Analysis of National Reports of the EU Biofuel Directive: Prospects and Barriers for 2005.* ECN (Energy Research Centre of the Netherlands) `www.ecn.nl/docs/library/report/2005/c05042.pdf` (last accessed October 2009).

Difiglio, C. (1997). Using advanced technologies to reduce motor vehicle greenhouse gas emissions. *Energy Policy*, **25**, 1173–1178.

Din, N., H.G. Damude, N.R. Gilkes, R.C. Miller, R.A.J. Warren and D.G. Kilburn (1994). C1-Cx revisited: intramolecular synergism in a cellulase. *Proc. Natl. Acad. Sci*., **91**, 11383–11387.

Divne, C., J. Ståhlberg, T. Reinikainen, L. Ruohonen, G. Pettersson, J. K. C. Knowles, T. T. Teeri, and T. A. Jones (1994). The three-dimensional crystal structure of the catalytic core of cellobiohydrolase I from *Trichoderma reesei. Science,* **265**, 524–528.

Dizhbite, T., G. Zakis, A. Kizima, E. Lazareva, G. Rossinskaya, V. Jurkjane, G. Telysheva and U. Viesturs (1999). Lignin – a useful bioresource for the production of sorption-active materials, *Bioresource Technology*, **67**, 221–228.

DOE announces up to $200 million in funding for biorefineries: small- and full-scale projects total up to $585 million to advance President Bush's Twenty in Ten Initiative (2007). United States Department of Energy. Press release, `www.energy.gov/news/5031.htm`, May 1st.

Donaldson, L.A., K.K.Y. Wong, K.L. Mackie (1988). Ultrastructure of steam-exploded wood. *Wood Sci Technol*, **22,** 103-114.

Douglas, J.M. (1988). *Conceptual design of chemical processes*, McGraw-Hill Book Co., New York (U.S.A.).

Dufey, A (2006). *Biofuels production, trade and sustainable development: emerging issues. Sustainable markets discussion, paper no. 2*, International Institute for Environment and Development, London (U.K.), November 2006.

Duff, S.J.B., W.D. Murray (1996). Bioconversion of forest products industry waste cellulosics to fuel ethanol: a review. *Biores Technol*, **55,** 1-33.

Elander, T.E., V.L. Putsche (1996). Ethanol from corn: Technology and economics. In: *Handbook on bioethanol: Production and utilization*.Wyaman, C.E., Washington (U.S.A.), pp. 351-347.

Energy technology perspectives 2006 – in support of the G8 plan of action – scenarios and strategies to 2050 (2006). Technical Report of International Energy Agency (IEA)/Organisation for Economic Co-operation and Development (OECD), Paris (France).

Ericsson, K. and L.J. Nilsson (2004). International biofuel trade—a study of the Swedish import, *Biomass Bioenergy*, **26,** 205–220.

Eriksson, T., J. Borjesson, F. Tjerneld (2002). Mechanism of surfactant effect in enzymatic hydrolysis of lignocellulose. *Enzyme Microb Technol*, **31**, 353– 364.

European transport policy for 2010: time to decide (2001). European Commission (EC). White Paper, Brussels (Belgium); `http://www.europa.eu.int` (last accessed October 2009)

Fan, L., Y. Lee, D. Beardmore (1981). The influence of major structural features of cellulose on rate of enzymatic hydrolysis. *Biotechnol Bioeng*, **23**, 419-424.

Fan, L.T. , Y.H. Lee, M.M. Gharpuray (1982). The nature of lignocellulosics and their pretreatments for enzymatic hydrolysis. *Adv. Biochem. Eng*., **23**, 158-187.

Fan, L.T., Y.-H. Lee (1983). Kinetics studies of enzymatic hydrolysis of insoluble cellulose: derivation of a mechanistic kinetics model. *Biotechnol Bioeng*, **25**, 2707–2733.

Fan, L.T., Y.-H. Lee, D.H. Beardmore (1980). Mechanism of the enzymatic hydrolysis of cellulose: effects of major structural features of cellulose on enzymatic hydrolysis. *Biotechnol Bioeng*, **22,** 177– 199.

Fan, L.T., Y.H. Lee, M..M. Gharpuray (1982). The nature of lignocellulosics and their pretreatments for enzymatic hydrolysis. *Adv. Biochem. Eng*, **23**, 158-187.

Feasibility study on an effective and sustainable bioethanol production program by least developed countries as alternative to cane sugar export. Ministry of Agriculture, Nature and Food Quality (LNV) (2005). Dutch Sustainable Development Group (DSD), The Hague (The Netherlands), May 20. <library.wur.nl/WebQuery/catalog/lang/1845441>.

Fengel, D., G. Wegener (1989). *Wood: chemistry, ultrastructure, reactions.* Walter de Gruyter & Co., Berlin (Germany).

Fenske, J.J., M.H. Penner, J.P. Bolte (1999). A simple individual-based model of insoluble polysaccharide hydrolysis: the potential for autosynergism with dual-activity glycosidases. *J Theor Biol*, **199**,113–118.

Fierobe, H.P., E.A. Bayer, C. Tardif, M. Czjzek, A. Mechaly, A. Bélaïch, R. Lamed, Y. Shoham, J.P. Bélaıch (2002). Degradation of Cellulose Substrates by Cellulosome Chimeras: substrate targeting versus proximity of enzyme components. *J Biol Chem*, **277**, 49621-49630.

Foyle, T., L. Jennings and P. Mulcahy (2006). Compositional analysis of lignocellulosic materials: evaluation of methods used for sugar analysis of waste paper and straw, *Bioresource Technology*, **98**, 3026–3036.

Franceschin, G., A. Zamboni, F. Bezzo and A. Bertucco (2008). Ethanol from corn: a technical and economic assessment based on different scenarios, *Chem Eng Res Des,* **86**, 488–498.

Galbe M. and G. Zacchi (2007). Pretreatment of lignocellulosic materials for efficient bioethanol production, *Adv Biochem Eng Biotechnol*, **108**, 41–65.

Gama, F.M., and M. Mota (1997). Enzymatic hydrolysis of cellulose (I): relationship between kinetics and physico-chemical parameters. *Biocatalysis Biotrans*., **15**, 221–236.

Gan, Q., S.J. Allen, G. Taylor (2003). Kinetic dynamics in heterogeneous enzymatic hydrolysis of cellulose: an overview, an experimental study and mathematical modeling, *Process Biochem,* **38**, 1003–1018.

Gauss, W.F., S. Suzuki, M. Takagi (1976*). Manufacture of alcohol from cellulosic materials using plural ferments.* Patent US3990944.

Gharpuray, M.M., Y.H. Lee, L.T. Fan (1983). Structural modification of lignocellulosic by pretreatments to enhance enzymatic hydrolysis. *Biotechnol Bioeng,* **25**,157–172.

Ghose, T.K. (1987). Measurement of cellulase activities. *Pure & Appl Chem*, **59,** 257-268.

Ghosh, P., T.K. Ghose (2003). Bioethanol in India: recent past and emerging future. *Advances in Biochemical Engineering/Biotechnology,* **85**, 1–27.

Gilkes, N.R., E. Jervis, B. Henrissat, B. Tekant, R.C. Jr Miller, R.A.J. Warren, D.G. Kilburn (1992). The adsorption of a bacterial cellulase and its two isolated domains to crystalline cellulose. *J Biol Chem*, **267**, 6743– 6749.

Glick, B.R. and J.J. Pasternak (1989). Isolation, characterization and manipulation of cellulase genes. *Biotechnol. Adv.,* **7**, 361–386.

Gong, C.S., M.R. Ladisch and G.T. Tsao (1977). Cellobiase from *Trichoderma viride:* purification, properties, kinetics, and mechanism. *Biotechnol. Bioeng*., **19**, 959–981.

Gong, C.S., N.J. Cao, J. Du, G.T. Tsao (1999). Ethanol production from renewable resources. Advances in Biochemical Engineering/Biotechnology, **65**, 207–241.

Gonzalez, G., G. Caminal, C. de Mas, Lopez-Santin (1989). A kinetic model pretreated wheat straw saccharification by cellulose. *J Chem Technol Biotechnol*, **44**, 275– 288.

Graf, A. and T. Koehler (2000). *Oregon Cellulose-Ethanol Study*. Oregon Office of Energy. Salem OR (USA).

Greenergy International Limited. Bioethanol–a greenergy perspective. London (2007) `http://www.greenergy.com` (last accessed October 2009)

Gregg, D., J. Saddler (1995). Bioconversion of lignocellulosic residue to ethanol: process flowsheet development. *Biomass and Bioenergy,* **9** (1– 5), 287–302.

Gregg, D.J., A. Boussaid, J.N. Saddler (1998). Techno-economic evaluation of a generic wood-ethanol process: effect of increased cellulose yields and enzyme recycle. *Bioresour Technol*, **63**, 7-12.

Gregg, D.J., J.N. Saddler (1996). Factors affecting cellulose hydrolysis and the potential of enzyme recycle to enhance the efficiency of an integrated wood to ethanol process. *Biotechnol. Bioeng*, **51,** 375-383.

Grethlein, A.J., M.K. Jain (1993). Bio-processing of coal-derived synthesis gases by anaerobic bacteria. *Trends Biotechnol*., **10**, 418-423.

Grethlein, H.E. (1985). The effect of pore size distribution on the rate of enzymatic hydrolysis of cellulose substrates. *Bio/Technology*, **3,** 155–160.

Grethlein, H.E., D.C. Allen, A.O. Converse (1984). A comparative stdy of the enzymatic hydrolysis of the acid-pretreated white pine and mixed hardwood, *Biotechnol. Bioeng*, **26,** 1498-1505.

Gueret, C., M. Daroux and F. Billaud (1997). Methane pyrolysis: thermodynamics, *Chem Eng Sci,* **5,** 815–827.

Gulati, M., P.J. Westgate, M. Brewer, R. Hendrickson and M.R. Ladisch (1996). Sorptive recovery of dilute ethanol from distillation column bottoms stream, *Applied Biochemistry and Biotechnology,* **57/58**, 103–119.

Gunata, Z. and M.J. Vallier (1999). Production of a highly glucose-tolerant extracellular β-glucosidase by three *Aspergillus* strains. *Biotechnol. Lett.,* **21**, 219–223.

Guo, G.L., W.H. Chen, L.C. Men, W.S. Hwang (2008). Characterization of dilute acid pretreatment of silvergrass for ethanol production. *Bioresource Technol*, **99,** 6046-6053.

Gusakov, A.V., A.P. Sinitsyn (1992). A theoretical analysis of cellulase product inhibition: effect of cellulase binding constant, enzyme/substrate ratio, and h-glucosidase activity on the inhibition pattern. *Biotechnol Bioeng*, **40**, 663– 671.

Gusakov, A.V., A.P. Sinitsyn, A.A. Klyosov (1985a). Kinetics of the enzymatic hydrolysis of cellulose. 1. A mathematical model for a batch reactor process. *Enzyme Microb Technol,* **7**, 346–352.

Gusakov, A.V., A.P. Sinitsyn, A.A. Klyosov (1985b). Kinetics of the enzymatic hydrolysis of cellulose. 2. A mathematical model for process in a plugflow column reactor. *Enzyme Microb Technol,* **7**, 383– 388.

Gusakov, A.V., A.P. Sinitsyn, J.A. Manenkova and O.V. Protas (1992). Enzymatic saccharification of industrial and agricultural lignocellulosic wastes—main features of the process. *Appl. Biochem*. Biotechnol., **34–35**, 625–637.

Gusakov, A.V., A.P. Sinitsyn, V.B. Gerasimas, R.Y. Savitskene, Y.Y. Steponavichus (1985c). A product inhibition study of cellulases from Trichoderma longibrachiatum using dyed cellulose. *J Biotechnol,* **3**, 167– 174.

Hahn-Hägerdal, B., M. Galbe, M.F. Gorwa-Grauslund and G. Zacchi (2006). Bioethanol – the fuel of tomorrow from the residues of today, *Trends Biotechnol*, **24,** 549–556.

Hamelinck, C. N. and A.P.C. Faaij (2005). Outlook for advanced biofuels, *Energy Policy,* **34,** 3268–3283.

Hamelinck, C. N., G. van Hooijdonk e A. Faaij (2005). Ethanol from lignocellulosic biomass: techno-economic performance in short-, middle- and long-term. *Biomass and Bioenergy*, **28**, 384-410.

Hamelinck, C.N. and A.P.C. Faaij (2001). *Future prospects for production of methanol and hydrogen from biomass*. Report NWS-E-2001-49, Utrecht University, Utrecht (The Netherlands).

Hammerschlag, R. (2006). Ethanol's energy return on investment. A survey of the literature 1990–present, *Environ Sci Technol*, **40**, 1744–1750.

Henrissat, B., B. Vigny, S. Perez (1988a). Possible adsorption sites of cellulases on crystalline cellulose. *FEBS Lett*, **231**, 177– 182.

Henrissat, B., H. Driguez, C. Viet, M. Schülein (1985). Synergism of cellulases from Trichoderma reesei in the degradation of cellulose. *Bio/Technology*, **3,** 722–726.

Henrissat, B., T.T. Teeri and R.A.J. Warren (1998b). A scheme for designating enzymes that hydrolyse the polysaccharides in the cell walls of plants. *FEBS Lett*., **425**, 352–354.

Himmel M.E., M.F. Ruth, C.E. Wymand (1999). Cellulase for commodity products from cellulosic biomass. *Current Opinion in Biotechnology*, **10,** 358-364.

Hinman, N.D., D.J. Schell, C.J. Riley, P.W. Bergeron and P.J. Walter (1992). Preliminary estimate of the cost of ethanol production for SSF technology, *Appl Biochem Biotechnol*, **34–35**, 639–649.

Holtzapple, M., M. Cognata, Y. Shu and C. Hendrickson (1990). Inhibition of *Trichoderma reesei* cellulase by sugars and solvents. *Biotechnol. Bioeng.*, **36**, 275–287.

Holtzapple, M.T., H.S. Caram, A.E. Humphrey (1984a). The HCH-1 model of enzymatic cellulose hydrolysis. *Biotechnol Bioeng*, **26**, 775– 780.

Holtzapple, M.T., H.S. Caram, A.E. Humphrey (1984b). Determining the inhibition constants in the HCH-1 model of cellulose hydrolysis. *Biotechnol Bioeng*, **26**, 735–757.

Holtzapple, M.T., H.S. Caram, A.E. Humphrey (1984c). A comparison of two empirical models for the enzymatic hydrolysis of pretreated poplar wood. *Biotechnol Bioeng*, **26**, 936–941.

Howell, J.A., J.D. Stuck (1975). Kinetics of Solka Floc cellulose hydrolysis by Trichoderma viride cellulase. Biotechnol Bioeng 17:873– 893.

Howell, J.A., J.D. Stuck (1975). Kinetics of Solka Floc cellulose hydrolysis by Trichoderma viride cellulase. *Biotechnol Bioeng*, **17**, 873– 893.

Huang, A.A. (1975). Kinetic studies on insoluble cellulose-cellulase system. *Biotechnol Bioeng,* **17**, 1421–1433.

Jacquet, F., L.Bamiere, J.C. Bureau, L. Guinde (2007). Recent developments and prospects for the production of biofuels in the EU: can they really be "part of solution"? In: *Proceedings of the conference on "biofuels, food and feed tradeoffs"*, Missouri (U.S.A.), April 12–13th.

Jaques, K., T.P. Lyons, D.R. Kelsall. (2003). *The alcohol textbook – A reference for the beverage, fuel and industrial alcohol industries*. (K. Jaques, T.P. Lyons, D.R. Kelsall Editors), Nottingham (U.K.).

Jefferson, M. (2006). Sustainable energy development: performance and prospects. *Renew Energy,* **31**, 571–82.

Jeoh, T., D.B. Wilson, L.P. Walker (2002). Cooperative and competitive binding in synergistic mixtures of Thermobifida fusca cellulases Cel5A, Cel6B, and Cel9A. *Biotechnol Prog*, **18**, 760–769.

Jusarek, L. (1979). Enzymic hydrolysis of pretreated aspen wood. *Dev. Indust. Microb*., **20,** 177-183.

Kadam, K.L., E.C. Rydholm, J.D. McMillan (2004). Development and validation of a kinetic model for enzymatic saccharification of lignocellulosic biomass, *Biotechnol Progr*, **20**, 698-705.

Karrer, P., P. Schubert, W. Whrli (1925). Polysaccharide XXXIII: uber enzymatischen abbau von kunstseide und nativer cellulose. *Helv Chim Acta*, **8,** 797– 810.

Kaster, J.A., D.L. Michelsen, W.H. Velander (1990). Increased Oxygen Transfer in a Yeast Fermentation Using a Microbubble Dispersion. *Appl. Biochem. Biotechnol.,* **24-25**, 469-484.

Kaylen, M., D. Van Dyne, Y.-S. Choi and M. Blasé (2000). Economic feasibility of producing ethanol from lignocellulosic feedstocks. *Bioresource Technology*, **72**, 19–32.

Kilpinen, P., M. Hupa and J. Leepälahti (1991). *Nitrogen chemistry at gasification – a thermodynamic analysis Report 91-14,* Combustion Chemistry Research Group, Abo Academi University, Finland.

Kim D.W., Y.H. Jang, J.K. Jeong (1998). Adsorption kinetics and behaviour of two cellobiohydrolases from *Trichoderma reesei* on microcrystalline cellulose. *Biotechnol Appl Biochem*, **27,** 97–102.

Kim, D.W., T.S. Kim, Y.K. Jeong, J.K. Lee (1992). Adsorption kinetics and behaviours of cellulase components on microcrystalline cellulose. *J Ferm Bioeng*, **73,** 461-466.

Kim, D.W., Y.K. Jeong, Y.H. Jang, and J.K. Lee (1994). Purification and characterization of endoglucanase and exoglucanase components from *Trichoderma viride. J. Ferment. Bioeng*., **77**, 363–369.

Kim, S. and B.E. Dale (2004). Global potential bioethanol production from wasted crops and crop residues, *Biomass Bioenergy,* **26**, 361–375.

Klass, D.L. (1998) *Biomass for renewable energy, fuels, and chemicals*, Academic Press, San Diego (U.S.A.).

Kleywegt, G.J., J.Y. Zou, C. Divne, G.J. Davies, I. Sinning, J. Ståhlberg, T. Reinikainen, M. Srisodsuk, T.T. Teeri and T.A. Jones (1997). The crystal structure of the catalytic core domain of endoglucanase I from *Trichoderma reesei* at 3.6 Å resolution, and a comparison with related enzymes. *J. Mol. Biol*., **272**, 383–397.

Klyosov, A.A (1990). Trends in biochemistry and enzymology of cellulose degradation. *Biochemistry*, **29,** 10577–10585.

Knauf, G., J. Maier, N. Skuce, A. Sugrue (2005). The challenge of sustainable bioenergy: balancing climate protection, biodiversity and development policy. A discussion paper, Forum Entwicklung und Umwelt, Bonn (Germany).

Kojima, M., D. Mitchell, W. Ward (2007). *Considering trade policies for liquid biofuels*. Energy Sector Management Assistance Program, Special Report 004/07, World Bank, Washington, DC (U.S.A.).

Koullas, D.P., P. Christakopoulos, D. Kekos, B.J. Macris, E.G. Koukios (1992). Correlating the effect of pretreatment on the enzymatic hydrolysis of straw. *Biotechnol Bioeng*, **39,** 113– 116.

Krassig, H.A. (1993). *Cellulose: structure, accessibility and reactivity*. Gordon & Breach Yverdon (Switzerland).

Kristensen, J., L. Thygesen, C. Felby, H. Jørgensen, T. Elder (2008). Cell-wall structural changes in wheat straw pretreated for bioethanol production. *Biotechnol Biofuels*, **16**, 1-5.

Kubicek, C.P. and M.E. Penttilä (1998). Regulation of production of plant polysaccharide degrading enzymes by *Trichoderma*, p. 49–72. In: *Trichoderma and Gliocladium* vol. 2 (G. E. Harman and C. P. Kubicek, Ed.), Taylor & Francis Ltd., London (United Kingdom).

Kyriacou, A., R.J. Neufeld, C.R. MacKenzie (1988). *Effect of physical parameters on the adsorption characteristics of fractionated Trichoderma reesei cellulase components*. *Enzyme Microb Technol*, **10,** 675–681.

Ladisch, M.R. and K. Dyck (1979). Dehydration of ethanol: new approach gives positive energy balance, *Science*, **205**, 898–900.

Ladisch, M.R., J. Hong, M. Voloch, G.T. Tsao (1981). Cellulase kinetics. In: Hollaender A, Rabson R, Rogers, P., A. San Pietro, R. Valentine, R. Wolfe (). *Trends in the biology of fermentations for fuels and chemicals.* New York (U.S.A.). p 55– 83.

Ladisch, M.R., M. Voloch, J. Hong, P. Bienkowski and G.T. Tsao (1984). Cornmeal Adsorber for Dehydrating Ethanol Vapors, *I&EC Process Design and Development,* **23**, 437–443.

Latif, F. and M.I. Rajoka (2001). Production of ethanol and xylitol from corn cobs by yeasts, *Bioresource Technology*, **77**, 57–63

Lawford, H.G., J.D. Rousseau (2003). Cellulosic fuel ethanol. Alternative fermentation process designs with wild-type and recombinant Zymomonas mobilis. *Applied Biochemistry and Biotechnology*, **105–108**, 457–469.

Leathers, T.D. (2003). Bioconversions of maize residues to value-added coproducts using yeast-like fungi, *FEMS Yeast Research* **3**, 133–140.

Lee, J. (1997). Biological conversion of lignocellulosic biomass to ethanol, *J. biotechnol*, **56,** 1-24.

Lee, N.E., and J. Woodward (1989). Kinetics of the adsorption of *Trichoderma reesei* C30 cellulase to DEAE-Macrosorb. ***J. Biotechnol***., **11**, 75–82.

Lee, S.B., H.S. Shin, D.D.Y. Ryu (1982). Adsorption of cellulase on cellulose: effect of physiochemical properties of cellulose on adsorption and rate of hydrolysis. *Biotechnol Bioeng*, **24,** 2137– 2153.

Lee, S.B., I.H. Kim, S.S.Y. Ryu, H. Taguchi (1983). Structural properties of cellulose and cellulase reaction mechanism. *Biotechnol Bioeng*, **25,** 33-52.

Lee, Y.-H. and L. T. Fan (1983). Kinetic studies of enzymatic hydrolysis of insoluble cellulose. II. Analysis of extended hydrolysis times. ***Biotechnol. Bioeng.*** **25**, 939–966.

Lee, Y.-H., L.T. Fan (1982). Kinetic studies of enzymatic hydrolysis of insoluble cellulose: analysis of the initial rates. *Biotechnol Bioeng*, **24**, 2383–2406.

Lee, Y.L. and J.M. Sanchez (1997). Theoretical study of thermodynamics relevant to tetramethylsilane pyrolysis, *J Cryst Growth,* **178,** 513–517.

Lehtio, J., J. Sugiyama, M. Gustavsson, L. Fransson, M. Linder, T.T. Teeri (2003). The binding specificity and affinity determinants of family 1 and family 3 cellulose binding modules. *Proc Natl Acad Sci USA*, **100**, 484– 489.

Lenze, J., H. Esterbauer, W. Sattler, J. Schurz, E. Wrentschur (1990). Changes of structure and morphology of regenerated cellulose caused by acid and enzymatic hydrolysis. *J Appl Poly Sci*, **41**, 1315– 1326.

Lin, J.K., M.R. Ladisch, J.A. Patterson and C.H. Noller (1987). Structural properties of cellulose and cellulase reaction mechanism. ***Biotechnol. Bioeng.***, **29**, 976–981.

Lin, Y., S. Tanaka (2006). Ethanol fermentation from biomass resources: current state and prospects. *Applied Microbiology and Biotechnology,* **69,** 627–642.

Linde, M., M. Galbe and G. Zacchi (2008). Bioethanol production from non-starch carbohydrate residues in process streams from a dry-mill ethanol plant, *Bioresour Technol* , **99,** 6505–6511.

Linde, M., M. Galbe, G. Zacchi (2006). Steam pretreatment of acid-sprayed and acid-soaked barley straw for production of ethanol, ***Appl. Biochem. Biotechnol***., **129-132**, 564-562.

Linder, M., and T. T. Teeri (1996). The cellulose-binding domain of the major cellobiohydrolase of *Trichoderma reesei* exhibits true reversibility and a high exchange rate on crystalline cellulose. ***Proc. Natl. Acad. Sci. USA***, **93,**12251–12255.

Linnhoff, B. and J.R. Flower (1978). Synthesis of heat exchanger networks: systematic generation of energy optimal networks, *AIChE J,* **24,** 633–654.

Luo, J., L. Xia, J. Lin, P. Cen (1999). Kinetics of simultaneous saccharification and lactic acid fermentation process. *Biotechnol Prog*, **13**, 762– 767.

Lynd, L.R. (1996). Overview and evaluation of fuel ethanol from cellulosic biomass: technology, economics, the environment, and policy, *Annual Reviews, Energy Environment,* **21,** 403–465.

Lynd, L.R. , R.T. Elander and C.E. Wyman (1996). Likely features and costs of mature biomass ethanol technology, *Appl Biochem Biotechnol*, **57–58**, 741–761.

Lynd, L.R. and M.Q. Wang (2004). A product-nonspecific framework for evaluating the potential of biomass-based products to displace fossil fuels, *J Ind Ecol,* **7**, 17–32.

Lynd, L.R., P.J. Weimer, W.H. van Zyl, I.S. Pretorious (2002). Microbial cellulose utilization: fundamentals and biotechnology. *Microbiology and Molecular Biology Reviews,* **66**, 506–577.

Mac Donald, D.G., J.F. Mathews (1979). Effect of steam treatment in the hydrolysis of aspen by commercial enzymes. *Biotech. Bioeng*. **21,** 1091-1096.

Mackie, K.L. (1985). Effect of sulphur dioxide and sulphuric acid on steam explosion of aspen wood. *J. Wood. Chem. Tech.,* **5,** 405-425.

MacLean, H.L. and L.B. Lave (2003). Evaluating automobile fuel/propulsion system technologies, *Prog Energy Combus Sci,* **29**, 1–69.

Magnusson, H. (2005). Process simulation in Aspen Plus of an integrated ethanol and CHP plant. Master thesis in Energy Engineering. Umea University (Sweden).

Malça, J. and F. Freire (2006). Renewability and life-cycle energy efficiency of bioethanol and bio-ethyl tertiary butyl ether (bioETBE): assessing the implications of allocation, *Energy,* **31,** 3362–3380.

Mandels, M. and E.T. Reese (1957). Induction of cellulase in *Trichoderma viride* as influenced by carbon sources and metals. *J. Bacteriol*., **73,** 269–278.

Mandels, M., J. Kostick, R. Parizek (1971). The use of adsorbed cellulase in the continuous conversion of cellulose to glucose. *J Polymer Sci*, **36**, 445– 459.

Mandfield, S.D., C. Mooney, J.N. Saddler (1999). Substrates and enzyme characteristics that limit cellulose hydrolysis. *Biotechnol Prog*, **15,** 804– 816.

Marshall, K., D. Sixsmith (1974). Some physical characteristics of microcrystalline cellulose. Powders for pharmaceutical use. *Drug Dev Commun*, **1,** 51-71.

Mason, WH. (1927). *Apparatus for and process of explosion fibration of lignocellulosic material*. U.S. Patent no. 1655618 (10 January 1929).

McAloon, A., F. Taylor, W. Yee, K. Ibsen, R. Wooley (2000). *Determining the cost of producing ethanol from corn starch and lignocellulosic feedstocks.* Technical Report NREL/TP-580-28893. National Renewable Energy Laboratory, Golden, CO (U.S.A.), 35pp.

McCormick-Brennan, K., C. Bomb, E. Deurwaarder and T. Kåberger (2007). Biofuels for transport in Europe: lessons from Germany and the UK, *Energy Policy,* **35,** 2256–2267.

McLaren, J.S. (2005). Crop biotechnology provides an opportunity to develop a sustainable future, *Trends in Biotechnology*, **23**, 339–342.

McMillan, M.M., D.W. Newman (1999). Templeton and A. Mohagheghi, Simultaneous saccharification and cofermentation of dilute-acid pretreated yellow poplar hardwood to ethanol using xylose-fermenting *Zymomonas mobilis*, *Applied Biochemistry and Biotechnology*, **77–79**, 649–665.

Medve, J., J. Karlsson, D. Lee, F. Tjerneld (1998). Hydrolysis of microcrystalline cellulose by cellobiohydrolase I and endoglucanase II from Trichoderma reesei: adsorption, sugar production pattern and synergism of the enzymes. *Biotechnol Bioeng,* **59,** 621–634.

Medve, J., J. Ståhlberg and F. Tjerneld (1994). Adsorption and synergism of cellobiohydrolase I and cellobiohydrolase II of *Trichoderma reesei* during hydrolysis of microcrystalline cellulose. *Biotechnol. Bioeng.,* **44**, 1064–1073.

Medve, J., J. Ståhlberg, F. Tjerneld (1997). Isotherms for adsorption of cellobiohydrolase I and II from Trichoderma reesei on microcrystalline cellulose. *Applied Biochem and Biotechnol*, **66,** 39-56.

Messner, R., K. Hagspiel and C.P. Kubicek (1990). Isolation of a β-glucosidase- binding and activating polysaccharide from cell walls of *Trichoderma reesei. Arch. Microbiol*., **154**, 150–155.

Michalowicz, G., B. Toussaint, M.R. Vignon (1991). Ultrastructural changes in poplar cell wall during steam explosion treatment. *Holzforschung*, **45,** 175-179.

Mielenz, J.R. (1997). Feasibility studies for biomass-to-ethanol production facilities in Florida and Hawaii. *Renewable Energy,* **10** (2/3), 279–284.

Millett, M.A., M.J. Effland, D.P. Caulfield (1979). Influence of fine grinding on the hydrolysis of cellulosic materials—acid versus enzymatic, *Advances in Chemistry Series*, **181**, 71–89.

Mississippi Ethanol LCC (2002). *Final report from Mississippi Ethanol LLC to the National Renewable Energy Laboratory*. Report NREL/SR-510-31720, NREL, Golden, CO (U.S.A.)

Miyamoto, S., K. Nisizawa (1942). Model for cellulose hydrolysis by cellulase. *J Vet Soc Arm Jpn*, **396**, 778– 784.

Monique, H., A. Faaij, R. van den Broek, G. Berndes, D. Gielen, W. Turkenburg (2003) Exploration of the ranges of the global potential of biomass for energy. *Biomass Bioenergy*, **25**, 119–133.

Mooney, C., S. Mandfield, M. Touhy, J. Saddler (1998). The effect of the initial pore volume and lignin content on the enzymatic hydrolysis of softwoods. *Bioresource Technol*, **64,** 113-119.

Mosier, N., C. Wyman, B. Dale, R. Elander, Y.Y. Lee, M. Holtzapple, M. Ladisch (2005). Features of promising technologies for pretreatment of lignocellulosic biomass. *Bioresource Technol*, **96,** 673-686.

Mosier, N.S., P. Hall, C.M. Ladisch and M.R. Ladisch (1999). Reaction kinetics, molecular action, and mechanisms of cellulolytic proteins. *Adv. Biochem. Eng. Biotechnol*., **65,** 23–40.

Mulder, K. and N.J. Hagens (2008). Energy return on investment: toward a consistent framework, *Ambio*, **37**, 74–79.

Nagle, N., K. Ibsen, E. Jennings (1999). A process economic approach to develop a dilute-acid cellulose hydrolysis process to produce ethanol from biomass. *Applied Biochemistry and Biotechnology,* **77–79**, 595–607.

Naik, S.N., V.V. Goud, P.K. Rout, A.K. Dalai (2010). Production of first and second generation biofuels: A comprehensive review. *Renewable and Sustainable Energy Reviews*, **14**, 578-597.

Neuman, R.P., L.P. Walker (1992). Solution exclusion from cellulose in packed columns; process modeling and analysis. *Biotechnol Bioeng,* **40,** 226– 234.

Neureiter, M., H. Danner, C. Thomasser, B. Saidi, R. Braun (2002). Dilute acid hydrolysis of sugarcane bagasse at varying conditions. *Appl. Biochem. Biotechnol*., **98-100**, 49-58.

Nexant Inc. (2005). *Equipment design and cost estimation for small modular biomass systems, synthesis gas cleanup, and oxygen separation equipment, task 9: mixed alcohols from syngas state of technology.* For National Renewable Energy Laboratory, Golden, CO (U.S.A.).

Nguyen, Q.A., J.N. Saddler (1991). An integrated model for the technical and economic evaluation of an enzymatic biomass conversion process, *Bioresour Technol*, **35,** 275-282.

Nguyen, Q.A., J.H. Dickow, B.W. Duff, J.D. Farmer, D.A. Glassner, K.N. Ibsen, M.F. Ruth, , D.J. Schell, I.B. Thompson, M.P. Tucker (1996). NREL/DOE ethanol pilot-plant: current status and capabilities. *Bioresource Technology,* **58**, 189–196.

Nidetzky, B. and W. Steiner (1993). A new approach for modeling cellulase-cellulose adsorption and the kinetics of the enzymatic hydrolysis of microcrystalline cellulose. *Biotechnol. Bioeng*., **42,** 469-479.

Nidetzky, B., W. Steiner, M. Hayn, M. Claeyssens (1994a). Cellulose hydrolysis by the cellulase from Trichoderma reesei: a new model for synergistic interaction. *Biochem J*, **298**, 705– 710.

Nidetzky, B., W. Zachariae, G. Gercken, M. Hayn, and W. Steiner (1994b). Hydrolysis of cellooligosaccharides by *Trichoderma reesei* cellobiohydrolases. Experimental data and kinetic modeling. *Enzyme Microb. Technol*., **16,** 43–52.

Nieves, R.A., C.I. Ehrman, W.S. Adney, R.T. Elander and M.E. Himmel (1998). Technical communication: survey and analysis of commercial cellulase preparations suitable for biomass conversion to ethanol. *World J. Microbiol. Biotechnol*., **14,** 301–304.

Nogawa, M., M. Goto, H. Okada and Y. Morikawa (2001). L-Sorbose induces cellulase gene trancription in the cellulolytic fungus *Trichoderma reesei*. *Curr. Genet*., **38,** 329–334.

Norde, W., C.A. Haynes (1995). *Reversibility and mechanism of protein adsorption. In: Proteins at Interfaces II, Fundamentals and Applications* (Horbett TJ, Brash JL Eds.), ACS Symposium Series 602, American Chemical Society, Washington, DC (U.S.A.).

Nutor, J.R.K., A.O. Converse (1991). The effect of enzyme and substrate levels on the specific hydrolysis rate of pretreated poplar wood. *Appl Biochem Biotechnol*, **28/29**, 75– 81.

Oh, K.-K., S.-W. Kim, Y.-S. Jeong, S.-I. Hong (2001). Bioconversion of cellulose into ethanol by nonisothermal simultaneous saccharification and fermentation. *Appl Biochem Biotechnol,* **89,** 15–30.

Öhgren, K., G. Zacchi, M. Galbe (2005), Optimisation of steam pretreatment of SO_2 impregnated corn stover for fuel ethanol production. *Appl. Biochem. Biotechnol*., **121-124**, 1055-1067.

Öhman, M., C. Boman, H. Hedman and R. Eklund (2006). Residential combustion performance of pelletized hydrolysis residue from lignocellulosic ethanol production, *Energy and Fuels*, **20**, 1298–1304.

Ohmine, K., H. Ooshima, Y. Harano (1983). Kinetic study of enzymatic hydrolysis of cellulose by cellulase from Trichoderma viride. *Biotechnol Bioeng*, **25**, 2041–2053.

Okazaki M., M. Moo-Young (1978). Kinetics of enzymatic hydrolysis of cellulose: analytical description of a mechanistic model. *Biotechnol Bioeng*, **20,** 637– 663.

Oliveria, M.E.D., B.E. Vaughan and E.J. Rykiel Jr. (2005). Ethanol as fuel: energy, carbon dioxide balances, and ecological footprint, *Bioscience,* **55**, 593–602.

Ooshima, H., D.S. Burns, A.O. Converse (1990). Adsorption of cellulase from Trichoderma reesei on cellulose and lignacious residue in wood pretreated by dilute sulfuric acid with explosive decompression. *Biotechnol Bioeng*, **36**,446–452.

Ooshima, H., K. Ohime, Y. Ishitani, Y. Harano (1982). Applicability of an empirical rate expression to enzymatic hydrolysis of cellulosic materials. *Biotechnol Lett,* **4,** 729– 734.

Ooshima, H., M. Kurakake, J. Kato, Y. Harano (1991). Enzymatic activity of cellulase adsorbed on cellulose and its change during hydrolysis. *Appl Biochem Biotechnol*, **31,** 253– 266.

Ooshima, H., M. Sakata, Y. Harano (1983). Adsorption of cellulase from Trichoderma viride on cellulose. *Biotechnol Bioeng*, **25,** 3103-3104.

Ozcimen, D., F. Karaosmanoglu (2004). Production and characterization of bio-oil and biochar from rapeseed cake. *Renew Energy*, **29**, 779–87.

Palonen, H., F. Tjerneld, G. Zacchi, M. Tenkanen (2004). Adsorption of Trichoderma reesei CBH I and EG II and their catalytic domains on steam pretreated softwood and isolated lignin. *J Biotechnol*, **107,** 65-72.

Palonen, H., M. Tenkanen and M. Linder (1999). Dynamic interaction of *Trichoderma reesei* cellobiohydrolases Ce16A and Ce17A and cellulose at equilibrium and during hydrolysis. *Appl. Environ. Microbiol.,* **65,** 5229–5233.

Pan, X., C. Arato, N. Gilkes, D. Gregg, W. Mabee, K. Pye, Z. Xiao, X. Zhang, J. Saddler (2005). Biorefining of softwoods using ethanol organosolv pulping: preliminary evaluation of process streams for manufacture of fuel-grade ethanol and co-products. *Biotechnology and Bioengineering*, **90 (4)**, 473–481.

Peitersen, N., E.W. Ross (1979). Mathematical model for enzymatic hydrolysis and fermentation of cellulose by Trichoderma. *Biotechnol Bioeng*, **21**, 997– 1017.

Philippidis, G.P. and C. Hatzis (1997). Biochemical engineering analysis of critical process factors in the biomass-to-ethanol technology, *Biotechnology Progress*, **13**, 222–231.

Philippidis, G.P., D.D. Spindler, C.E. Wyman (1992). Mathematical modelling of cellulose conversion to ethanol by the simultaneous saccharification and fermentation process. *Appl Biochem Biotechnol*, **34/35**, 543–556.

Philippidis, G.P., T. K. Smith, C.E. Wyman (1993). Study of the enzymatic hydrolysis of cellulose for production of fuel ethanol by the simultaneous saccharification and fermentation process. *Biotechnol Bioeng*, **41**, 846–853.

Phillips, S., A. Aden, J. Jechura, and D. Dayton (2007). *Thermochemical ethanol via indirect gasification and mixed alcohol synthesis of lignocellulosic biomass.* Technical Report NREL/TP-510-41168, Golden, CO: National renewable Energy Laboratory.

Piccolo, C., F. Bezzo (2007). Ethanol from lignocellulosic biomass: a comparison between conversion technologies, In: *Computer-Aided Chemical Engineering 24, 17th European Symp. on Computer Aided Process Engineering* (V. Plesu and P.S. Agachi, Eds.), Elsevier, Amsterdam, Paesi Bassi, 1277-1282.

Piccolo, C., F. Bezzo (2009). A techno-economical comparison between two technologies for bioethanol production from lignocellulose. *Biomass and Bioenergy*, **33**, 478-491.

Piccolo, C., G. Lidén, F. Bezzo (2009). Effect of substrate specific area on lignocellulose enzymatic hydrolysis: An experimental and modeling investigation, In: *Computer-Aided Chemical Engineering 27, 10th International Symp. on Process Systems Engineering* (R.M. Brito-Alves,

C.A. Oller do Nascimento, E.C. Biscaia Jr., Eds.), Elsevier, Amsterdam, Paesi Bassi, 1701-1706.

Piccolo, C., M. Wiman, F. Bezzo, G. Lidén (2010). Enzyme adsorption on SO_2 catalyzed steam-pretreated wheat and spruce material. *Enzyme and Microbial Technology*, **46**, 159-169.

Pimentel, D., and Pimentel M. (2008). Corn and Cellulosic Ethanol Cause Major Problems. *Energies*, **1**, 35-37.

Powelson, R. (2006). Company plans big ethanol plant in Oak Ridge. 1 May 2006 article accessed 20th September 2009 at http://www.knoxnews.com/kns/local_news/article/0,1406,KNS_347_4664543,00.html.

Prins, M.J., K.J. Ptasinski and F.J.J.G. Janssen (2007). From coal to biomass gasification: comparison of thermodynamic efficiency, *Energy*, **32**, 1248–1259.

Process Systems Enterprise Ltd. (2009). *gPROMS User's Guide.*

Proposal for a directive of the European Parliament and of the Council on the promotion of the use of energy from renewable source (2008). European Commission (EC) Brussels (Belgium), January 23.

Puls, J., T.M. Wood (1991). The degradation pattern of cellulose by extracellular cellulases of aerobic and anaerobic microorganisms. *Biores Technol*, **36**, 15–19.

Rabinovich, M.L., V.M. Chernoglazov, and A.A. Klesov (1983). Isoenzymes of endoglucanase in cellulase complexes: different affinity for cellulose and different role in the hydrolysis of an insoluble substrate. *Biochemistry*, **48,** 321–329.

Ragauskas, A.J., C.K. Williams, B.H. Davison, G. Britovsek, J. Cairney, C.A. Eckert, W.J. Frederick Jr., J.P. Hallett, D.J. Leak, C.L. Liotta, J.R. Mielenz, R. Murphy, R. Templer, T. Tschaplinski (2006). The path forward for biofuels and biomaterials. *Science*, **311**, 484-488.

Ramos, L.P., C. Breuil, J.N. Saddler (1992). Comparison of steam pretreatment of eucalyptus, aspen, and spruce wood chips and their enzymatic hydrolysis. *Appl. Biochem. Biotechnol*, **34,** 37-48.

Ramos, L.P., M.M. Nazhad, J.N. Saddler (1993). Effect of enzymatic hydrolysis on the morphology and fine structure of pretreated cellulosic residues. *Enzyme Microb Technol*, **15,** 821-831.

Reczey, K., A. Brumbauer, M. Bollok, Z. Szengyel and G. Zacchi (1998). Use of hemicellulose hydrolysate for β-glucosidase fermentation. *Appl. Biochem. Biotechnol*., **70–72**, 225–235.

Reese, E.T. (1956). A microbiological process report: enymatic hydrolysis of cellulose. *Appl. Microbiol.,* **4,** 39–45.

Reese, E.T. and M. Mandels (1971). Enzymatic degradation. In: *Cellulose and cellulose derivatives* (N. M. Bikales and L. Segal, Ed.), Wiley Interscience, New York (U.S.A.). pp. 1079–1094.

Reese, E.T., R.G.H. Siu, H.S. Levinson (1950). The biological degradation of soluble cellulose derivatives and its relationship to the mechanism of cellulose hydrolysis. *J Bacteriol*, **59,** 485-497.

Reijnders, L. (2006). Conditions for the sustainability of biomass based fuel use. *Energy Policy*, **34**, 863–76.

Reinikainen, T., O. Teleman, T.T. Teeri (1995). Effects of pH and high ionic strength on the adsorption and activity of native and mutated cellobiohydrolase I from Trichoderma reesei. *Proteins*, **22**, 392–403.

Reith, J. H., H. den Uil, H. van Veen, W. T. A. M. de Laat, J. J. Niessen, E. de Jong, H. W. Elbersen, R. Weusthuis, J. P. van Dijken e L. Raamsdonk (2002). Co-production of bio-ethanol, electricity and heat from biomass residues. Presented at *12th European Conference and Technology Exhibition on Biomass for Energy, Industry and Climate Protection*, Amsterdam, Netherlands, 17-21 giugno.

Rivers, D.B., G.H. Emert (1987). Lignocellulose pretreatment: a comparison of wet and dry ball attrition, *Biotechnology Letter,* **9,** 365–368.

Rostami, A.A., M.R. Hajaligol and S.E. Wrenn (2004). A biomass pyrolysis submodel for CFD applications, *Fuel,* **83,** 1519–1525.

Rouvinen, J., T. Bergfors, T.T. Teeri, J.K. Knowles and T.A. Jones (1990). Three-dimensional structure of cellobiohydrolase II from *Trichoderma reesei*. *Science*, **249,** 380–386.

Ruiz, R., T. Ehrman (1996). *Dilute acid hydrolysis procedure for determination of total sugars in the liquid fraction of process samples.* NREL, Golden, CO (U.S.A.).

Ryu, D.D.Y., C. Kim and M. Mandels (1984). Competitive adsorption of cellulase components and its significance in a synergistic mechanism. *Biotechnol. Bioeng*. **26,** 488–496.

Ryu, D.D.Y., S.B. Lee (1982). Effect of compression milling on cellulose structure and on enzymatic hydrolysis kinetics. *Biotechnol Bioeng*, **24**, 1047– 1067.

Saddler, J.N. (1992). Biotechnology for the conversion of lignocellulosics. Biomass and *Bioenergy,* **2**, 229–238.

Saha, B.C. (2003), Hemicellulose bioconversion, Journal of Industrial Microbiol and Biotechnol, 30, 279-291.

Sanchez, O.J. and C.A. Cardona (2008). Trends in biotechnological production of fuel ethanol from different feedstocks, *Bioresour Technol*, **99**, 5270–5295.

Sandgren, M., A. Shaw, T.H. Ropp, S. Wu, R. Bott, A.D. Cameron, J. Ståhlberg, C. Mitchinson and T.A. Jones (2000). The X-ray crystal structure of the Trichoderma reesei family 12 endoglucanase 3, Cel12A, at 1.9 Å resolution. *J. Mol. Biol*., **308,** 295–310.

Sassner, P., M. Galbe, G. Zacchi (2007). Techno-economic evaluation of bioethanol production from three different lignocellulosic materials. *Biomass. Bioen*., **32**, 422-430.

Sattler, W., H. Esterbauer, O. Glatter, W. Steiner (1989). The effect of enzyme concentration on the rate of the hydrolysis rate of cellulose. *Biotechnol Bioeng,* **33,**1221–1234.

Scheiding, W., M. Thoma, A. Ross, K. Schugerl (1984). Modeling of the enzymatic hydrolysis of cellobiose and cellulose by a complex enzyme mixture of Trichoderma reesei QM9414. *Appl Microbiol Biotechnol*, **20,** 176– 182.

Schell, D.J., C.J. Riley, N. Dowe, J. Farmer, K.N. Ibsen, M.F. Ruth, S.T. Toon, R.E. Lumpkin (2004). A bioethanol process development unit: initial operating experiences and results with a corn fiber feedstock. *Bioresource Technology,* **91**, 179–188.

Schnepf, R. (2006). *European Union biofuels policy and agriculture: an overview*. Congressional Research Service Report, RS22404, Washington, DC (U.S.A.), March 16th .

Schurz, J., J. Billiani, A. Honel, W.D. Eigner, A. Jànosi, M. Hayn, H. Esterbauer (1985). Reaktionsmechanismus und Strukturnderungen beim enzymatischen Abbau von Cellulose durch Trichoderma-reesei-Cellulase. *Acta Polymer*, **36**, 76–80.

Schwald, W., H.H. Brownell, J.N. Saddler (1988). Enzymatic hydrolysis of steam treated aspen wood: Influence of partial hemicellulose and lignin removal prior to pretreatment. *J Wood Chem Technol*, **8,** 543-560.

Sheehan, J. and M. Himmel (1999). Enzymes, energy, and the environment: a strategic perspective on the U.S. Department of Energy's research and development activities for bioethanol. *Biotechnol. Prog*., **15**, 817–827.

Sheehan, J., V. Cambreco, J. Duffield, M. Garboski, H. Shapouri (1998*). An overview of biodiesel and petroleum diesel life cycles.* A report by US Department of Agriculture and Energy, p. 1–35.

Shimizu, K. (1991), Chemistry of Hemicellulose, chapter 5 in Hon D.N.S. and Shiraishi N.: Wood and cellulosic chemistry (Marcel Dekker, inc., New York and Basel).

Sin, G., A.S. Meyer, K.V. Gernaey (2009). Are Mechanistic Cellulose-Hydrolysis Models Reliable for Use in Biofuel Process Design? - Identifiability and Sensitivity Analysis. In: *Proceedings of FOCAPD-2009, 7th International Conference on Foundations of Computer-Aided Process Design* (M. El-Halwagi and A. Linninger, Eds.) Taylor & Francis, London, UK, pp. 93-106.

Singh, A., P.K.R. Kumar and K. Schugerl (1991). Adsorption and reuse of cellulases during saccharification of cellulosic materials. *J. Biotechnol*. **18,** 205–212.

Sinitsyn, A.P., A.V. Gusakov, E.Y. Vlasenko (1991). Effect of structural and physico-chemical features of cellulosic substrates on the efficiency of enzymatic hydrolysis. *Appl Biochem and Biotechnol*, **30,** 43-59.

Sinitsyn, A.P., O.V. Mitkevich, A.V. Gusakov (1989). Decrease in reactivity and change of physico-chemical parameters of cellulose in the course of enzymatic hydrolysis. *Carbohydr Polymer*, **10**, 1– 14.

Sluiter, A., B. Hames, R. Ruiz, C. Scarlata, J. Sluiter, D. Templeton, D. Crocker (2008). *Determination of structural carbohydrates and lignin in biomass*. Technical Report NREL/TP-510-42618 NREL, Golden, CO (U.S.A.) `http://devafdc.nrel.gov/pdfs/9572.pdf`.

Smith, A.M. (2008). Prospects for increasing starch and sucrose yields for bioethanol production, *Plant J,* **54**, 546–558.

Solomon, B.D., J.R. Barnes, K.E. Halvorsen (2007). Grain and cellulosic ethanol: history, economics, and energy policy. *Biomass and Bioenergy*, **31**, 416-425.

South, C.R., D.A. Hogsett and L.R. Lynd (1993). Continuous fermentation of cellulosic biomass to ethanol, *Applied Biochemistry and Biotechnology*, **39/40**, 587–600.

South, C.R., D.A.L. Hogsett and L.R. Lynd (1995). Modeling simultaneous saccharification and fermentation of lignocellulose to ethanol in batch and continuous reactors, *Enzyme and Microbial Technology*, **17**, 797–803.

Spath, P.L. and D.C. Dayton (2003). *Preliminary screening – technical and economic assessment of synthesis gas to fuels and chemicals with emphasis on the potential for biomass-derived syngas.* Report NREL/TP-510-34929, NREL, Golden, CO (U.S.A.).

Steiner, W., W. Sattler, H. Esterbauer (1988). Adsorption of Trichoderma reesei cellulase on cellulose experimental-data and their analysis by different equations, *Biotechnol Bioeng*, **32,** 853– 865.

Stenberg, K., C. Tengborg, M. Galbe, G. Zacchi (1998). Optimization of Steam Pretreatment of SO_2- Impregnated Mixed Softwoods for Ethanol Production. *J Chem Technol Biotechnol*, **71,** 299-308.

Sternberg, D., P. Vijayakumar and E.T. Reese (1977). β-Glucosidase: microbial production and effect on enzymatic hydrolysis of cellulose. *Can. J. Microbiol*., **23,** 139–147.

Stevens, D.J., M. Wörgetter, J. Saddler (2004). *Biofuels for transportation: an examination of policy and technical issues.* IEA Bioenergy Task 39, Liquid Biofuels Final Report 2001–2003, Paris (France).

Stone, J.E., A.M. Scallan, E. Donefer, E. Ahlgren (1969). Digestibility as a simple function of a molecule of a similar size to a cellulase enzyme. *Adv Chem Ser*, **95**, 219–241.

Strategic energy review – an energy policy for Europe (2007). European Commission (EC), Brussels (Belgium), January 10th .

Strobel, H.J., F.C. Caldwell, and K.A. Dawson (1995). Carbohydate transport by the anaerobic thermophilic *Clostridium thermocellum* LQRI. *Appl. Environ. Microbiol*., **61,** 4012–4015.

Stutzenberger, F. and G. Lintz. (1986). Hydrolysis products inhibit adsorption of *Trichoderma reesei* C30 cellulases to protein-extracted lucerne fibres. *Enzyme Microb. Technol*., **8,** 341–344.

Ståhlberg, J., G. Johandson, G. Pettersson (1991). A new model for enzymatic hydrolysis of cellulose based on the two domain-structure of cellobiohydrolase I. *Bio/Technology,* **9,** 286-290.

Suga, K., G. van Dedem, M. Moo-Young (1975). Degradation of polysaccharides by endo and exo enzymes: a theoretical analysis. *Biotechnol Bioeng*, **17**, 433– 439.

Sun, Y., J. Cheng (2002). Hydrolysis of lignocellulosic materials for ethanol production: a review. *Biores Technol*, **83,** 1– 11.

Sutcliffe R, J. Saddler (1986). The role of lignin in the adsorption of cellulases during enzymatic treatment of lignocellulosic material. *Biotechnol Bioeng*, **17**, 749-762.

Szengyel, Z. (2000). Ethanol from wood—Cellulase enzyme production. *PhD thesis*, Lund University/Chemical Engineering Department at Lund (Sweden).

Söderström J., L. Pilcher, M. Galbe, G. Zacchi (2002). Two step steam pretreatment of softwood with SO_2 impregnation for ethanol production, *Appl. Biochem. Biotechnol*, **98-100**, 5-21.

Takagi, M., S. Abe, S. Suzuki, G.H. Emert and N. Yata (1977). A method for production of ethanol directly from cellulose using cellulase and yeast. In: Proceedings of *Bioconversion Symposium*,T.K. Ghose, Editor, IIT, Delhi (India), pp. 551–571.

Takashima, S., A. Nakamura, M. Hidaka, H. Masaki and T. Uozumi (1999). Molecular cloning and expression of the novel fungal beta-glucosidase genes from *Humicola grisea* and *Trichoderma reesei*. *J. Biochem*., **125,** 728– 736.

Tassinari, T., C. Macy, L. Spano (1982). Technology advances for continuous compression milling pretreatment of lignocellulosics for enzymatic hydrolysis, *Biotechnology and Bioengineering* **24**, 1495–1505.

Teeri, T.T. (1997). Crystalline cellulose degradation: new insight into the function of cellobiohydrolases. *Trends Biotechnol.,* **15,** 160–167.

Teeri, T.T., A. Koivula, M. Linder, G. Wohlfahrt, C. Divne and T. A. Jones (1998a). *Trichoderma reesei* cellobiohydrolases: why so efficient on crystalline cellulose? *Biochem. Soc. Trans*., **26,** 173–178.

Teeri, T.T., A. Koivula, M. Linder, G. Wohlfahrt, L. Ruohonen, J. Lehtio, T. Reinikainen, M. Srisodsuk, K. Kleman-Leyer, T.K. Kirk, T.A. Jones (1998b). Cellulose-cellulase interactions of native and engineered cellobiohydrolases from Trichoderma reesei. In: *Carbohydrates from Trichoderma reesei and other mciroorganisms: structures, biochemistry, genetics and applications (*Claeyssens M, Nerinckx W, Piens K, editor), Cambridge (U.K.), p 3 –12.

Thompson, D.N., H.C. Chen, H.E. Grethlein (1992). Comparison of pretreatment methods on the basis of available surface area. *Bioresource Technol*, **39,** 155-163.

Tolan, J.S. (2002). Iogen's process for producing ethanol from cellulosic biomass. *Clean Technologies and Environmental Policy,* **3**, 339–345.

Tomme, P., V. Heriban, M. Claeyssens (1990). Adsorption of two cellobiohydrolases from Trichoderma reesei to Avicel: evidence for exoexo synergism and possible loose complex formation. *Biotechnol Lett*,**12**, 525– 530.

Trostle, R. (2008). *Global Agricultural supply and demand: factors contributing to the recent increase in food commodity prices.* USDA Economic Research Service, Report WRS-0801, Washington, DC (U.S.A).

Ture, S., D. Uzun, I.E. Ture (1997). The potential use of sweet sorghum as a non-polluting source of energy. *Energy*, **22**, 17–9.

Usami, S., K. Kirimura, M. Imura, and S. Morikawa (1990). Cellular localization of the constitutive ß-glucosidase in *Trichoderma viride. J. Ferment. Bioeng*., **70**, 185-187.

Wald, S., C.R. Wilke, H.W. Blanch (1984). Kinetics of the enzymatic hydrolysis of cellulose. *Biotechnol Bioeng*, **26,** 221– 230.

Van den Broek, R. (2000) Sustainability of biomass electricity systems—an assessment of costs, macro-economic and environmental impacts in Nicaragua, Ireland and the Netherlands. Eburon, Delft (The Netherlands), p.216.

Van der Laaka, S.R.P, J.M. Raven and G.P.J. Verbong (2007). Strategic niche management for biofuels: analysing past experiments for developing new biofuel policies, *Energy Policy*, **35,** 3213–3225.

Van Kasteren, J. M. N., D. Dizdarevic, W. R. van der Waall, J. Guo, R. Verberne (2005), *Bio-ethanol from syngas*.

Van Tilbeurgh, H., G. Pettersson, R. Bhikabhai, H. De Boeck, M. Claeyssens (1985). Studies of the cellulolytic system of Trichoderma reesei QM 9414. Reaction specificity and thermodynamics of interactions of small substrates and ligands with the 1,4-beta-glucan cellobiohydrolase II, *Eur J Biochem*, **148,** 329–334.

Wang, W. (2002). Cassava production for industrial utilization in China – present and future perspective. In: *Cassava research and development in Asia: exploring new opportunities for an ancient crop*, 7th Regional Cassava Workshop, Bangkok (Thailand), October 28th– November 1st; 2002, pp. 33–38.

Ward, O.P., A. Singh (2002). Biotechnol technology development and perspectives. *Adv Appl. Microbiol,* **51**, 53-80.

Varhegyi, G., M.J.J. Antal, E. Jakab and P. Szabo (1997). Kinetic modelling of biomass pyrolysis, *J Anal Appl Pyrolysis*, **42**, 73–87.

Watanabe, T., T. Sato, S. Yoshioka, T. Koshijima and M. Kuwahara (1992). Purification and properties of *Aspergillus niger* β-glucosidase. *Eur. J. Biochem*., **209**, 651–659.

Weimer, P. J., J.M. Hackney and A.D. French (1995). Effects of chemical treatments and heating on the crystallinity of cellulose and their implications for evaluating the effect of crystallinity on cellulose biodegradation. *Biotechnol. Bioeng.*, **48,** 169–178.

Weimer, P.J., J.M. Lopez-Guisa, A.D. French (1990). Effect of cellulose fine structure on kinetics of its digestion by mixed ruminal microorganisms in vitro. *Appl Environ Microbiol*, **56,** 2421 – 2419.

White, A.R., R.M. Jr. Brown (1981). Enzymatic hydrolysis of cellulose: visual characterization of the process. *Proc Natl Acad Sci USA*, **78**, 1047– 1051.

Wilkie, A.C., K.J. Riedesel and J.M. Owens (2000). Stillage characterization and anaerobic treatment of ethanol stillage from conventional and cellulosic feedstocks. *Biomass and Bioenergy,* **19,** 63–102.

Wingren, A., M. Galbe and G. Zacchi (2003). Techno-Economic Evaluation of Producing Ethanol from Softwood: Comparison of SSF and SHF and Identification of Bottlenecks. *Biotechnol. Prog.,* **19**, 1109-1117.

Vinzant, T.B., L. Ponfick, N.J. Nagle, C.J. Ehrman, J.B. Reynolds, M. Himmel (1994). SSF comparison of selected woods from southern sawmills, *Appl Biochem Biotechnol*, **45-46**, 611-626.

Wiselogel, A., S. Tyson, D. Johnson (1996), Biomass feedstock resources and composition, chapter 6. In: *Handbook on bioethanol: Production and utilization* (Wyman C.E.), Taylor & Francis, Washington (U.S.A.).

Von Blottnitz, H., M..A. Curran (2007). A review of assessments conducted on bioethanol as a transportation fuel from a net energy, greenhouse gas, and environmental life-cycle assessment, *Journal of Cleaner Production*, **15**, 607–619.

Von Sivers, M., G. Zacchi (1995). A techno-economical comparison of three processes for the production of ethanol from pine. *Bioresource Technology,* **51**, 43–52.

Wong, K.K.Y., K.F. Deverell, K.L. Mackie, T.A. Clark, L.A. Donaldson (1988). The relationship between fiber-porosity and cellulose digestibility in steam-exploded Pinus radiata. *Biotechnol Bioeng*, **31,** 447-456.

Wood, T.M. (1975). Properties and Mode of action of cellulases. *Biotechnol Bioeng Symp,* **5**, 111–137.

Wood, T.M. (1992). Fungal cellulases. *Biochem. Soc. Trans*., **20,** 46–53.

Wood, T.M., N. Saddler (1988). Increasing the availability of cellulose in biomass materials In: *Methods in Enzymology*, W.A. Wood and S.T. Kellogg Editors, **160,** 3–11.

Wood, T.M., S.I. McCrae, K.M. Bhat (1989). The mechanism of fungal cellulase action. *Biochem J*, **260,** 37-43.

Woodward, J., M.K. Hayes, and N.E. Lee (1988). Hydrolysis of cellulose by saturating and non-saturating concentrations of cellulase: implications for synergism. *Bio/Technology*, **6**, 301–304.

Wooley, R., K. Ibsen (2000). Rapid evaluation of research proposals using Aspen Plus. In: *Aspen World 2000*, Orlando, FL (U.S.A.).

Wooley, R., M. Ruth, J. Sheehan, K. Ibsen, H. Majdeski, A. Galvez (1999a). *Lignocellulosic biomass to ethanol process design and economics utilizing co-current acid prehydrolysis and enzymatic hydrolysis. Current and futuristic scenarios*. Report No. NREL/TP-508-26157. National renewable Energy Laboratory, Golden, CO (U.S.A.)

Wooley, R., M. Ruth, D. Glassner, J. Sheejan (1999b). Process design and costing of bioethanol technology: a tool for determining the status and direction of research and development. *Biotechnology Progress,* **15**, 794–803.

Wooley, R., V. Putsche (1996). *Development of an ASPEN PLUS physical property database for biofuels components*. Report No. NREL/MP-425-20685. Golden, CO: National renewable Energy Laboratory.

Worden, R.M., M.D. Bredwell, A.J. Grethlein (1997). *Fuels and Chemicals from Biomass,* ACS Symposium Series No 666, Washington, DC (U.S.A.), pp. 320-336.

Wyman, C.E. (1994). Ethanol from lignocellulosic biomass: technology, economics, and opportunities, *Bioresource Technology*, **50,** 3–16.

Wyman, C.E., B.E. Dale, R.T. Elander, M. Holtzapple, M.R. Ladisch and Y.Y. Lee (2005). Coordinated development of leading biomass pretreatment technologies, *Bioresour Technol* **96**, 1959–1966.

Wyman, C.E., D.D. Spindler and K. Grohmann (1992). Simultaneous saccharification and fermentation of several lignocellulosic feedstocks to fuel ethanol, *Biomass and Bioenergy*, **3**, 301–307.

Väljamäe, P., V. Sild, G. Pettersson, and G. Johansson (1998). The initial kinetics of hydrolysis by cellobiohydrolases I and II is consistent with a cellulose surface—erosion model. *Eur. J. Biochem*., **53**, 469–475.

Yan, T.R. and C.L. Lin (1997). Purification and characterization of a glucose-tolerant β-glucosidase from *Aspergillus niger* CCRC 31494. *Biosci. Biotechnol. Biochem*., **61**, 965–970.

Yau, W.W., J.J. Kirkland, D.D. Bly (1979). *Model size—exclusion liquid chromatography*. John Wiley & Sons, New York (U.S.A.).

Yu, X., R.H. Atalla (1998). A staining technique for evaluating the pore structure variations of microcrystalline cellulose powders. *Powder Technol*, **98,** 135-138.

Zanzi, R., K. Sjostrom and E. Bjornbom (1996). Rapid high-temperature pyrolysis of biomass in a free-fall reactor, *Fuel,* **75,** 545–550.

Zarzyycki, A., W. Polska (2007). Bioethanol production from sugar beet – European and polish perspective. Presented at 1st TOSSIE Workshop on technology improvement opportunities in the European sugar industry, Ferrara (Italy), January 25–26th.

Zeng, M., N.S. Mosier, C.P. Huang, D.M. Sherman, M.R. Ladisch (2007). Microscopic examination of changes of plant cell structure in corn stover due to hot water pretreatment and enzymatic hydrolysis. *Biotechnol Bioeng*, **97,** 265-278.

Zhang, S., D. E. Wolfgang, and D. B. Wilson (1999). Substrate heterogeneity causes the nonlinear kinetics of insoluble cellulose hydrolysis. *Biotechnol. Bioeng.,* **66**, 35–41.

Zhang, Y.H.P., L.R. Lynd (2004). Toward an aggregated understanding of enzymatic hydrolysis of cellulose: Noncomplexed cellulase systems. *Biotechnol. Bioeng*., **88,** 797-824.

Zhang, Y.H.P., L.R. Lynd (2006). A functionally-based model for hydrolysis of cellulose by fungal cellulase. *Biotechnol. Bioeng*., **94**, 888-898.

Websites

`www.biofuels-platform.ch` (Website of ENERS Energy Concept) [accessed on October 5th, 2009]

`www.novafuels.com` (Website of Nova Fuels, Inc.) [accessed on October 5th, 2009]

`www.ott.doe.gov/biofuels` (Website of US DOE) [accessed on January 7th, 2010]

`www.powerenergy.com` (Website of Power Energy Fuels, Inc.) [accessed on October 5th, 2009]

`www.rangefuels.com` (Website of Range Fuels, Inc.) [accessed on October 12th, 2009]

`www.syntecbiofuel.com` (Website of Syntec Biofuel, Inc.) [accessed on October 15th, 2009]

Acknowledgements

My supervisor, Ing. Fabrizio Bezzo deserves my deepest and most sincere gratitude: thank you for the many the opportunities and the many challenges you offered me in these past three years. Thank you for your excellent guidance and support, not only concerning research, but life itself. Thank you for your tolerance, understanding and your encouragement during the, not really infrequent actually, “dark moments” I had during my PhD. Finally thank you for every CAPE-luganega, every CAPE-mountain tour, and every funny informal chat and because, in very few words, *you care*…

Thank you, or better *Tack!* (one of the few words of my *very pocket* Swedish vocabulary) to my supervisor at Chemical Engineering Department of Lund University, Prof. Gunnar Lidén. Thank you for the opportunity to stay and for welcome me so warmly in the cold Sweden, thank you for your help, for every suggestion and interesting discussion we had. Thank you because, despite you were always so busy you have always been generous in time with me.
I gratefully thank Prof. Guido Zacchi, Doctor Mats Galbe and Prof. Folke Tjerneld for sharing their invaluable knowledge.
Special thanks to Magnus, Kim, Karen, Cristhian, Benny, Krisztina, Sanam, Kerstin, Christian, Ola, Birgitta for being always kind and helpful and for teaching me how to survive in the lab.

Grazie Stefano, *zio dado*, per tutte le volte che mi hai aiutato, dentro e fuori dal KC, per le nostre chiacchierate sulla panchina in pausa caffè, per tutte le volte che mi hai detto “dai, non fare la nonna” (*o peggio*), per quel sabato passato insieme in laboratorio a fare la NREL. Grazie perché, è vero che è difficile creare amicizie profonde quando si fa solo una “comparsata” in un posto come ho fatto io, ma ci sono le eccezioni… e tu sei una delle mie eccezioni… grazie, perché la nostra forza è l’innata capacità di unire gli opposti con un sorriso.

Tornando al DIPIC un grazie sincero a Giada, Andrea, Federico, Madda, Maria per tutti i caffè, i discorsi e le risate condivisi, per tutto l’aiuto che mi avete dato in questi anni, e in particolare nell’ultimo periodo.
Grazie al Prof. Max Barolo e a tutto il CAPE-Lab per tutte le iniziative, l’entusiasmo e la passione contagiosi.
Grazie a tutti i docenti, i tecnici, i post-doc, i dottorandi, presenti e passati, che con una parola, una battuta, un sorriso, hanno reso piacevole e meno pesante la permanenza al DIPIC.

Infine, *last but not least*, grazie alla mia insostituibile famiglia allargata, perché insieme, anche nei momenti difficili, ce l'abbiamo sempre fatta (*If you have a problem, if no one else can help, and if you can find them.*… altro che A-Team!).

Grazie, mamma e papà, perché non mi fate mai mancare il vostro supporto, anche quando, lo so, non condividete le mie scelte. Grazie perché avete capito che, come un aquilone, ho bisogno che mi *lasciate spago* per volare, ma non per questo mancate di farmi sentire la vostra mano salda al capo del filo.

Grazie Paola, Michele, Claudia, Sofia e Mauro, perché quando ci ritroviamo tutti insieme è sempre una festa, perché *squadra che vince non si cambia* e su di noi scommetterei sempre.

Grazie Nicola… e va bene così… senza parole…